ABSTRACT

Glaucoma is an optic neuropathy with multifactorial etiologies, commonly associated with elevated intraocular pressure (IOP) and characterized by degeneration of the optic nerve, loss of retinal ganglion cells (RGC), cupping of optic disc and visual field deficits, which could ultimately lead to vision loss. In most cases, glaucoma is a chronic, asymptomatic and gradually progressing neurodegenerative disease, sometimes referred to as the "silent thief of sight", hence, routine eye examinations by an ophthalmologist are critical to determine if there is a likelihood of developing the disease. Elevated IOP is a primary and the only modifiable risk factor in glaucoma. Currently, reducing IOP remains the only proven treatment to delay the progression of RGC death; however, some patients continue to have neurodegenerative effects despite lowering IOP. Therefore, development of novel neuroprotection strategies as an adjunct therapy to IOP-lowering agents will provide a valuable therapeutic strategy in glaucoma. One of the promising targets for neuroprotection is the endothelin system of peptides and their receptors.

The endothelin (ET) system comprises of three vasoactive peptides (ET-1, ET-2 and ET-3), which act through two types of G-protein coupled receptors, namely, ET_A and ET_B receptors. Originally discovered in the cardiovascular system, the diverse expression pattern of endothelin peptides and their receptors implicate their involvement in a variety of physiological processes in the body. A growing body of evidence suggests that endothelins and their receptors are associated with neurodegeneration in glaucoma. Previous studies have demonstrated that ET-1 levels are elevated in aqueous humor (AH) and plasma of glaucoma patients. Our lab previously demonstrated that in an ocular hypertension model in rats, there was an increase in ET_B as well as ET_A receptor expression primarily in RGCs compared to contralateral eyes. Following IOP elevation, RGC loss was significantly attenuated in the ET_B

receptor-deficient rats, pointing to a causative role of the ET_B receptor in glaucomatous neurodegeneration. However, the precise cellular and molecular mechanisms by which ET-1 promotes neurodegeneration through its actions on the endothelin receptors are not completely understood. Previous studies have shown that ET_B receptor stimulation increases the oxidative stress and production of superoxide anions, in sympathetic neurons. Several studies point to the role of mitochondrial dysfunction and oxidative stress as contributors to glaucomatous damage in animal models of glaucoma. To investigate various molecular events contributing to the ET-1 mediated RGC loss in glaucoma, we carried out RNA-seq analysis of the translatome in rat primary RGCs following ET-1 treatment. We identified several key mitochondrial and neurodegenerative gene candidates including Atp5h, Cox17, Foxo1, Moap1 and Map3k11 that were differentially expressed in the translatome by ET-1 treatment in RGCs. Based on our RNA-seq findings, we hypothesized that ***ET-1 causes an increase in reactive oxygen species (ROS) by acting through the ET_B receptor that produces a subsequent decline in mitochondrial function and bioenergetics ultimately predisposing RGCs to cell death***. To test this hypothesis, we used an *in vitro* approach by utilizing rat primary culture of RGCs treated with ET-1 as well as an *in vivo* approach by intravitreal ET-1 injections in rodents and the Morrison's model of glaucoma in rats. Our data showed that there is a significant decrease in the expression of cytochrome c oxidase 17 copper chaperone (COX17) and ATP synthase, H^+ transporting, mitochondrial F_0 complex, subunit D (ATP5H), both of which are critical components of the electron transport chain and oxidative phosphorylation pathway. Using a Seahorse mitostress assay, we also found a significant decline of several mitochondrial parameters following ET-1 treatment in primary RGCs, which indicated the possibility of a disruption in the mitochondrial quality control machinery. Hence, we also explored the effect of the ET-1 treatment on the

mitophagy pathway, specifically in RGCs. Our findings suggest that there is a decrease in mitophagosome formation in RGCs in the Morrison ocular hypertensive model as well as in GFP-LC3 mice injected with ET-1, indicating an impairment in the mitochondrial quality control mechanism. Our studies reveal several novel candidates that could be targeted for the development of neuroprotective approaches to treat glaucoma.

ENDOTHELIN-1 MEDIATED DECLINE IN MITOCHONDRIAL FUNCTION CONTRIBUTES TO NEURODEGENERATION IN GLAUCOMA

DISSERTATION

Presented to the Graduate Council of the

Graduate School of Biomedical Sciences

University of North Texas Health Science Center at Fort Worth

In Partial Fulfillment of the Requirements

For the Degree of

DOCTOR OF PHILOSOPHY

By

Renuka M. Chaphalkar, M.S.

Fort Worth, Texas

May 2020

ACKNOWLEDGEMENTS

Firstly, I would like to express my profound gratitude and sincere thanks to my mentor Dr. Raghu Krishnamoorthy who accepted me as a graduate student in his lab and mentored me through my graduate program. This journey would not have been possible without his continued support and guidance. His constant encouragement during times of rejection and failed experiments motivated me to work harder for my projects. I am grateful to him for giving me the opportunity to explore my work independently and chose for myself the research directions I wanted to proceed with. He has always encouraged me to ask questions and taught me to plan and organize my experiments meticulously. In addition to his professional guidance, he has also helped me in my personal growth and development. His valuable scientific expertise will be of immense help as I further pursue my career in research.

I would like to thank my co-mentor and committee member Dr. Dorota Stankowska who has always had her door open for answering all my questions and concerns. She has always been considerate and understanding whenever I made any mistakes in my experiments. Her quick suggestions in troubleshooting my experiments have helped me to improve my work and obtain data in a timely manner.

I would also like to thank my committee member Dr. Abe Clark who has been supportive and understanding during this period. His critical observations and insightful comments on my experimental results has helped me to improvise my data and understanding minute details in an experimental design. I am extremely appreciative of Dr. Gulab Zode for providing significant

inputs in my research work. His critical feedback and challenging questions to my work has helped in shaping my PhD project in an extremely positive way. I would also like to extend thanks to my university member Dr. Keisa Mathis for being supportive and present for all my committee meetings.

I want to thank the current members of the lab Dr. Shaoqing He and Dr. Bindu Kodati for all the scientific discussions and random conversations we shared together in the breakroom. You have always made the lab environment fun and full of excitement.

Lastly, I am deeply thankful to my parents Makarand Chaphalkar and Sunita Chaphalkar, who have been patient, supportive and a constant source of strength during this journey and never raised an eyebrow when I claimed my manuscript or thesis would be finished in '2 weeks' for nearly 2 years. I am also grateful to my sister Manasi Chaphalkar and my brother in law Manjunath Karantha for their love and moral support. To my friends back home in India and in US, whenever I needed a helping hand and motivation.

TABLE OF CONTENTS

- **LIST OF FIGURES**

CHAPTER I

CHAPTER II

CHAPTER III

CHAPTER I

INTRODUCTION

Glaucoma is a heterogeneous group of diseases with different etiologies and clinical presentations that lead to optic neuropathy. Glaucoma is a leading cause of global irreversible blindness worldwide and greatly impacts the everyday lives of millions of patients. The global prevalence of glaucoma in 2020 has been estimated to be 76 million and projecting to 111.8 million in 2040. In most cases, the disease progresses without major symptoms, pain or discomfort, hence glaucoma is sometimes referred to as the 'sneak thief of sight' and by the time patients come to the clinic, they have lost a substantial part of their peripheral vision. Glaucoma is commonly characterized by elevation of **IOP**, accompanied by degeneration of the optic nerve, loss of retinal ganglion cells (**RGCs**), thinning of the retinal nerve fiber layer and optic disc cupping (Jonas et al. 2017).

There are two major forms of glaucoma, namely open-angle and closed-angle glaucoma, which are defined and revealed by the gonioscopic evaluation of the anterior chamber angle of the eye. In patients with primary open angle glaucoma (POAG), the drainage angle between iris and cornea remains open, however, there is an increased resistance to aqueous outflow resulting in a gradual increase in IOP. In primary angle closure glaucoma, there is an obstruction in the aqueous humor drainage due to a closed iridocorneal angle and blockade of the drainage canal resulting in a sudden rise in IOP. A major risk factor in primary open angle glaucoma is elevated intraocular pressure (IOP), which is the only modifiable risk factor as well as treatable risk factor. Other factors contributing to glaucomatous neurodegeneration include, IOP fluctuations, advancing age, family

history of glaucoma, reduced central corneal thickness, elevated cup to disc ratio, disc asymmetry and disc hemorrhages (McMonnies 2017; Bron et al. 2008).

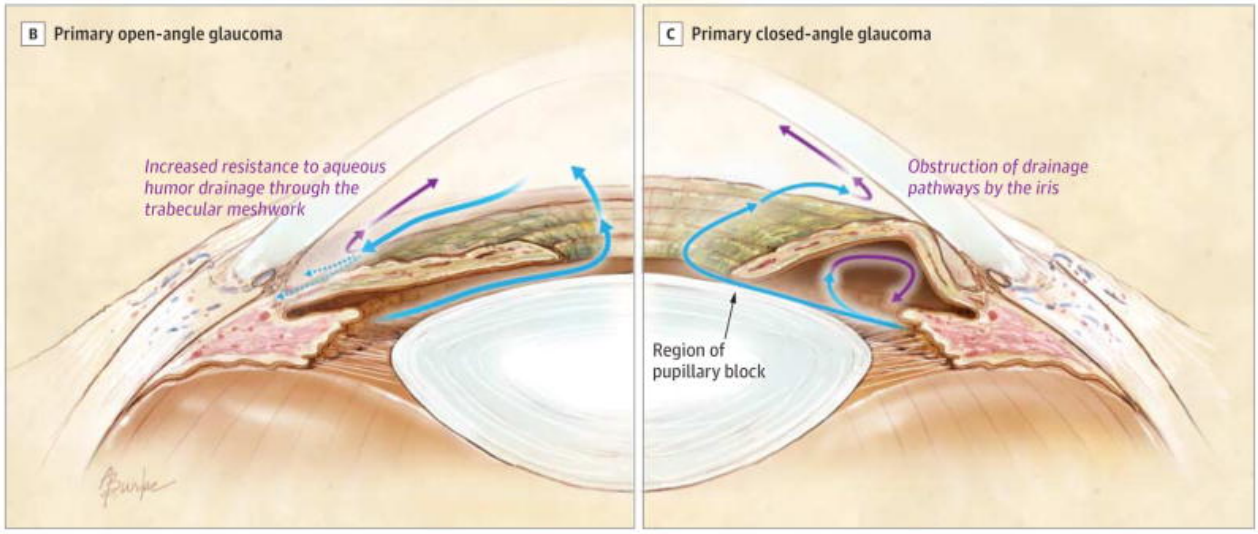

Figure 1. Illustration showing aqueous drainage pathways in open-angle glaucoma and angle-closure glaucoma. Reproduced from *Weinreb, Robert N et al. "The pathophysiology and treatment of glaucoma: a review." JAMA vol. 311,18 (2014): 1901-11.*

IOP elevation in glaucoma can be attributed to various reasons. Some of them are depicted below:

1) **Extracellular matrix (ECM) remodeling**

The trabecular meshwork (TM) is the primary site for regulation of AH outflow, with the structure of triangular wedge of tissue that encircles the eye at the irido-corneal angle. Aqueous humor is a nutritive fluid, produced in the ciliary body which flows from the posterior to the anterior chamber through the pupil. Along its route, it provides for the nutrition of tissues in the anterior segment and is drained from the TM into Sclemm's canal and aqueous veins and finally into the episceral veins. The TM is a dynamic tissue divided into 3 layers- the uveal meshwork, corneoscleral meshwork and juxtacanalicular region. Under normal conditions, the rate of aqueous humor formation (2 to 3 µl/min in humans) is balanced by an equal rate of aqueous humor drainage.

However, changes in the ECM protein expression/deposition within these tissues disrupts aqueous humor dynamics by reducing the rate of aqueous humor drainage. Excessive accumulations of collagen IV and VI (Tawara et al. 2008; Tripathi et al. 1994), and fibronectin (Medina-Ortiz et al. 2013; Tawara et al. 2008; Tovar-Vidales et al. 2008) are thought to contribute to clogging of the trabecular meshwork, leading to IOP elevation, commonly observed in POAG.

2) **Myocilin mutations**

Myocilin or trabecular meshwork-inducible glucocorticoid response (TIGR) protein, is a secreted 55-57 kDa glycoprotein that is found intracellularly as well as in the extracellular matrix of the normal and glaucomatous trabecular meshwork cells. The myocilin protein has different structural domains including, myosin-like, leucine zipper and olfactomedin domains. Nearly 3-5% of patients with primary open-angle glaucoma harbor myocilin gene mutations found mainly in the olfactomedin domain of the protein. Mutant myocilin causes a decline in secretion of the translated protein in trabecular meshwork cells, which could be a contributor to decreased aqueous outflow leading to an increase in IOP (Clark et al. 2001; O'Brien, Ren, and Wang 2000; Tamm 2002). A substantial increase in myocilin expression, from barely detectable levels to greater than 2% of total cellular mRNA, was found following 10 days exposure of dexamethasone in TM cells (Nguyen et al. 1998). However, previous studies suggest that increased IOP may not be associated with myocilin overexpression.

In a study screening steroid responders and control patients for mutations in the myocilin gene, no significant association was found between variations in myocilin and the steroid response. The precise role of mutations in the myocilin gene and their role in steroid-induced ocular hypertension is still an active area of investigation. Nevertheless, a transgenic mouse model of POAG made by incorporating the Y437H MYOC mutation, referred to as Tg-MYOC(Y437H)

mice, has proved to be good model for POAG and recapitulate many of the key pathological features of glaucoma such as degeneration of the optic nerve and RGC loss (Zode et al. 2011).

3) **Steroid induced**

IOP elevation could be iatrogenic due to local or systemic use of corticosteroids which was first reported by (Becker and Mills, 1963). The prevalence of glaucoma was higher among systemic lupus erythematosus (SLE) patients under chronic glucocorticoid therapy (Carli et al. 2013). Steroid treatment produces IOP elevation in 90% of POAG patients, compared to 30% in control subjects. The mechanism for this steroid sensitivity was elucidated in a pioneering work carried out by Zhang et al., (2005). The authors demonstrated that the glucocorticoid (GRβ) receptor is a negative regulator of dexamethasone sensitivity. They found that trabecular meshwork cell lines derived from glaucoma patients have lower expression of the GRβ receptor, compared to normal trabecular meshwork cells (Zhang, Clark, and Yorio 2005). Another elegant model of secondary glaucoma that resembles POAG was developed by Zode et al., (2014), by topical administration of dexamethasone in mice eyes, which produced IOP elevation and subsequent optic nerve axon injury and RGC loss. Use of different animal models is helpful in understanding key cellular events in the pathogenesis of glaucoma.

Advances in glaucoma therapies

Current glaucoma therapies are aimed at lowering IOP to a predetermined target IOP level., the standard of care is to lower IOP by 17-27% (Crawley et al. 2012). This reduction in IOP is achieved through two major approaches that involve either reducing aqueous humor formation or increasing its drainage.

Medications

Decreasing aqueous humor formation: β-blockers including timolol and betaxolol reduce aqueous humor production and typically produce a 20 to 27% decrease from baseline IOP.

Topical carbonic anhydrase inhibitors including brinzolamide and dorzolamide bring about 17 to 20% reduction in IOP, compared to baseline. Adrenergic/cholinergic agonists have vasoconstrictive effects on the blood vessels of the ciliary body stroma, which ultimately causes a reduction in aqueous humor formation.

Increasing aqueous humor outflow: The unconventional uveoscleral outflow pathway is targeted by prostaglandins analogues that include, latanoprost, travoprost, tafluprost, which have similar IOP lowering effects as timolol. Treatment with these prostaglandin analogs produces a robust 20 to 35% reduction in IOP.

Rho kinase inhibitors: Two new ocular hypotensive agents targeting the Rho kinase pathway were recently approved for clinical use: ripasudil in Japan and Netarsudil in the United States (Tanna and Johnson, 2018). This is a significant development in the field since this treatment is the first to target the trabecular pathway to enhance outflow of aqueous humor (Rao et al., 2016). This was the culmination of 15 years of research on the role of Rho kinases in the trabecular meshwork carried out in David Epstein's group as well as other labs. Rho kinase acts as an effector of the small G protein Rho GTPase which regulates actin dynamics in cells. Inhibition of Rho kinase was found to lower IOP mediated by relaxation of the trabecular meshwork, thereby promoting increased drainage of aqueous humor. This development opens the possibilities for development of additional therapeutics that directly target the trabecular meshwork.

NO-donor:

This is a recently approved new class of glaucoma medication. Vyzulta (latanoprostene bunod ophthalmic solution) is a dual-action medication which reduces intraocular pressure (IOP) primarily by increasing AH outflow through the uveoscleral pathway with latanoprost acid and targeting the trabecular meshwork outflow with nitric oxide. It is metabolized into latanoprost and a moiety that donates nitric oxide once the medication is in the eye. The IOP reduction is facilitated by combining the complementary mechanisms of these two molecules.

Surgery: In patients where IOP reduction is not effectively reduced by pharmacotherapy, an alternative or additive means to control IOP is by surgery. Trabeculectomy (gold standard) is a surgical procedure that involves creating a "flap" to allow additional outflow from the eye for the aqueous humor. Other treatments include laser treatments of the trabecular meshwork (trabeculoplasty) or the ciliary body.

EX-Press Tube Shunts: Another approach gaining wide acceptance is the implantation of aqueous shunts. Aqueous shunts (glaucoma drainage devices, tube implants, setons) are being increasing used to lower IOP to 8 to 10 mmHg. A "bleb" is created by inserting a small metal shunt to drain the fluid from inside of the eye, Trabeculoplasty – Argon/diode/YAG LASER delivered to the TM to improve the drainage of fluid from the eye.

Despite numerous advances in pharmacological and surgical management of glaucoma, neurodegeneration of the optic nerve, RGC loss, axonal injury and visual field damage continues to occur in some patients. Moreover, the IOP-lowering glaucoma medications exhibit high risk of systemic and ocular side-effects, although in very few patients (5-7%). "Neuroprotection" as an approach to slow down the functional loss in glaucoma by an IOP-independent mechanism or synergistic to IOP-lowering medications is emerging as a promising therapeutic strategy.

However, there are no medications currently available for a neuroprotective treatment of glaucoma. Hence, there is a pressing need for additional neuroprotective treatments for glaucoma to delay axonal injury and enhance the survival of RGCs.

The endothelin system of vasoactive peptides and their receptors have emerged as potential targets for the development of a neuroprotective treatment of glaucoma.

Endothelin system of vasoactive peptides and their receptors

Endothelin-1 (ET-1) is a prototypical member of the endothelin system of vasoactive peptides and was originally discovered from research work in cardiovascular system. In the 1980s, it was found that the acetyl choline dependent relaxation of vascular smooth muscle required presence of endothelial cells. This relaxation was mediated by release of an endothelium derived relaxation factor subsequently identified as nitric oxide (Furchgott 1983; Furchgott and Zawadzki 1980). In contrast, it was also found that the endothelial cells in culture secrete a potent vasoconstrictor important in regulating the vascular smooth muscle contractility (Hickey et al. 1985). This endogenous vasoconstrictor, endothelin, was subsequently isolated from porcine aortic endothelial cells (Yanagisawa, Kurihara, et al. 1988). To identify the pathophysiological role of this vasoconstrictor, rat endothelin was used to study sequence analysis and biological activity (Yanagisawa, Inoue, et al. 1988). Subsequent studies by Inoue and colleagues suggested the existence of three endothelin isopeptides encoded by three distinct genes: Endothelin-1(ET-1), Endothelin-2 (ET-2) and Endothelin-3 (ET-3) which differ in structure and exhibit different pharmacological activities (Inoue et al. 1989). These three isoforms of endothelins have a high sequence homology to a rare snake venom, sarafotoxin (S6c). ET-1 represents the most predominant isoform *in vivo*, since it is constitutively synthesized and secreted by the vascular

endothelium. Besides, the vascular endothelial cells, ET-1 has been detected in wide variety of tissues such as epithelial cells of lungs, kidney, and colon; smooth muscle cells of blood vessels, heart, lung, brain, gastrointestinal tract and eye. The cellular distribution of ET-2 has not been as extensively studied but the peptide has been detected in vasculature, heart, lung, kidney, intestine, ovaries and eye, while ET-3 expression predominates in the brain (Davenport et al. 2016; Rubanyi and Polokoff 1994).

Endothelins are trasnscribed as prepro-ET mRNA, which encodes a 212-amino acid precursor, prepro-ET. Removal of a short secretory sequence of amino acid generates proET-1, which in turn is cleaved by furin-like enzymes (belonging to a subtilisin-like proprotein convertase family) to yield a 38 amino acid precursor, Big ET. Big ET is converted to a mature, biologically active peptide ET by a family of metalloprotease enzymes, endothelin converting enzymes (ECE). Synthesis of ET-2 has steps that are similar to that of ET-1 (Figure 3).

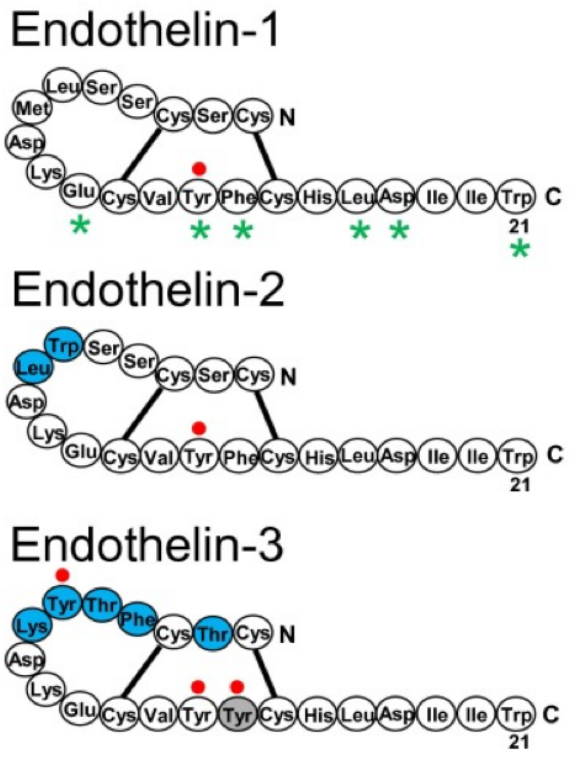

Figure 2. Amino-acid sequence and structure of endothelin peptides.

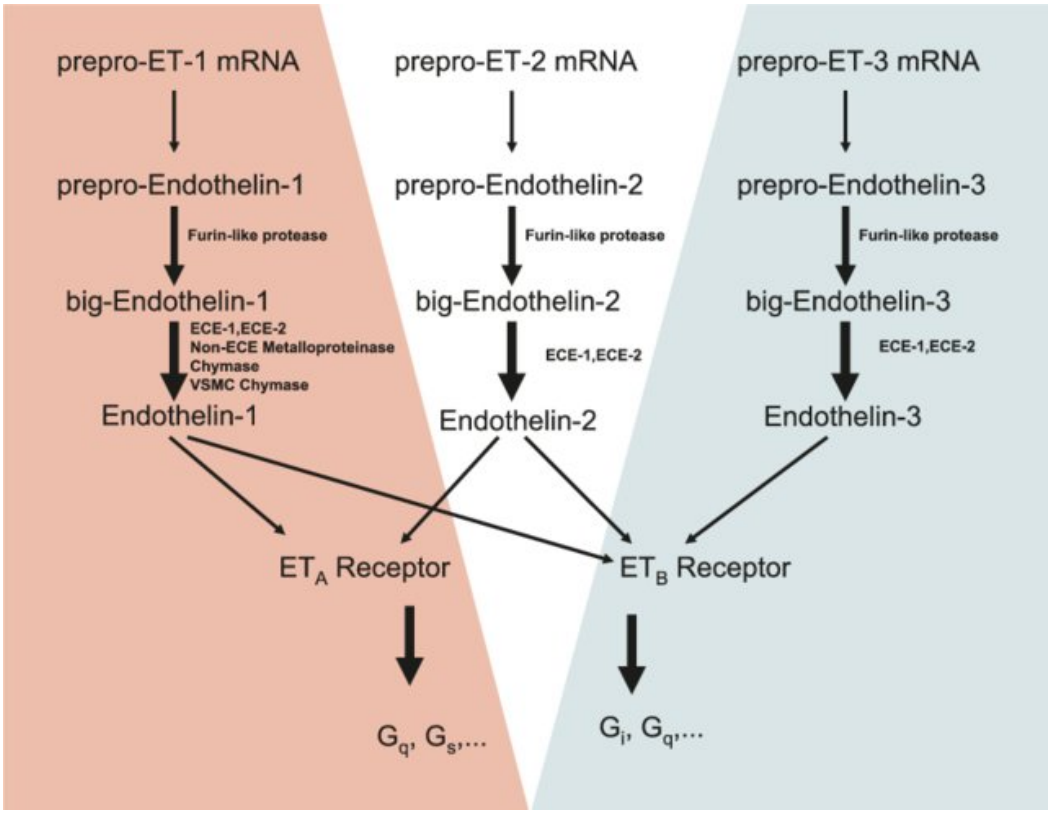

Figure 3. Biosynthesis of the components of the endothelin system. Reproduced from *Can J Physiol Pharmacol 2008; 86: 485-498.*

ETs mediate their actions via two classes of seven transmembrane G-protein coupled receptors (GPCRs), namely, endothelin A (ET_A) receptor or endothelin B (ET_B) receptor. In the vasculature, the ET_A receptor is predominantly expressed in vascular smooth muscle cell and cardiomyocytes, whereas the ET_B receptor is abundantly expressed in endothelial cells and to an extent on vascular smooth muscle cells. The two classes of endothelin receptors differ in their relative affinities for the endothelin peptides. The ET_A receptor has equal affinity for the ET-1 and ET-2 peptides and lower affinity for the ET-3 peptide (ET-1=ET-2>>>ET-3). On the other hand, the ET_B receptor binds with equal affinity, with all the endothelin peptides (ET-1=ET-2=ET-3) Hence, ET-3 is considered a selective agonist of the ET_B receptor.

The intracellular signalling pathway following activation of ET_A and ET_B receptor by ET-1 involves the heterotrimeric G proteins G_q, G_s and G_i to induce various signalling second messenger through effector enzymes and ion channels, including, phospholipase C (PLC) leading to production of inositol triphosphate (IP_3), diacylglycerol (DAG) and adenylyl cyclase to elevate cAMP (Sandoval et al. 2014; Sugden 2003). Production of IP_3 rapidly increases intracellular $Ca^{2+,}$ by promoting the mobilization of intracellular calcium stores (mainly the endoplasmic reticulum) and extracellular Ca^{+2}. This Ca^{+2} entry depolarizes the cell, leading to opening of a cascade of ion channels and also activating the Ca^{2+}-dependent pathways and Ca^{2+}/calmodulin-dependent pathways. In the vasculature, ET-1 produced by endothelial cells bind to both ET_A and ET_B receptors in the vascular wall. In smooth muscle cells, ET-1 binds to ET_A receptor causing a rapid increase in release of Ca^{+2} by an increase in PLC and consecutive production of IP_3 leading to a vasoconstriction of the vessels (Schneider, Boesen, and Pollock 2007). However, ET-1 also induces vasodilation via the endothelial cell ET_B receptors by promoting release of endothelial nitric oxide synthase (eNOS) derived nitric oxide (NO) release through a Ca^{+2} dependent calmodulin pathway. The NO release reduces the concentration of intracellular Ca+2 causing vasodilation. This explains the biphasic effect of intravenous administration to ET-1 in lab animals: a transient hypotension due to ET_B receptor mediated NO release from vascular endothelial cells followed by a prolonged hypertension due to ETA receptor mediated elevation of Ca^{+2} in vascular smooth muscle cells.

Endothelins in the ocular system

In the eye, endothelin (ET) expression was predominantly observed in the iris, in the Descemet's membrane, corneal endothelium, choroid and retina and ET binding sites were observed in the cornea (endothelial layer) and Descemet's membrane, and in the choroid, and the

retina (MacCumber and D'Anna 1994). Subsequent studies using the immunogold labelling in the retina demonstrated ET-1 immunoreactivity in the photoreceptor inner segments and in the outer plexiform layer (OPL). In retinal vasculature, robust ET-1 expression was found in choroidal and retinal vessels (Stitt et al. 1996). In the retina, ET-1 immunoreactivity was found in inner nuclear layer and in the inner segments of photoreceptors, retinal pigment epithelium cells, ganglion cell layers as well as optic nerve head astrocytes (Ripodas et al. 2001). All these studies point to the paracrine effects of ET-1 since the binding sites were observed in close proximity to the site of its synthesis, indicative of local actions of the peptide. The exact endogenous role of endothelins is not known and additional studies are needed to understand its physiological role in ocular tissues.

Endothelins in glaucoma

ET-1 was found to be elevated in the aqueous humor in animal models of glaucoma including the congenital Beagle model, the Morrison model in rats (Källberg et al. 2002; Prasanna et al. 2005b). Recent studies have shown that ET-1 levels are elevated in aqueous humor and plasma of glaucoma patients (Chen et al. 2013; Lopez-Riquelme et al. 2015). However, these findings did not indicate if ET-1 is a cause or consequence of the disease process of glaucoma. Intracameral administration of ET-1 in rabbits and monkeys produced a profound lowering of IOP, possibly mediated by ET-1's effect on contraction of the ciliary muscle (Erickson-Lamy, Rohen, and Grant 1991; Okada et al. 1995). On the other hand, ET-1 produces contraction of human trabecular meshwork cells in a dose dependent manner from 0.1 pM to a maximum effect at 100 pM (Dismuke et al. 2014). In primary and transformed human TM cells, TGF-β_2 induced a significant increase in ET-1 secretion at 1ng/ml and was maximal at 2.5ng/ml partly through a non-canonical Rho G-protein–mediated mechanism (Von Zee et al., 2012). These observations

suggest that ET-1 could produce an increase in IOP, mediated through a contraction of the TM. It is evident from these studies that the effect on ET-1 on aqueous humor dynamics depends on the net effect of ET-1 on both the ciliary muscle and the trabecular meshwork. This could vary depending on the species, which could account for the disparate findings of the effects of ET-1 in the anterior segment of the eye. ET-1 concentrations were also found to be increased in several animal models of glaucoma (Källberg et al. 2002; Prasanna et al. 2005b; Thanos and Naskar 2004). Both intravitreal and peribulbar administration of ET-1 has been shown to produce axon loss, RGC loss and disruption of nerve fiber layer (Chauhan et al. 2004; Krishnamoorthy et al. 2008; Lau, Dang, et al. 2006b). A growing body of evidence suggests that endothelins and their receptors are associated with neuronal damage in glaucoma (McGrady et al. 2017a; Howell et al. 2011; Howell et al. 2014; Yorio, Krishnamoorthy, and Prasanna 2002b; Krishnamoorthy et al. 2008; Minton et al. 2012b). In particular, Minton et al. (2012) demonstrated that RGC loss and damage to optic nerve axons were significantly attenuated in ET_B receptor-deficient rats, compared to those in wild type rats. This suggests that the ET_B receptor plays a causative role in promoting neurodegeneration during IOP elevation in rats.

In glaucomatous optic nerve degeneration, there is a decrease in blood flow at the optic nerve head, associated with vascular dysregulation, producing damage to the optic nerve and degeneration of RGCs (Flammer et al., 2001; Werner and Shen 2019). An increase in preproendothelin mRNA levels was detected following 1 hour of hypoxia (1% oxygen, 5% CO_2, 94% N_2) in human endothelial cells (Kourembanas et al. 1991). ET-1 promoter contains a HIF-1α binding site, which could account for an increase in ET-1 expression by hypoxia (Hu et al. 1998). Another study demonstrated the hypoxia augmented and TNF-α-mediated release of endothelin-1 (ET-1) from human optic nerve head astrocytes leading to their proliferation. Using an $ET_{A/B}$

receptor antagonist completely blocked these responses demonstrating that human optic nerve head astrocytes secrete ET-1, which could act on its receptors by autocrine signalling mechanisms to produce neurodegenerative effects (Desai et al. 2004). In the retina and optic nerve head of glaucomatous eyes, immunostaining for HIF-1α, an indicator of hypoxic stress, exhibited an increased expression, indicating that HIF-1α signalling may have a pathophysiological role in the development progression of neurodegeneration in the glaucomatous eyes (Tezel and Wax 2004). These observations, suggest that ET-1 could be a contributor of hypoxia-induced oxidative stress and possibly act as a causative factor in glaucomatous neurodegeneration.

Oxidative stress and glaucoma

A significant increase in biomarkers associated with oxidative stress, inflammation, apoptosis was found in the AH and plasma samples of glaucoma patients (Kamel, Farrell, and O'Brien 2017; Tang et al. 2019; Ung et al. 2017). An increase in putative biomarkers, including, malonyldialdehyde, interleukin-6 (IL-6) was observed in the AH of the POAG patients, indicative of damage due to lipid peroxidation and inflammation (Pinazo-Duran et al. 2013). Release of free radicals and reactive oxygen species (ROS) produce oxidative damage in target tissues, altering the biochemical composition of the vitreous humor, ultimately affecting the viability and function of trabecular meshwork and the optic nerve head. Hypoxia and vascular changes could produce oxidative damage to the human trabecular meshwork and also promote apoptotic changes in RGCs (Kimura et al. 2017; Zhao et al. 2016). Hence, mediators of oxidative stress involved in glaucoma pathogenesis could be pertinent targets for prevention and therapy in primary open-angle glaucoma (Saccà and Izzotti 2008). Oxidative stress, inflammatory response, and activation of apoptotic pathways also play a central role in retinal neurodegenerative diseases including age-related

macular degeneration, diabetic retinopathy and retinitis pigmentosa (Masuda, Shimazawa, and Hara 2017).

The mitochondria which play a central role in oxidative phosphorylation are also the site of origin of reactive oxygen species. Under normal conditions, the mitochondria play a pivotal role in complete oxidation of metabolic fuels including glucose and free fatty acids. The oxidation of these molecules through the Krebs cycle leads to the generation of energy, and electron-rich molecules, namely, NADH and $FADH_2$. High energy electrons from NADH and $FADH_2$ are transported along the carriers of the electron transport chain to molecular oxygen. The energy inherent in the downhill transport of electrons along the electron transport chain is utilized to pump proton across the mitochondrial inner membrane to create a proton gradient, which is utilized for the generation of ATP. One of the by by-products of oxidative metabolism and electron transport chain is the formation of ROS which can cause detrimental effects in highly metabolically active cells (such as RGCs and photoreceptors) and surrounding tissues. Accumulation of ROS causes mitochondrial outer membrane pore permeabilization and release of cytochrome c and other apoptotic proteins. Oxidative stress resulting in retina remodelling, including, functional changes in the retina and also generate cellular responses due to retinal injuries due to alterations in molecular pathways. Due to this retinal remodelling phenomenon, retinal neurodegenerative diseases may require a combination of several types of therapies like administration of neurotrophic factors, vitamins, antioxidants, anti-apoptotic and anti-inflammatory compounds (Cuenca et al. 2014). To summarize, oxidative stress and impairment in anti-oxidant machinery is a major underlying mechanism in pathogenesis of several neurodegenerative disorders including glaucoma.

RGCs and mitochondria

Mitochondria are abundant in RGCs, particularly, within the soma region (initial unmyelinated part) and synaptic terminals, as opposed to the post-laminar and myelinated region. Retrograde and anterograde transport of mitochondria is a continuous process along the axons of neurons. Hence, any disturbance of axonal transport due to mitochondrial abnormalities and a compromise in the mitochondrial function can lead to severe metabolic crises because of energy depletion (Osborne 2010). The impairment in axonal transport can be observed commonly in diseases such as Amyotrophic Lateral Sclerosis and Leber's Hereditary Optic Neuropathy (Osborne and del Olmo-Aguado 2013). Mitochondrial function decreases with age and since RGCs are largely dependent on their mitochondria, the prevalence of POAG increases with age possibly due to a decline in mitochondrial function. A decrease in the blood supply in the optic nerve head causing ischemia is a major risk factor in glaucoma since the RGCs would constantly be subjected to oxidative stress under these conditions. In addition, with increasing duration of ischemia, there could be an accumulation of nitric oxide, TNF-α and glutamate which in turn affect the RGCs which are already under oxidative stress (Osborne, Alvarez, and del Olmo Aguado 2014).

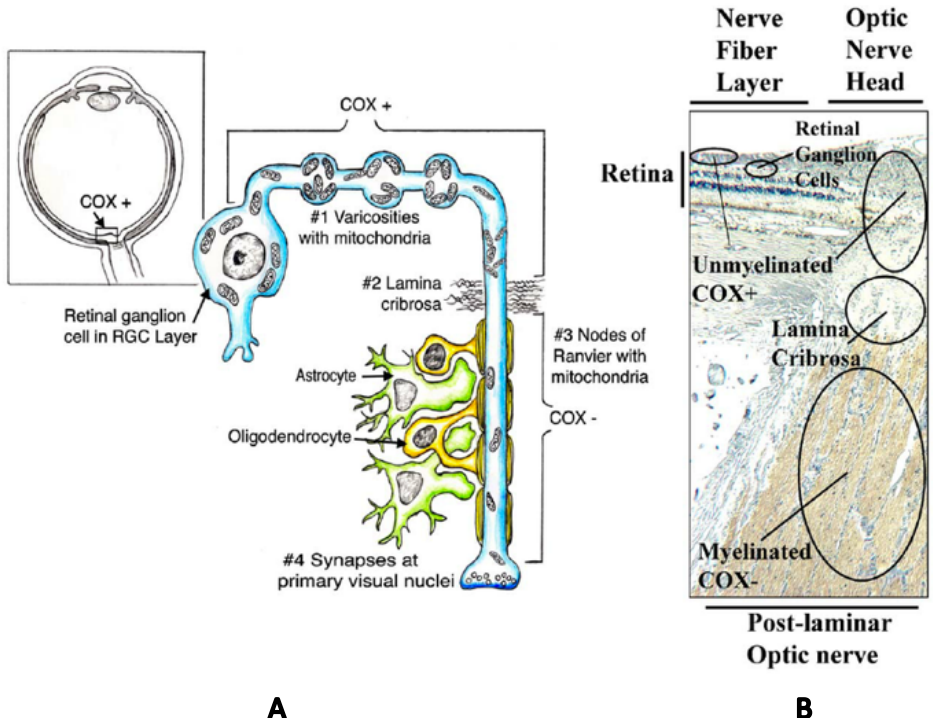

Figure 4. Diagrammatic view of pattern of immunostaining for COX in RGCs.

Mitochondrial distribution shown from the RGC soma through the unmyelinated (COX+) portion of the axon and penetrating the lamina cribrosa at the optic nerve head. **A.** Mitochondrial accumulations are represented in the varicosities within the NFL, and in the prelaminar region. There is a drastic decrease in mitochondrial numbers within the retrolaminar portion (COX−). Mitochondria, in this part of the RGC axon, are mostly located under the unmyelinated nodes of Ranvier. **B.** Illustration of a histological sagittal section of a normal human eye stained by a method using immunoperoxidase for myelin basic protein and showing a parallel transition from the retina to the optic nerve head, the lamina cribrosa and a portion of the myelinated retrolaminar optic nerve. Figure adapted from *Carelli et al., (2004) Mitochondrial dysfunction as a cause of optic neuropathies. Prog Retin Eye Res. Review*.

During normal mitochondrial respiration, electrons derived from NADH and FADH2 are transferred along a series of protein-bound electron carriers (Complex I through IV) and ultimately transferred to molecular oxygen.

Complex I (The NADH dehydrogenase complex) - is largest of these respiratory enzyme complexes. It accepts electrons from NADH and passes them through a flavin mononucleotide to ubiquinone resulting in the reduction of ubiquinone.

Complex II (Succinate dehydrogenase) – Electrons from oxidation of succinate by succinate dehydrogenase are fed into the electron-transport chain in the form of FADH2 which adds its electron to ubiquinone, producing reduced ubiquinone. Although it is embedded in the mitochondrial crista membrane, Complex II does not pump protons and contribute to proton motive force.

Complex III (Cytochrome oxidoreductase) – Ubiquinone accepts electrons from both Complex I and Complex II to form the reduced form of ubiquinone (ubiquinol) which then transfers its electrons to cytochrome c. Complex III pumps also protons across the inner mitochondrial membrane contributing to proton gradient across the membrane.

Complex IV (Cytochrome c oxidase) - Electrons from cytochrome c pass through this complex via bound copper ions and hemes to an oxygen molecule bound between the heme group and a copper ion. Four protons are then pumped out of the matrix into the intermembrane space accompanied by the reduction of O2 which combines with H+ ions to form water.

Complex V (F_1F_0ATP synthase) – Pumps protons from the intermembrane space to the matrix through the inner mitochondrial membrane to power ATP synthesis by the promotive force inherent in the proton gradient, driving ATP production in the mitochondrial matrix.

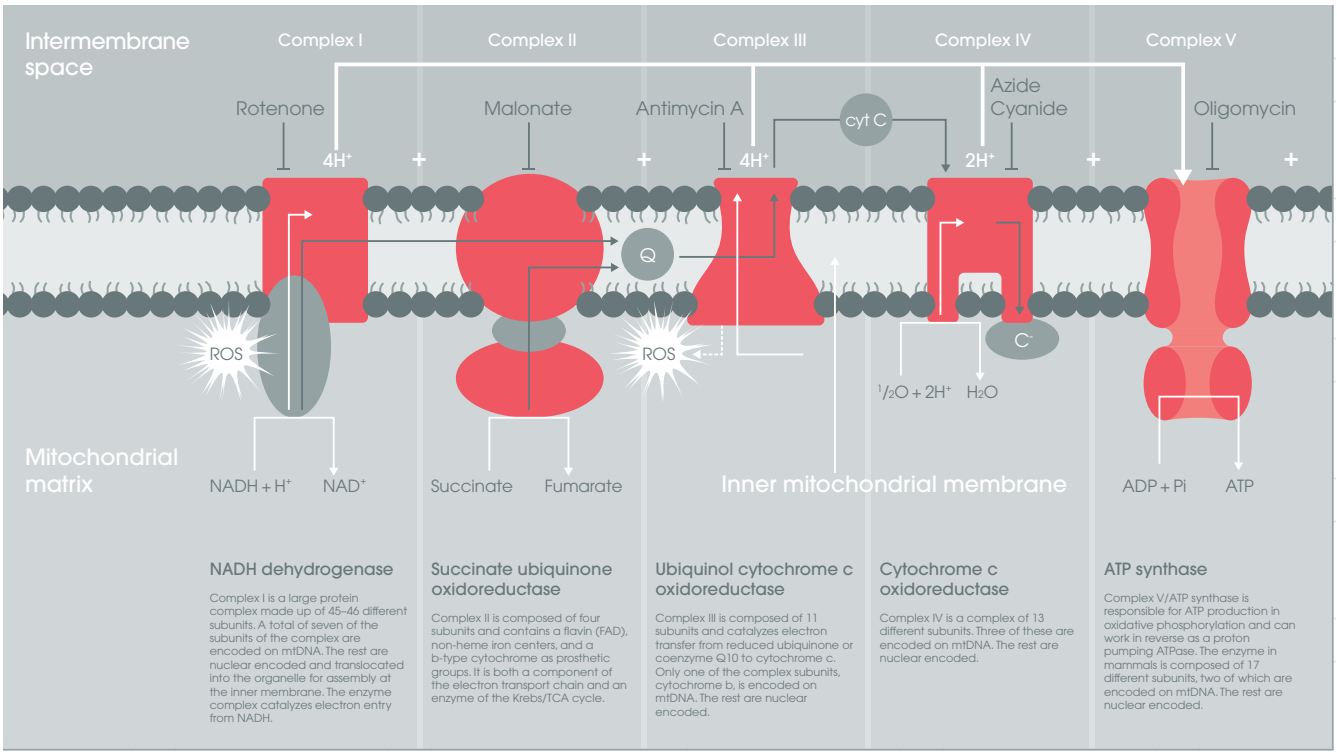

Figure 5. Oxidative phosphorylation pathway showing the electron transfer through five different complexes (Complex I-V) and their respective inhibitors. *Adapted from abcam*

In this study, we assessed mitochondrial mechanisms involved in ET-1 mediated neurodegeneration of RGCs, both in culture as well as in an ocular hypertension model in rats. We also assessed ET-1-mediated changes in bioenergetics in RGCs which underlie some of these degenerative effects. The study elucidates hitherto unknown mechanisms by which ET-1 promotes degeneration of RGCs. The basic information gained from the study will be helpful in developing novel strategies for neuroprotection in glaucoma and translating this knowledge to develop endothelin receptor antagonists in the future.

References

1. Becker, B, and Mills DW. 1963. 'Corticosteroids and Intraocular Pressure', *Archives of Ophthalmology*, 70: 500-07.

2. Bron, A., G. Chaine, M. Villain, J. Colin, J. P. Nordmann, J. P. Renard, and J. F. Rouland. 2008. '[Risk factors for primary open-angle glaucoma]', *J Fr Ophtalmol*, 31: 435-44.

3. Chauhan, Balwantray C., Terry L. LeVatte, Christine A. Jollimore, Paula K. Yu, Herbert A. Reitsamer, Melanie E. M. Kelly, Dao-Yi Yu, François Tremblay, and Michele L. Archibald. 2004. 'Model of Endothelin-1–Induced Chronic Optic Neuropathy in Rat', *Investigative Ophthalmology & Visual Science*, 45: 144-52.

4. Chen, H. Y., Y. C. Chang, W. C. Chen, and H. Y. Lane. 2013. 'Association between plasma endothelin-1 and severity of different types of glaucoma', *J Glaucoma*, 22: 117-22.

5. Clark, A. F., K. Kawase, S. English-Wright, D. Lane, H. T. Steely, T. Yamamoto, Y. Kitazawa, Y. H. Kwon, J. H. Fingert, R. E. Swiderski, R. F. Mullins, G. S. Hageman, W. L. Alward, V. C. Sheffield, and E. M. Stone. 2001. 'Expression of the glaucoma gene myocilin (MYOC) in the human optic nerve head', *Faseb j*, 15: 1251-3.

6. Crawley, L., S. M. Zamir, M. F. Cordeiro, and L. Guo. 2012. 'Clinical options for the reduction of elevated intraocular pressure', *Ophthalmol Eye Dis*, 4: 43-64.

7. Cuenca, N., L. Fernandez-Sanchez, L. Campello, V. Maneu, P. De la Villa, P. Lax, and I. Pinilla. 2014. 'Cellular responses following retinal injuries and therapeutic approaches for neurodegenerative diseases', *Prog Retin Eye Res*, 43: 17-75.

8. Davenport, A. P., K. A. Hyndman, N. Dhaun, C. Southan, D. E. Kohan, J. S. Pollock, D. M. Pollock, D. J. Webb, and J. J. Maguire. 2016. 'Endothelin', *Pharmacol Rev*, 68: 357-418.

9. Desai, D., S. He, T. Yorio, R. R. Krishnamoorthy, and G. Prasanna. 2004. 'Hypoxia augments TNF-alpha-mediated endothelin-1 release and cell proliferation in human optic nerve head astrocytes', *Biochem Biophys Res Commun*, 318: 642-8.

10. Dismuke, W. M., J. Liang, D. R. Overby, and W. D. Stamer. 2014. 'Concentration-related effects of nitric oxide and endothelin-1 on human trabecular meshwork cell contractility', *Exp Eye Res*, 120: 28-35.

11. Erickson-Lamy, K., J. W. Rohen, and W. M. Grant. 1991. 'Outflow facility studies in the perfused human ocular anterior segment', *Exp Eye Res*, 52: 723-31.

12. Flammer, J., M. Pache, and T. Resink. 2001. 'Vasospasm, its role in the pathogenesis of diseases with particular reference to the eye', *Prog Retin Eye Res*, 20: 319-49.

13. Furchgott, R. F. 1983. 'Role of endothelium in responses of vascular smooth muscle', *Circ Res*, 53: 557-73.

14. Furchgott, R. F., and J. V. Zawadzki. 1980. 'The obligatory role of endothelial cells in the relaxation of arterial smooth muscle by acetylcholine', *Nature*, 288: 373-6.

15. Hickey, K. A., G. Rubanyi, R. J. Paul, and R. F. Highsmith. 1985. 'Characterization of a coronary vasoconstrictor produced by cultured endothelial cells', *Am J Physiol*, 248: C550-6.

16. Howell, G. R., D. G. Macalinao, G. L. Sousa, M. Walden, I. Soto, S. C. Kneeland, J. M. Barbay, B. L. King, J. K. Marchant, M. Hibbs, B. Stevens, B. A. Barres, A. F. Clark, R. T. Libby, and S. W. John. 2011. 'Molecular clustering identifies complement and endothelin induction as early events in a mouse model of glaucoma', *J Clin Invest*, 121: 1429-44.

17. Howell, G. R., K. H. MacNicoll, C. E. Braine, I. Soto, D. G. Macalinao, G. L. Sousa, and S. W. John. 2014. 'Combinatorial targeting of early pathways profoundly inhibits neurodegeneration in a mouse model of glaucoma', *Neurobiol Dis*, 71: 44-52.

18. Hu, Jing, Daryl J. Discher, Nanette H. Bishopric, and Keith A. Webster. 1998. 'Hypoxia Regulates Expression of the Endothelin-1 Gene through a Proximal Hypoxia-Inducible Factor-1 Binding Site on the Antisense Strand', *Biochemical and Biophysical Research Communications*, 245: 894-99.

19. Inoue, A., M. Yanagisawa, S. Kimura, Y. Kasuya, T. Miyauchi, K. Goto, and T. Masaki. 1989. 'The human endothelin family: three structurally and pharmacologically distinct isopeptides predicted by three separate genes', *Proc Natl Acad Sci U S A*, 86: 2863-7.

20. Jonas, Jost B., Tin Aung, Rupert R. Bourne, Alain M. Bron, Robert Ritch, and Songhomitra Panda-Jonas. 2017. 'Glaucoma', *The Lancet*, 390: 2183-93.

21. Källberg, Maria E., Dennis E. Brooks, Gustavo A. Garcia-Sanchez, Andras M. Komàromy, Nancy J. Szabo, and Lili Tian PhD. 2002. 'Endothelin 1 Levels in the Aqueous Humor of Dogs With Glaucoma', *Journal of Glaucoma*, 11: 105-09.

22. Kamel, K., M. Farrell, and C. O'Brien. 2017. 'Mitochondrial dysfunction in ocular disease: Focus on glaucoma', *Mitochondrion*, 35: 44-53.

23. Kimura, A., K. Namekata, X. Guo, T. Noro, C. Harada, and T. Harada. 2017. 'Targeting Oxidative Stress for Treatment of Glaucoma and Optic Neuritis', *Oxid Med Cell Longev*, 2017: 2817252.

24. Kourembanas, S., P. A. Marsden, L. P. McQuillan, and D. V. Faller. 1991. 'Hypoxia induces endothelin gene expression and secretion in cultured human endothelium', *The Journal of Clinical Investigation*, 88: 1054-57.

25. Krishnamoorthy, Raghu R., Vidhya R. Rao, Rachel Dauphin, Ganesh Prasanna, Christina Johnson, and Thomas Yorio. 2008. 'Role of the ETB receptor in retinal ganglion cell death in glaucomaThis article is one of a selection of papers published in the special issue (part 1 of 2) on Forefronts in Endothelin', *Canadian Journal of Physiology and Pharmacology*, 86: 380-93.

26. Lau, Jonathan, Matthew Dang, Karlo Hockmann, and Alexander K. Ball. 2006. 'Effects of acute delivery of endothelin-1 on retinal ganglion cell loss in the rat', *Experimental Eye Research*, 82: 132-45.

27. Lopez-Riquelme, N., C. Villalba, C. Tormo, A. Belmonte, C. Fernandez, G. Torralba, and F. Hernandez. 2015. 'Endothelin-1 levels and biomarkers of oxidative stress in glaucoma patients', *Int Ophthalmol*, 35: 527-32.

28. MacCumber, Mathew W., and Salvatore A. D'Anna. 1994. 'Endothelin Receptor-Binding Subtypes in the Human Retina and Choroid', *Archives of Ophthalmology*, 112: 1231-35.

29. Masuda, T., M. Shimazawa, and H. Hara. 2017. 'Retinal Diseases Associated with Oxidative Stress and the Effects of a Free Radical Scavenger (Edaravone)', *Oxid Med Cell Longev*, 2017: 9208489.

30. McGrady, Nolan R., Alena Z. Minton, Dorota L. Stankowska, Shaoqing He, Hayden B. Jefferies, and Raghu R. Krishnamoorthy. 2017. 'Upregulation of the endothelin A (ET(A)) receptor and its association with neurodegeneration in a rodent model of glaucoma', *BMC neuroscience*, 18: 27-27.

31. McMonnies, Charles W. 2017. 'Glaucoma history and risk factors', *Journal of optometry*, 10: 71-78.

32. Medina-Ortiz, W. E., R. Belmares, S. Neubauer, R. J. Wordinger, and A. F. Clark. 2013. 'Cellular fibronectin expression in human trabecular meshwork and induction by transforming growth factor-beta2', *Invest Ophthalmol Vis Sci*, 54: 6779-88.

33. Minton, Alena Z., Nitasha R. Phatak, Dorota L. Stankowska, Shaoqing He, Hai-Ying Ma, Brett H. Mueller, Ming Jiang, Robert Luedtke, Shaohua Yang, Colby Brownlee, and Raghu R. Krishnamoorthy. 2012. 'Endothelin B Receptors Contribute to Retinal Ganglion Cell Loss in a Rat Model of Glaucoma', *PLOS ONE*, 7: e43199.

34. Nguyen, T. D., P. Chen, W. D. Huang, H. Chen, D. Johnson, and J. R. Polansky. 1998. 'Gene structure and properties of TIGR, an olfactomedin-related glycoprotein cloned from glucocorticoid-induced trabecular meshwork cells', *J Biol Chem*, 273: 6341-50.

35. O'Brien, E. T., X. Ren, and Y. Wang. 2000. 'Localization of myocilin to the golgi apparatus in Schlemm's canal cells', *Invest Ophthalmol Vis Sci*, 41: 3842-9.

36. Okada, K., K. Sugiyama, M. S. Haque, T. Taniguchi, and Y. Kitazawa. 1995. 'The effects of endothelin-1 on intraocular pressure and pupillary diameter in rabbits', *Jpn J Ophthalmol*, 39: 233-41.

37. Osborne, N. N. 2010. 'Mitochondria: Their role in ganglion cell death and survival in primary open angle glaucoma', *Exp Eye Res*, 90: 750-7.

38. Osborne, N. N., C. N. Alvarez, and S. del Olmo Aguado. 2014. 'Targeting mitochondrial dysfunction as in aging and glaucoma', *Drug Discov Today*, 19: 1613-22.

39. Osborne, N. N., and S. del Olmo-Aguado. 2013. 'Maintenance of retinal ganglion cell mitochondrial functions as a neuroprotective strategy in glaucoma', *Curr Opin Pharmacol*, 13: 16-22.

40. Pinazo-Duran, M. D., V. Zanon-Moreno, J. J. Garcia-Medina, and R. Gallego-Pinazo. 2013. 'Evaluation of presumptive biomarkers of oxidative stress, immune response and apoptosis in primary open-angle glaucoma', *Curr Opin Pharmacol*, 13: 98-107.

41. Prasanna, Ganesh, Christina Hulet, Devashish Desai, Raghu R. Krishnamoorthy, Santosh Narayan, Anne-Marie Brun, Angela M. Suburo, and Thomas Yorio. 2005. 'Effect of

elevated intraocular pressure on endothelin-1 in a rat model of glaucoma', *Pharmacological Research*, 51: 41-50.

42. Ripodas, Ainhoa, Jose Juan, Manuela Roldán-Pallarés, M. Rosa Bernal-Lopez, José Moya, Montserrat Chao, Araceli López, Arturo Fernández-Cruz, and Raquel Fernández-Durango. 2001. 'Localisation of endothelin-1 mRNA expression and immunoreactivity in the retina and optic nerve from human and porcine eye. Evidence for endothelin-1 expression in astrocytes', *Brain Research*, 912: 137-43.

43. Rubanyi, G. M., and M. A. Polokoff. 1994. 'Endothelins: molecular biology, biochemistry, pharmacology, physiology, and pathophysiology', *Pharmacol Rev*, 46: 325-415.

44. Saccà, S. C., and A. Izzotti. 2008. 'Oxidative stress and glaucoma: injury in the anterior segment of the eye', *Progress in brain research*, 173: 385-407.

45. Sandoval, Yessica-Haydee Gomez, Mohammed Emehdi Atef, Louis-Olivier Levesque, Yuan Li, and Madhu B. Anand-Srivastava. 2014. 'Endothelin-1 signaling in vascular physiology and pathophysiology', *Current vascular pharmacology*, 12: 202-14.

46. Schneider, Markus P., Erika I. Boesen, and David M. Pollock. 2007. 'Contrasting actions of endothelin ET(A) and ET(B) receptors in cardiovascular disease', *Annual review of pharmacology and toxicology*, 47: 731-59.

47. Stitt, A. W., U. Chakravarthy, T. A. Gardiner, and D. B. Archer. 1996. 'Endothelin-like immunoreactivity and receptor binding in the choroid and retina', *Current Eye Research*, 15: 111-17.

48. Sugden, P. H. 2003. 'An overview of endothelin signaling in the cardiac myocyte', *J Mol Cell Cardiol*, 35: 871-86.

49. Tamm, E. R. 2002. 'Myocilin and glaucoma: facts and ideas', *Prog Retin Eye Res*, 21: 395-428.

50. Tang, Binghua, Shengjie Li, Wenjun Cao, and Xinghuai Sun. 2019. 'The Association of Oxidative Stress Status with Open-Angle Glaucoma and Exfoliation Glaucoma: A Systematic Review and Meta-Analysis', *Journal of Ophthalmology*, 2019: 1803619.

51. Tawara, Akihiko, Norihiko Tou, Toshiaki Kubota, Yukinori Harada, and Kiyomi Yokota. 2008. 'Immunohistochemical evaluation of the extracellular matrix in trabecular meshwork in steroid-induced glaucoma', *Graefe's Archive for Clinical and Experimental Ophthalmology*, 246: 1021-28.

52. Tezel, G., and M. B. Wax. 2004. 'Hypoxia-inducible factor 1alpha in the glaucomatous retina and optic nerve head', *Arch Ophthalmol*, 122: 1348-56.

53. Thanos, S., and R. Naskar. 2004. 'Correlation between retinal ganglion cell death and chronically developing inherited glaucoma in a new rat mutant', *Exp Eye Res*, 79: 119-29.

54. Tovar-Vidales, T., R. Roque, A. F. Clark, and R. J. Wordinger. 2008. 'Tissue transglutaminase expression and activity in normal and glaucomatous human trabecular meshwork cells and tissues', *Invest Ophthalmol Vis Sci*, 49: 622-8.

55. Tripathi, B. J., M. Hansen, J. Li, and R. C. Tripathi. 1994. 'Identification of type VI collagen in the trabecular meshwork and expression of its mRNA by trabecular cells', *Exp Eye Res*, 58: 181-7.

56. Ung, L., U. Pattamatta, N. Carnt, J. L. Wilkinson-Berka, G. Liew, and A. J. R. White. 2017. 'Oxidative stress and reactive oxygen species: a review of their role in ocular disease', *Clin Sci (Lond)*, 131: 2865-83.

57. Von Zee, C. L., K. A. Langert, and E. B. Stubbs, Jr. 2012. 'Transforming growth factor-beta2 induces synthesis and secretion of endothelin-1 in human trabecular meshwork cells', *Invest Ophthalmol Vis Sci*, 53: 5279-86.

58. Werner, A. C., and L. Q. Shen. 2019. 'A Review of OCT Angiography in Glaucoma', *Semin Ophthalmol*, 34: 279-86.

59. Yanagisawa, M., A. Inoue, T. Ishikawa, Y. Kasuya, S. Kimura, S. Kumagaye, K. Nakajima, T. X. Watanabe, S. Sakakibara, K. Goto, and et al. 1988. 'Primary structure, synthesis, and biological activity of rat endothelin, an endothelium-derived vasoconstrictor peptide', *Proc Natl Acad Sci U S A*, 85: 6964-7.

60. Yanagisawa, M., H. Kurihara, S. Kimura, Y. Tomobe, M. Kobayashi, Y. Mitsui, Y. Yazaki, K. Goto, and T. Masaki. 1988. 'A novel potent vasoconstrictor peptide produced by vascular endothelial cells', *Nature*, 332: 411-5.

61. Yorio, Thomas, Raghu Krishnamoorthy, and Ganesh Prasanna. 2002. 'Endothelin: Is It a Contributor to Glaucoma Pathophysiology?', *Journal of Glaucoma*, 11: 259-70.

62. Zhang, X., A. F. Clark, and T. Yorio. 2005. 'Regulation of glucocorticoid responsiveness in glaucomatous trabecular meshwork cells by glucocorticoid receptor-beta', *Invest Ophthalmol Vis Sci*, 46: 4607-16.

63. Zhao, J., S. Wang, W. Zhong, B. Yang, L. Sun, and Y. Zheng. 2016. 'Oxidative stress in the trabecular meshwork (Review)', *Int J Mol Med*, 38: 995-1002.

64. Zode, G. S., M. H. Kuehn, D. Y. Nishimura, C. C. Searby, K. Mohan, S. D. Grozdanic, K. Bugge, M. G. Anderson, A. F. Clark, E. M. Stone, and V. C. Sheffield. 2011. 'Reduction of ER stress via a chemical chaperone prevents disease phenotypes in a mouse model of primary open angle glaucoma', *J Clin Invest*, 121: 3542-53.

65. Zode GS, Sharma AB, Lin X, Searby CC, Bugge K, Kim GH, Clark AF, Sheffield VC. (2014) Ocular-specific ER stress reduction rescues glaucoma in murine glucocorticoid-induced glaucoma. J Clin Invest. 2014 May;124(5):1956-65. Epub 2014 Apr 1. PubMed PMID: 24691439; PubMed Central PMCID: PMC4001532.

CHAPTER II

Endothelin-1 Mediated Decrease in Mitochondrial Gene Expression and Bioenergetics Contribute to Neurodegeneration of Retinal Ganglion Cells.

Renuka M. Chaphalkar[1], Dorota L. Stankowska[1], Shaoqing He[1], Bindu Kodati[1], Nicole Phillips[2], Jude Prah[3], Shaohua Yang[1] and Raghu R. Krishnamoorthy[1*]

Scientific Reports February 2020

North Texas Eye Research Institute, [1]Department of Pharmacology and Neuroscience, UNT Health Science Center, Fort Worth, Texas 76107, United States. [2]Department of Microbiology, Immunology and Genetics, UNT Health Science Center, Fort Worth, Texas 76107, United States. [3] Department of Basic and Translational Sciences, School of Dental Medicine, University of Pennsylvania, Philadelphia, PA 19104, United States. Correspondence and requests for materials should be addressed to R.R.K. (email: raghu.krishnamoorthy@unthsc.edu)

Abstract

Endothelin-1 (ET-1) is a vasoactive peptide that is elevated in aqueous humor as well as circulation of primary open angle glaucoma (POAG) patients. ET-1 has been shown to promote degeneration of optic nerve axons and apoptosis of retinal ganglion cells (RGCs), however, the precise mechanisms are still largely unknown. In this study, RNA-seq analysis was used to assess changes in ET-1 mediated gene expression in primary RGCs, which revealed that 23 out of 156 differentially expressed genes (DEGs) had known or predicted mitochondrial function, of which

oxidative phosphorylation emerged as the top-most enriched pathway. ET-1 treatment significantly decreased protein expression of key mitochondrial genes including cytochrome C oxidase copper chaperone (COX17) and ATP Synthase, H^+ transporting, Mitochondrial Fo Complex (ATP5H) in primary RGCs and in vivo following intravitreal ET-1 injection in rats. A Seahorse ATP rate assay revealed a significant decrease in the rate of mitochondrial ATP production following ET-1 treatment. IOP elevation in Brown Norway rats showed a trend towards decreased expression of ATP5H. Our results demonstrate that ET-1 produced a decrease in expression of vital components of mitochondrial electron transport chain, which compromise bioenergetics and suggest a mechanism by which ET-1 promotes neurodegeneration of RGCs in glaucoma.

Introduction

Glaucoma is an optic neuropathy with an approximate prevalence of 60.5 million people worldwide and is projected to reach 111 million by 2040 (Quigley and Broman 2006; Tham et al. 2014). The disease is commonly associated with elevated intraocular pressure (IOP), accompanied by optic nerve degeneration and loss of retinal ganglion cells (RGCs)(Quigley 1999, 2019). RGC death via apoptosis is a culminating event in the pathophysiology of glaucoma, stemming from optic nerve axonal injury, leading to visual field loss. Elevated IOP is a major risk factor in primary open-angle-glaucoma and current therapeutic approaches are aimed at lowering IOP with medications, laser treatment, or surgery ('The Advanced Glaucoma Intervention Study (AGIS): 7. The relationship between control of intraocular pressure and visual field deterioration.The AGIS Investigators' 2000; Vass et al. 2007). However, in some patients, the progression of the disease continues to occur slowly (Leske et al. 2003) despite lowering IOP, hence there is a compelling

need for neuroprotection of RGCs and optic nerve axons and as an additional therapeutic modality. The molecular changes occurring specifically in the RGCs, during the progression of glaucoma, contributing to neurodegeneration, are still poorly understood; hence identifying new therapeutic targets could provide more efficacious neuroprotective treatments.

ET-1 is a 21 amino acid vasoactive peptide that acts through two G-protein coupled receptors namely, ET_A and ET_B receptors, to produce diverse effects in various ocular tissues (Prasanna et al. 2002; Stokely, Brady, and Yorio 2002; Narayan et al. 2003; Krishnamoorthy et al. 2008). A growing body of evidence suggests that endothelins and their receptors are major contributors to neuronal damage in glaucoma (Yorio, Krishnamoorthy, and Prasanna 2002; Krishnamoorthy et al. 2008; Howell et al. 2011; Howell et al. 2014; McGrady et al. 2017; Minton et al. 2012). The role of endothelins in glaucomatous neurodegeneration has been the subject of several review articles (Yorio, Krishnamoorthy, and Prasanna 2002; Chauhan 2008; Rosenthal and Fromm 2011). However, the detailed cellular and molecular mechanisms that contribute to ET-1 mediated-neurodegeneration are not completely understood. ET-1 concentrations were also found to be increased in several animal models of glaucoma (Kallberg et al. 2002; Prasanna et al. 2005; Thanos and Naskar 2004). Both intravitreal and peribulbar administration of ET-1 has been shown to produce axon loss, RGC loss and disruption of nerve fiber layer (Chauhan et al. 2004; Lau, Dang, et al. 2006; Krishnamoorthy et al. 2008).

Several studies point to the role of mitochondrial dysfunction and oxidative stress as contributors to glaucomatous damage in animal models of glaucoma (Cuenca et al. 2014; Pinazo-Duran et al. 2013; Tezel 2008; Zanon-Moreno et al. 2009). There is an abundance of mitochondria in retinal ganglion cells (RGCs) within the soma region and the initial unmyelinated axons

(anterior to the lamina cribrosa) of the optic nerve and synaptic terminals as opposed to the post-laminar and myelinated region. Hence, RGCs are typically more sensitive to mitochondrial dysfunction than other neuronal populations (Carelli, Ross-Cisneros, and Sadun 2004). Retrograde and anterograde transport of mitochondria which occurs continuously along the axons of neurons, is vital for synaptic function. Hence, any disturbance of axonal transport due to mitochondrial abnormalities and a compromise in the mitochondrial function can lead to severe metabolic crises because of energy depletion (Osborne 2010). The impairment in axonal transport can be observed commonly in diseases such as Amyotrophic Lateral Sclerosis and Leber's Hereditary Optic Neuropathy (Osborne and del Olmo-Aguado 2013). Mitochondrial function decreases with age and as RGCs are largely dependent on their mitochondria, the prevalence of primary open angle glaucoma (POAG) increases with age possibly due to a decline in mitochondrial function (Kong et al. 2009). Impaired mitochondrial dysfunction is a phenomenon observed in most, if not all, neurodegenerative disorders (Yu-Wai-Man 2012; Ji et al. 2019; Boyman, Karbowski, and Lederer 2019; Williams, Harder, and John 2017). ET-1 elevates reactive oxygen species by acting through the ET_B receptor, which could be one mechanism by which ET-1 alters mitochondrial function (Lau, Galligan, et al. 2006).

The effect of ET-1 on mitochondrial gene expression and function and their potential impact on neurodegeneration of RGCs has not been adequately explored. The purpose of this study was to use RNA-seq to investigate ET-1 mediated changes in gene expression of mitochondrial genes and proteins in primary RGCs treated with ET-1, as well as in vivo following either ET-1 administration or IOP elevation in rat eyes.

Methods

Isolation of primary retinal ganglion cells

Primary rat RGCs isolation was performed according to the method of Barres et al (Barres et al. 1988). All protocols and procedures were in accordance with the policies of the Association for Research in Vision and Ophthalmology (ARVO) for use of animals in research and approved by the Institutional Animal Care and Use Committee (IACUC) (animal protocol #IACUC-2017-0024) at University of North Texas Health Science Center at Fort Worth, TX, USA. Post-natal day 4-7 rat pups were euthanized, and the isolated retinas were treated with 4.5 units/ml of papain solution to dissociate the cells. The cell suspension was subsequently incubated for 10 minutes with a rabbit anti-macrophage antibody and transferred to a petri dish coated with a goat anti-rabbit IgG (H+L chain) antibody for 35 minutes. Cells that were not attached to the coated anti-rabbit IgG were transferred to a petri-dish coated with anti-Thy1.1 antibody for 1 hour with intermittent shaking. Cells were then detached by trypsin treatment and collected by centrifugation. Cells were seeded either directly in a 6-well plate or on coverslips coated with poly-D lysine and mouse-laminin and cultured in serum-free Dulbecco's modified Eagle's medium containing brain-derived neurotrophic factor (BDNF) (50 ng/ml; Peprotech, Rocky Hill, NJ, USA), ciliary neurotrophic factor (10 ng/ml; Peprotech), and forskolin (5 ng/ml; Sigma-Aldrich Corp.). Cells were incubated at 37°C in a humidified atmosphere of 10% CO_2 and 90% air. One-third volume of the culture medium was changed every two days. The purity of the culture was determined by counting RBPMS and Brn3a positive cells per 100 cells from different regions in an image. The purity of the culture obtained is routinely between 90%-95% in most batches of isolated RGCs.

ET-1 treatment

ET-1 peptide was purchased from Bachem (Torrance, CA) and dissolved to a stock concentration of 500 μM and working stocks of 100 μM. The seeding density of the primary RGCs was approximately 350,000 / well in a 6-well plate. After 1 week in culture to promote neurite outgrowth, the isolated RGCs were treated with 100 nM ET-1 (final concentration) for 24 hours while untreated RGCs served as a control.

Polysomal RNA isolation

Following ET-1 treatment, a brief incubation with cycloheximide (10 μg/ml) to inhibit protein synthesis was done, total polysomes were isolated by magnesium precipitation by a modification of the method of Palmiter et al (Palmiter 1974). Cells were washed, scraped in PBS and the cell pellet was suspended in 150 μl of homogenization buffer (25 mM Tris-HCl pH 7.5, 25 mM NaCl, 5 mM $MgCl_2$, and 1% Triton X-100). After an incubation on ice for 5 min, the homogenate was centrifuged at 10,000xg in a microfuge for 10 min at 4^{o}C to sediment the nuclei and mitochondria. The pellet was discarded and the supernatant was treated with an equal volume of polysome precipitation buffer (25 mM Tris-HCl pH 7.5, 25 mM NaCl, 250 mM $MgCl_2$ and 1 M sucrose). The content of the tubes was mixed by inverting and incubated on ice for one hour with intermittent mixing. The polysomal fraction was obtained by centrifugation at 40,000×g for 1 hr in a Beckman ultracentrifuge at 4^{o}C using the TLA-55 fixed angle rotor. The supernatant was discarded and the polysomal pellet was extracted using the Trizol reagent to isolate polysomal RNA according to the manufacturer's instructions.

Library preparation and RNA-seq analysis

Libraries for RNA-Seq were prepared in the UCLA core facility with Clonetech SMARTer Stranded Total RNA-Seq (Pico) Kit. The workflow consisted of first-strand synthesis, template switching, adaptor ligation, cleavage of ribosomal cDNA and PCR amplification. Different adaptors were used for multiplexing samples in one lane. Sequencing was performed on Illumina Hiseq3000 for a single read 50bp run. Data quality check was done on Illumina SAV. The reads were first mapped to the latest UCSC transcript set using Bowtie2 version 2.1.0 (Langmead and Salzberg 2012) and the gene expression level was estimated using RSEM v1.2.15 (Li and Dewey 2011). TMM (trimmed mean of M-values) was used to normalize the gene expression. Differentially expressed genes were identified using the edgeR program (Robinson, McCarthy, and Smyth 2010). Genes showing altered expression with $p<0.05$ and more than 1.5 fold changes were considered differentially expressed, since a fold increase of less than 1.5-fold would typically not produce appreciable phenotypic changes. Differentially expressed genes (DEGs) based on grouped comparison of untreated and treated cells were analyzed for biological and functional relevance using the *Rattus norvegicus* knowledgebase in PANTHER v.13.1; GO classifications based on cellular component, molecular function, biological process, and reactome pathways were analyzed. MitoMiner v.4.0 was used to identify the DEG subset that has a known or predicted mitochondrial function. A STRING network was constructed using the 156 genes to identify known and potential protein-protein interactions within the set of differentially expressed genes (DEGs). DEGs were ranked using the sign (fold change)*(1/p-value) method to identify genes that are both highly dysregulated (up/down fold change magnitude) and with a low probability of false discovery (low p-value).

Quantitative Real-Time PCR

Primary RGCs were isolated from post-natal day 4-6 rat pups (as described above) and total cellular RNA was extracted using the Trizol reagent (as described above). Complementary DNA was prepared from total cellular RNA using iScript Reverse Transcription Kit (BioRad, Hercules, CA), and Real-time PCR (SsoAdvanced™ SYBR® Green Supermix) was performed using cDNA as template to detect gene expression of some DEGs including Mitochondrial Ribosomal Protein L30 (Mrpl30), ATP Synthase, H^+ Transporting, Mitochondrial F0 Complex, Subunit D (Atp5h), cytochrome C oxidase copper chaperone (Cox17), Glucose-6-phosphate dehydrogenase (G6pd), Forkhead box protein (Foxo1), Mitogen-Activated Protein Kinase Kinase Kinase 11 (Map3k11) and Modulator Of Apoptosis 1 (Moap1). PCR conditions were as follows: 95°C for 3 minutes followed by 40 three-step cycles of 95°C for 10 seconds, 60°C for 30 seconds and 72°C for 30 seconds. PCR primers were validated and the authenticity of the amplicons were confirmed by their melting temperatures. RNA samples from 3-4 biological replicates were used for real-time PCR analysis. Data was expressed as mean ± SEM and normalized to cyclophilin-1. The results were presented as relative fold change compared to untreated control. The statistical significance was calculated by Student's *t*-test, and *p* values <0.05 were considered significant.

Immunocytochemistry

Purified RGCs were cultured for 7 days to promote neurite outgrowth. RGCs were then treated with 100 nM ET-1 for 24 h and fixed with 4% paraformaldehyde for 10 min. After permeabilization with 0.1% Triton X-100, the cells were blocked with 5% bovine serum albumin and 5% normal donkey serum at room temperature for 1 hour to prevent non-specific binding with the secondary antibody. Blocking was followed by overnight incubation at 4°C with primary antibodies against mitochondrial proteins ATP5H and Cox17. Primary antibodies used were rabbit

anti-COX 17 (1:100, #ab69611, Abcam), mouse anti-ATP5H (1:200, #ab110275, Abcam) and goat anti-Brn3a (1:200, #sc31984, Santa Cruz Biotechnology). Following primary antibody incubations, cells were washed with PBS and then incubated with the corresponding secondary antibody at room temperature (RT) in the dark. Secondary antibodies used were donkey anti-rabbit Alexa 647 (1:1000, Invitrogen), donkey anti-mouse Alexa 546 (1:1000, Invitrogen) and donkey anti-goat 488 (1:1000, Invitrogen). Immunostaining carried out with the exclusion of the primary antibody and using only the secondary antibody conjugated to the fluorophore served as the negative control, which was indicative of non-specific staining by the secondary antibody. Following the secondary antibody incubation, cells were washed with PBS and incubated with with 4′ 6 Diamidino-phenylindole dichloride (DAPI) to stain cell nuclei. The coverslips were mounted on slides with antifade medium (FluorSave; Calbiochem, La Jolla, CA, USA). Images were captured for each field of view using the Zeiss 510 meta confocal microscope.

Intravitreal injection of ET-1

ET-1 peptide was purchased from Bachem (Torrance, CA) and dissolved to a stock concentration of 500 μM. One group of male Brown Norway rats (n=6) were intravitreally injected in one eye with 4 μl of 500 μM ET-1 in 0.25% glacial acetic acid (adjusted to pH 7.0) while the contralateral eye served as control. The other group (n=6) received vehicle (0.25% glacial acetic acid, neutralized to pH 7.0) intravitreally in one eye, while the contralateral eye was control. Rats were euthanized 24 hours after injection by intraperitoneal pentobarbital injection (120 mg/kg body wt) followed with intracardiac pentobartital injection.

Morrison model of IOP elevation in rats

IOP elevation was carried out in one eye of four retired breeder female Brown Norway rats by injection of 100 µl of hypertonic saline through episcleral veins (Morrison et al. 1997). Briefly, rats were anesthetized by inhalation of isoflurane and ensured by lack of a toe pinch reflex. Following a conjunctival incision, hypertonic saline (1.8M NaCl) was injected into an episcleral vein using a glass needle (TIP01TW1F, WPI). The companion eye was used as the contralateral control eye. A flow rate of 309µL/min was maintained during the injection for 10 to 20 seconds, thereby injecting 50 to 100 µl of hypertonic saline into the episcleral veins. IOP was measured two times a week using a hand-held TonoLab tonometer (iCare, Finland). Six IOP readings were averaged from each IOP measurement and ten IOP measurements were obtained for each eye. IOP plots were generated from IOP values obtained from the surgically treated eye and contralateral control eye. The IOP exposure in each rat was computed by the integral product of the extent of IOP elevation and the number of days of IOP elevation (expressed as mm Hg-days).

Immunohistochemistry

Eyes were enucleated and a small incision (4 mm) was made posterior to the limbus and the eye was fixed in 4% paraformaldehyde (PFA) in phosphate buffered saline (PBS) for 30 min. Subsequently, an incision was made along the entire circumference of the limbus to remove the entire anterior segment. The optic cups were fixed in 4% PFA for an additional 3 hours. After fixation, the tissue was rinsed with 70% ethanol and later embedded in paraffin. Seven-micron sagittal retinal sections through the optic nerve head were obtained, de-paraffinized in xylene, and rehydrated with a graded series of ethanol. Following permeabilization with 0.1% Triton X-100 and blocking with 5% normal donkey serum containing 5% BSA in PBS, retinal sections were incubated with the appropriate primary antibodies overnight. Primary antibodies used were rabbit

anti-Cox 17 (1:100, #ab69611, Abcam), mouse anti-ATP5H (1:200, #ab110275, Abcam), goat anti-Brn3a (1:200, #sc31984, Santa Cruz Biotechnology) and mouse anti-β-III-Tubulin (1:500, Sigma). Secondary antibody incubation for 1 hr was carried out at room temperature. Secondary antibodies used were either donkey anti-rabbit Alexa 546 (1:1000, Invitrogen), donkey anti-mouse Alexa 647 (1:1000, Invitrogen) or donkey anti-goat 488 (1:1000, Invitrogen). Retinal sections incubated with no primary antibody served as the blank to assess non-specific staining by the secondary antibodies.

Seahorse XF Real-Time ATP rate assay

Agilent Seahorse XFe96 analyzer was used to measure multiple parameters including oxygen consumption rate (OCR), total ATP production by quantifying ATP production rate from both glycolytic and mitochondrial pathways and ATP rate index. Briefly, primary RGCs were isolated from post-natal day 4-6 rat pups. The RGCs were seeded in RGC medium in a poly-D-lysine coated seahorse plate and maintained in culture for one week to allow neurite outgrowth. The RGCs were either untreated or treated with ET-1 for 4h or 24 h in trophic factor-free medium. A day prior to the experiment seahorse sensor cartridge was hydrated with water and incubated in a non CO_2 incubator at 37°C. Two hours before the experiment, the water was replaced with a seahorse calibrant. On the day of the experiment, seahorse XF DMEM (pH=7.4) was supplemented with 1 mM pyruvate, 2 mM glutamine and 10 mM glucose (Agilent, USA). The RGC medium was then replaced with 180 µl of Seahorse XF base medium and the cells incubated in a non CO_2 incubator at 37°C for 1 hour. During this incubation period, oligomycin and Rotenone/antimycin (Agilent, USA) were prepared in the seahorse medium to achieve final concentrations of 1.5 µM and 0.5 µM respectively when injected. From these stock solutions, 20µl and 22µl of Oligomycin

and rotenone/antimycin respectively were then loaded into the drug delivery ports A and B of the hydrated sensor cartridge and loaded into the seahorse XF analyzer to calibrate for 30 minutes. The calibration plate was replaced with the cell culture plate and oxygen consumption (OCR) and extracellular acidification rate (ECAR) was monitored following the sequential injection of Oligomycin and rotenone/antimycin with each cycle set as 3 min mix, 2 min delay and measure for 3 minutes. According to the manufacturer's instructions (Agilent Technologies, Santa Clara, CA), the following equation was used to calculated mitochondrial ATP production:

OCR_{ATP} (pmol O_2/min) = $OCR_{Untreated}$ (pmol O_2/min) - $OCR_{Oligomycin}$ (pmol O_2/min).

The ATP production rate in ET-1 treated RGCs was compared to that of untreated RGCs for two time points of ET-1 treatment (4h and 24h). Data was normalized to the cell number of each well by Calcien AM assay.

Statistical Analysis

GraphPad Prism 7 (La Jolla, CA, USA) was used to perform statistical analysis. Student's t-test was used while comparing two experimental groups (control versus treated). Statistical significance of the experimental data was described as $*p < 0.05$; $**p < 0.01$. Data are presented as mean ±SEM.

Results

Characterization, Purity and Yield of Isolated Primary RGCs

By sequential double immunopanning with the Thy1.1 antibody, we isolated approximately 20,000 to 40,000 RGCs per retina, with a yield of 40% to 50% of the RGCs in post-natal day 4-7 (P4-P7) rat retinas [35]. To confirm the purity of the RGCs, immunostaining using RGC specific markers,

including, RBPMS (**Figure 1a**) and Brn3a (**Figure 1b**) was carried out and GFAP, an astrocyte marker was used as a negative control (**Figure 1c)**. It was found that approximately 90 to 95% of the cells were immunopositive for RBPMS and Brn3a and hence were characterized as RGCs, whereas 2% of the cells were immunoreactive for GFAP. Thus, the immunopanning technique yielded a highly enriched RGC culture.

Translatome analysis of primary RGCs following ET-1 treatment (100nM)

Primary cultures of RGCs were isolated and treated with ET-1 for 24 h, following which polysomal RNA was isolated. RNA-seq analysis of polysomal RNA from untreated (control) and ET-1-treated RGCs was performed and bioinformatics analysis was carried out**.** From the STRING network analysis (**Figure 2**), several mitochondrially-relevant genes which had a significant change in expression were identified. Gene Ontology (GO) classification with statistical overrepresentation tests indicate a significant enrichment in the differentially expressed genes (DEG) set for cellular components, including mitochondrion, endocytic vesicle membrane and cytoplasmic stress granules. The DEG set was also enriched for specific biological processes, including cation transport and metabolic processes. Twenty-three genes out of the 156 DEGs were identified to have a known or predicted mitochondrial function. Of the 23 genes, 14 of which are represented in the STRING network (indicated by the mitochondrial symbol on the node) are defined by some connected nodes. Four of the connected, mitochondrially-related genes were in the top 20 up-regulated and down-regulated genes in the list of 156 DEGs.

From the STRING network, mitochondrially-relevant genes were identified within the network and the direction of fold regulation was overlaid using red (up-regulated) and green (down-regulated) borders. It was found that 156 genes were differentially expressed following ET-

1 treatment in RGCs. The thickness of the color indicator denotes the ranking of the gene: thick indicators are ranked in the top or bottom 20 of the ranked DEG list; medium borders are in the top / bottom 20 genes based only on magnitude of fold change; thin lines just indicate direction of fold change. Analysis of differential gene expression revealed a significant change in expression of several genes involved in mitochondrial function, oxidative metabolism and cell survival pathways. An increase in an expression of mitochondrial proteins cytochrome c oxidase copper chaperone (COX17) (3- fold), and ATP synthase, H^+ transporting mitochondrial F0 complex (ATP5H) (3-fold) was found. On the other hand, a decrease in expression of glucose-6-phosphate dehydrogenase (5-fold), Forkhead box O1 (FOXO1) (986-fold), mitogen- activated protein kinase kinase kinase 11(Map3k11) (40-fold) and modulator of apoptosis (Moap1) (6255-fold) was observed.

Translatome changes in primary RGCs following ET-1 treatment

To explore the translatome differences in primary retinal RGCs between the control and ET-1 treated samples, a heatmap was generated showing log2 (fold-change) > 1.5. Hierarchical clustering was performed using the 156 DEGs to determine whether these gene expression profiles were different between the two groups, we analyzed RNA-seq data by Pearson correlation coefficient (**Figure 3a**). The results showed that the replicates cluster together based on similarities in gene expression, although there was some variability observed in the top genes between the replicates. Further, two clear sets of genes with increased expression as well as genes with decreased expression following ET-1 treatment emerged. In addition, principal component analysis (PCA) of the normalized gene expression values for the top 156 DEGs showed that axes 1 and 2 accounted for 76.3% and 19.4% of the total variation, respectively (**Figure 3b**). PC1

distinguishes the controls from the ET-1 treated replicates by the origin of the X-axis. Ingenuity Pathway Analysis (IPA) canonical pathway analysis of the gene set revealed that oxidative phosphorylation pathway is the top-most enriched pathway within the DEGs following ET-1 treatment (**Figure 3c**).

Validation of DEGs with qPCR

To validate RNA-seq findings, qPCR analysis was performed on several selected genes associated with either mitochondrial function, neurodegeneration or cell survival. A significant decrease in gene expression of Atp5h (30 %) and Moap-1 (17 %) was observed following treatment of primary RGCs with ET-1 (**Figure 4**). On the other hand, an increasing trend in the expression of FOXO1(31%) and Map3K11(179%) genes and a decreasing trend in the expression of Cox17 (17 %) and G6PD (15 %) genes were observed in ET-1 treated RGCs (**Figure 4**). However, these were not statistically significant. The expression pattern observed by conventional qPCR was different in comparison to the RNA-seq data for some DEGs including Atp5h, Cox17 FoxO1, and Map3k11. There was no appreciable change in the expression of mitochondrial ribosomal protein L30 (Mrpl30) gene following ET-1 treatment when analysed by qPCR **(Figure 4).**

ET-1 treatment causes a decline in key mitochondrial proteins COX17 and ATP5H in primary RGCs

Mitochondrial dysfunction and oxidative damage are associated with many neurodegenerative disorders including glaucoma. Hence, we focused our attention on the expression of some mitochondrial genes that are important components of the mitochondrial

oxidative phosphorylation pathway. To observe changes at the protein level, immunostaining for ATP5H and COX17 was carried out (**Figure 5a and 5b**). Staining for both ATP5H and COX17 was observed both in the soma and axonal processes of RGCs.

Immunocytochemical analysis revealed that ET-1 treatment produced a decrease in immunostaining of key mitochondrial proteins ATP5H and COX17, indicating that ET-1 has the potential to compromise the bioenergetics of RGCs. Quantitation of the immunofluorescence of both ATP5H and COX17 revealed a decrease in integrated density/100 Brn3a positive cells following ET-1 treatment. (**Figure 5c and Figure 5d**) However, immunostaining of only COX17 showed a significant ($p<0.05$) decrease in integrated density/100 Brn3a positive cells.

A significant decrease in mitochondrial rate of ATP production was observed following ET-1 treatment in primary RGCs

Since a decrease in immunostaining for ATP5H and COX17 was found in RGCs treated with ET-1, a Seahorse XF ATP rate assay was carried out to determine if a functional decline in mitochondrial ATP production was observed. As seen in **Figure 6a**, the OCR differed at the 4h and 24h timepoints of ET-1 treatment. At the 4-hour time point, RGCs had a higher basal level of OCR (35 pmol/min), compared to the 24 hour time point (20 pmol/min). At both 4h and 24 h time points of ET-1 treatment, the OCR was reduced, compared to the corresponding untreated controls. ET-1 treatment produced a significant decrease in the rate of mitochondrial ATP production at both 4h and 24h time points following treatment with 100 nM ET-1 (**Figure 6b**). The glycolytic ATP production rate showed a significant decrease following 4 h and a decreasing trend at 24 h following ET-1 treatment in RGCs. When the ratio of the mitochondrial to glycolytic ATP

production was calculated, a significant decrease of the ratio was found at both 4h and 24h time points of ET-1 treatment (**Figure 6c**).

Decrease in expression of mitochondrial proteins COX17 and ATP5H following intravitreal administration of ET-1

To determine if ET-1-mediated changes in ATP5H and COX17 were also observed *in vivo*, intravitreal injection of ET-1 was carried out in one eye of Brown Norway rats. The contralateral eye was injected with the vehicle used to dissolve ET-1. Rat retina section from vehicle-injected rat eyes showed immunoreactivity for ATP5H and COX17, which was assessed in multiple retinal layers including the nerve fiber layer (NFL), ganglion cell layer (GCL) and inner plexiform layer (IPL).

In the vehicle treated eyes, robust immunostaining for ATP5H was detected in the retinal ganglion cells, inner plexiform layer and outer plexiform layer (**Figure 7a**). On the other hand, immunostaining for COX17 was found predominantly in the nerve fiber layer, retinal ganglion cells and inner plexiform layer in vehicle treated rat eyes (**Figure 7a**). A semi-quantitative analysis measuring the change in integrated intensity was also performed using ImageJ software. Projections from confocal image z-stacks were analyzed for integrated density of ATP5H and COX17 expression in ET-1 treated and vehicle-treated eyes to determine fold change in expression. Compared to the vehicle-treated controls, retinas obtained from ET-1 treated eyes showed a statistically significant decrease in ATP5H expression mainly in the GCL (RFI= 0.4818 ± 0.1328, n=6, $p<0.01$) and IPL (RFI = 0.5633 ± 0.1333, n=6, $p<0.01$) (**Figure 7b**). Expression of ATP5H was co-localized with Brn3a (a RGC specific marker) in RGCs (**Figure 7b**). Additionally,

a modest decrease in immunostaining for ATP5H was also observed in the NFL compared to the vehicle-control. (RFI =0.645 ± 0.1814, n=6).

Similar to the pattern of expression observed for ATP5H, ET-1 treatment (24h) showed decreased immunoreactivity for COX17 in NFL, GCL and IPL in rat retinas (**Figure 7c**). A semi-quantitative analysis performed indicated a statistically significant decrease in COX17 expression in the NFL (RFI = 0.4914 ± 0.1738, n=7, $p < 0.05$) and GCs (RFI = 0.6483 ± 0.1518, n=6, $p < 0.05$) (**Figure 7c**). A statistically significant difference was not found in the IPL (RFI = 0.6867 ± 0.1593, n=6), however, the same trend of decrease as observed in ATP5H expression was still present. Taken together, the data suggest that there was a downregulation in the expression of the key mitochondrial proteins ATP5H and COX17, 24 hours following ET-1 treatment.

IOP elevation produced a modest decrease in immunoreactive levels of ATP5H

Retina sections were obtained from four retired breeder Brown Norway rats, which were IOP elevated in one eye, using the other eye as the contralateral control (**Figure 8a**). Immunostaining was carried out using antibodies to ATP5H and COX17 and images were taken on a Zeiss LSM580 confocal microscope. A semi-quantitative analysis measuring the change in integrated intensity was also performed using ImageJ software. Projections from the confocal image z-stacks were analyzed for integrated density of ATP5H and COX17 immunostaining and compared between the IOP-elevated eyes and their corresponding contralateral eyes (**Figure 8b**). It was found that IOP elevation produced a decreasing trend in immunostaining for ATP5H, compared to that of the corresponding contralateral eyes (**Figure 8d**). There was no appreciable change in immunostaining for COX17 between IOP elevated eyes and contralateral eyes (**Figure 8c**).

Discussion

ET-1 is a potent vasoactive peptide that has been shown to be elevated in both the aqueous humor and circulation of primary open angle glaucoma patients (Iwabe et al. 2010; Choritz, Machert, and Thieme 2012; Cellini et al. 2012; Chen et al. 2013). An elevation of both ET-1 and homocysteine was found in the plasma of primary open angle glaucoma patients, compared to normal tension glaucoma as well as control subjects, suggesting that elevated oxidative stress and ET-1 are involved in the early stages of glaucoma pathology (Lopez-Riquelme et al. 2015). Single nucleotide polymorphisms (SNPs) in both the ET-1 and ET_A receptor genes that affected ET-1 plasma concentrations and higher ET-1 levels correlated with increased visual field damage (Kosior-Jarecka et al. 2016). A recent meta-analysis that included seven studies (212 cases, 164 controls) for normal tension glaucoma and six studies (160 cases, 174 controls) for the POAG analysis demonstrated increased circulating ET-1 levels in glaucoma patients, compared to control subjects (Li et al. 2016).

Several studies have pointed to ET-1's key role in neurodegeneration, however, the precise mechanisms by which ET-1 produces neurodegenerative effects is still an active area of investigation. Previous studies from our laboratory have shown that intravitreal ET-1 injection in rats decreased anterograde axonal transport of vesicles associated with the mitochondrial subcomponent (Stokely, Brady, and Yorio 2002). Axonal transport is an energy dependent process, mediated by motor proteins which use the energy of ATP hydrolysis to produce force and movement along the microtubules. The decrease in fast axonal transport could be due to a decline ATP production, disruption of the cytoskeleton or a combination of these factors. Most of the ATP needed for cellular metabolism/activities is generated by oxidative phosphorylation in the mitochondria. This raises the possibility that ET-1 could alter mitochondrial dynamics as well as

oxidative metabolism in the optic nerve head during glaucoma. It has been shown that ET_B receptor stimulation by administration of sarafotoxin (ET_B receptor agonist) in rats increases the production of superoxide anions, in sympathetic neurons (Lau, Galligan, et al. 2006). Increased oxidative stress by endothelin receptor stimulation could have damaging effects on the mitochondria, thereby providing a strong rationale to assess expression of mitochondrial genes and their contribution to neurodegeneration.

Dysregulation of gene expression contributes to neurodegeneration in glaucoma, by acting on several cellular pathways, ultimately enhancing pro-apoptotic effects while suppressing anti-apoptotic gene expression (Nickells et al. 2012; Nickells and Pelzel 2015). Numerous studies have been carried out using total cellular RNA from either the retina or cultured RGCs to evaluate changes in gene expression in various models of optic neuropathy (Ahmed et al. 2004; White et al. 2015). While an assessment of changes in gene expression at the mRNA level is informative, it does not provide an indication of the corresponding changes in the protein levels. In the polysomal profiles, there is a drastic shift of distribution of mRNA and its association with multiple ribosomes, following metabolic insults before it is detected on the proteome level (Panda, Martindale, and Gorospe 2017). Hence, assessment of polysomal RNA will provide a reflection of the translatome, offering a glimpse into *de novo* protein synthesis which is an important manifestation of changes in gene expression at the protein level.

In the current study, using RNA-seq we analyzed the changes in gene expression of polysomal RNA which represent the pool of actively translated mRNAs. This provides a unique opportunity to identify novel genes whose expression are altered at the protein level during pathogenesis. Identification of novel genes that contribute to glaucomatous neurodegeneration will provide the basic information needed to develop new therapies aimed at neuroprotection in

glaucoma. To our knowledge, this is the first study to use RNA-seq analysis to investigate the RGC translatome profile following ET-1 treatment. Although other researchers have conducted microarray analyses of gene expression under glaucomatous conditions, most of these studies focused on mRNA expression which may not be reflected at the level of the protein expression (He et al. 2015; Yang et al. 2007; Johnson et al. 2011).

The results of the RNA seq analysis were confirmed by qPCR analysis of some of the candidate genes. Some of the data derived from the qPCR data were different from that found in the RNA-seq analysis. For instance, while an increase in Atp5h and Cox17 was found in the RNA-seq analysis, a decrease in the expression of these genes were found by qPCR analysis. Some of these variations could be related to the template half-life of the individual transcripts. Less abundant transcripts in RNA samples with low concentrations could be rapidly degraded, particularly with longer handling times. The differences in the handling time between RNA-seq analysis and qPCR analysis could be one plausible reason for the discrepancies in the findings between RNA-seq and qPCR, as well as account for the big variations observed in RNA expression that contributed to the lack of statistical significance in many of the qPCR analyses. On the other hand, at the protein level, the data was very consistent and a decrease in levels of ATP5H was observed both in cultured RGCs treated with ET-1 and in retinas of rats intravitreally injected with ET-1.

A notable finding from the RNA-seq analysis was that 23 out of 156 DEG in the RNA-seq analysis were identified with known or predicted mitochondrial function. Ingenuity Pathway Analysis revealed oxidative phosphorylation as the top significantly enriched canonical pathway, which points to the involvement of mitochondrial bioenergetics in RGCs with ET-1 treatment. To specifically assess the nuclear encoded genes in the mitochondrial respiratory chain complex and

oxidative phosphorylation, the mRNA and protein expression of Cox17, and Atp5h which are critical components of Complex I and Complex V, respectively, were determined. COX17 is the terminal enzyme of the mitochondrial respiratory chain while mitochondrial ATP synthase catalyzes ATP synthesis, utilizing an electrochemical gradient of protons across the inner membrane during oxidative phosphorylation (Srinivasan and Avadhani 2012; Carelli, Ross-Cisneros, and Sadun 2004). IOP elevation has previously shown to cause a reduction of Cytochrome c oxidase IV subunit 1 activity by damaging the mitochondria in response to mitochondrial fission (Ju et al. 2008). There is a decline of mitochondrial function during early stages of POAG due to reduction in ATP synthesis, particularly making RGCs susceptible for oxidative phosphorylation impairment (Lee et al. 2012). Mitochondrial mutation and mitochondrial genetic variation can also act as a potential risk factor in POAG pathogenesis (Abu-Amero, Morales, and Bosley 2006; Collins et al. 2016). Interestingly, a recent study showing association of mitochondrial proteins with the pathogenesis of POAG identified a number of key genes including Atp5h, Cox17, Ndufs7, Ndufb9, Uqcrc1 and Ak3 involved in oxidative phosphorylation in human POAG that were identical to some of the genes observed in our findings (Khawaja et al. 2016). In the current study, we identified that there was a decline in two important mitochondrial proteins ATP5H and COX17 both in primary RGCs treated with ET-1 as well as in rats intravitreally injected with ET-1. In addition, a decreasing trend in immunostaining for ATP5H was found following IOP elevation in Brown Norway rats.

The IOP elevation model is a chronic model and the data presented is indicative of IOP-mediated changes that occur over longer period of time, compared to the acute effects that occur following a bolus intravitreal administration of 2 nmole of ET-1. Nevertheless, a trend towards a decrease in ATP5H was observed following IOP elevation for 2 weeks in Brown Norway rats.

This suggests that a decline in mitochondrial function could compromise bioenergetics mediated by a decline in ATP levels. The Seahorse assay which exploits the coupling of ATP synthesis to oxygen consumption that occurs during oxidative phosphorylation, provided a clear evidence for the ability of ET-1 to significantly decline mitochondrial ATP production in RGCs. The use of oligomycin to inhibit mitochondrial ATP synthase and assess the decline in the oxygen consumption rate, provides a glimpse of ATP-linked respiration, which differed significantly between the control and the ET-1 treated RGCs. The data points to the ability of ET-1 to functionally impact ATP synthesis in RGCs. The findings have important implications for RGC death occurring through energy depletion, which could occur through opening of permeability transition pore, leading to mitochondrial depolarization and mitochondrial damage. It is well known that reactive oxygen species are a major contributor to mitochondrial outer membrane permeabilization. As mentioned earlier, ET_B receptor activation has been shown to result in elevation of oxidative stress as reported in dorsal root ganglion neurons (Lau, Galligan, et al. 2006). It is plausible that similar mechanisms could operate to generate oxidative stress through the actions of ET-1 on its receptors in RGCs.

Taken together, our findings have important implications for the role of mitochondria in the pathogenesis of glaucoma. Further work is required to understand the role of the genes identified in the RNA-seq analysis and elucidate the signalling pathways which contribute to the expression of these genes. The current study could provide an insight to advance our understanding of mitochondrial dynamics contributing to RGC loss in POAG.

Author Contributions

RMC designed, performed experiments, analyzed data and wrote the manuscript. DLS and SH designed and performed experiments and interpreted data. BK performed some experiments. NP carried out bioinformatics analysis and interpretation of the data. SY and JP aided in the design, performance and interpretation of the Seahorse assay. RK was involved in conceptualization, data analysis and writing the manuscript.

Acknowledgements

This work was supported by an extramural grant (EY028179) to RRK from the National Eye Institute.

Additional Competing Interests

Competing Interests: The authors declare no competing interests.

References

1. Abu-Amero, Khaled K., Jose Morales, and Thomas M. Bosley. 2006. 'Mitochondrial Abnormalities in Patients with Primary Open-Angle Glaucoma', *Investigative Ophthalmology & Visual Science*, 47: 2533-41.
2. 'The Advanced Glaucoma Intervention Study (AGIS): 7. The relationship between control of intraocular pressure and visual field deterioration.The AGIS Investigators'. 2000. *Am J Ophthalmol*, 130: 429-40.
3. Ahmed, Farid, Kevin M. Brown, Dietrich A. Stephan, John C. Morrison, Elaine C. Johnson, and Stanislav I. Tomarev. 2004. 'Microarray Analysis of Changes in mRNA Levels in the

Rat Retina after Experimental Elevation of Intraocular Pressure', *Investigative Ophthalmology & Visual Science*, 45: 1247-58.

4. Barres, B. A., B. E. Silverstein, D. P. Corey, and L. L. Chun. 1988. 'Immunological, morphological, and electrophysiological variation among retinal ganglion cells purified by panning', *Neuron*, 1: 791-803.
5. Boyman, L., M. Karbowski, and W. J. Lederer. 2019. 'Regulation of Mitochondrial ATP Production: Ca(2+) Signaling and Quality Control', *Trends Mol Med*.
6. Carelli, V., F. N. Ross-Cisneros, and A. A. Sadun. 2004. 'Mitochondrial dysfunction as a cause of optic neuropathies', *Prog Retin Eye Res*, 23: 53-89.
7. Cellini, M., E. Strobbe, C. Gizzi, N. Balducci, P. G. Toschi, and E. C. Campos. 2012. 'Endothelin-1 plasma levels and vascular endothelial dysfunction in primary open angle glaucoma', *Life Sci*, 91: 699-702.
8. Chauhan, Balwantray C. 2008. 'Endothelin and its potential role in glaucoma', *Canadian Journal of Ophthalmology*, 43: 356-60.
9. Chauhan, Balwantray C., Terry L. LeVatte, Christine A. Jollimore, Paula K. Yu, Herbert A. Reitsamer, Melanie E. M. Kelly, Dao-Yi Yu, François Tremblay, and Michele L. Archibald. 2004. 'Model of Endothelin-1–Induced Chronic Optic Neuropathy in Rat', *Investigative Ophthalmology & Visual Science*, 45: 144-52.
10. Chen, H. Y., Y. C. Chang, W. C. Chen, and H. Y. Lane. 2013. 'Association between plasma endothelin-1 and severity of different types of glaucoma', *J Glaucoma*, 22: 117-22.
11. Choritz, Lars, Maren Machert, and Hagen Thieme. 2012. 'Correlation of Endothelin-1 Concentration in Aqueous Humor with Intraocular Pressure in Primary Open Angle and Pseudoexfoliation Glaucoma', *Investigative Ophthalmology & Visual Science*, 53: 7336-42.

12. Collins, D. W., H. V. Gudiseva, B. Trachtman, A. S. Bowman, A. Sagaser, P. Sankar, E. Miller-Ellis, A. Lehman, V. Addis, and J. M. O'Brien. 2016. 'Association of primary open-angle glaucoma with mitochondrial variants and haplogroups common in African Americans', *Mol Vis*, 22: 454-71.
13. Cuenca, N., L. Fernandez-Sanchez, L. Campello, V. Maneu, P. De la Villa, P. Lax, and I. Pinilla. 2014. 'Cellular responses following retinal injuries and therapeutic approaches for neurodegenerative diseases', *Prog Retin Eye Res*, 43: 17-75.
14. He, Shaoqing, Yong H. Park, Thomas Yorio, and Raghu R. Krishnamoorthy. 2015. 'Endothelin-Mediated Changes in Gene Expression in Isolated Purified Rat Retinal Ganglion CellsEndothelin-Mediated Changes in Gene Expression', *Investigative Ophthalmology & Visual Science*, 56: 6144-61.
15. Howell, G. R., D. G. Macalinao, G. L. Sousa, M. Walden, I. Soto, S. C. Kneeland, J. M. Barbay, B. L. King, J. K. Marchant, M. Hibbs, B. Stevens, B. A. Barres, A. F. Clark, R. T. Libby, and S. W. John. 2011. 'Molecular clustering identifies complement and endothelin induction as early events in a mouse model of glaucoma', *J Clin Invest*, 121: 1429-44.
16. Howell, G. R., K. H. MacNicoll, C. E. Braine, I. Soto, D. G. Macalinao, G. L. Sousa, and S. W. John. 2014. 'Combinatorial targeting of early pathways profoundly inhibits neurodegeneration in a mouse model of glaucoma', *Neurobiol Dis*, 71: 44-52.
17. Iwabe, S., M. Lamas, C. G. Vasquez Pelaez, and F. G. Carrasco. 2010. 'Aqueous humor endothelin-1 (Et-1), vascular endothelial growth factor (VEGF) and cyclooxygenase-2 (COX-2) levels in Mexican glaucomatous patients', *Curr Eye Res*, 35: 287-94.

18. Ji, T., X. Zhang, Z. Xin, B. Xu, Z. Jin, J. Wu, W. Hu, and Y. Yang. 2019. 'Does perturbation in the mitochondrial protein folding pave the way for neurodegeneration diseases?', *Ageing Res Rev*, 57: 100997.
19. Johnson, E. C., T. A. Doser, W. O. Cepurna, J. A. Dyck, L. Jia, Y. Guo, W. S. Lambert, and J. C. Morrison. 2011. 'Cell proliferation and interleukin-6-type cytokine signaling are implicated by gene expression responses in early optic nerve head injury in rat glaucoma', *Invest Ophthalmol Vis Sci*, 52: 504-18.
20. Ju, W. K., K. Y. Kim, J. D. Lindsey, M. Angert, K. X. Duong-Polk, R. T. Scott, J. J. Kim, I. Kukhmazov, M. H. Ellisman, G. A. Perkins, and R. N. Weinreb. 2008. 'Intraocular pressure elevation induces mitochondrial fission and triggers OPA1 release in glaucomatous optic nerve', *Invest Ophthalmol Vis Sci*, 49: 4903-11.
21. Kallberg, M. E., D. E. Brooks, G. A. Garcia-Sanchez, A. M. Komaromy, N. J. Szabo, and L. Tian. 2002. 'Endothelin 1 levels in the aqueous humor of dogs with glaucoma', *J Glaucoma*, 11: 105-9.
22. Khawaja, Anthony P., Jessica N. Cooke Bailey, Jae Hee Kang, R. Rand Allingham, Michael A. Hauser, Murray Brilliant, Donald L. Budenz, William G. Christen, John Fingert, Douglas Gaasterland, Terry Gaasterland, Peter Kraft, Richard K. Lee, Paul R. Lichter, Yutao Liu, Felipe Medeiros, Syoko E. Moroi, Julia E. Richards, Tony Realini, Robert Ritch, Joel S. Schuman, William K. Scott, Kuldev Singh, Arthur J. Sit, Douglas Vollrath, Gadi Wollstein, Donald J. Zack, Kang Zhang, Margaret Pericak-Vance, Robert N. Weinreb, Jonathan L. Haines, Louis R. Pasquale, and Janey L. Wiggs. 2016. 'Assessing the Association of Mitochondrial Genetic Variation With Primary Open-Angle Glaucoma Using Gene-Set

AnalysesMitochondrial Genetic Variation and POAG', *Investigative Ophthalmology & Visual Science*, 57: 5046-52.

23. Kong, G. Y., N. J. Van Bergen, I. A. Trounce, and J. G. Crowston. 2009. 'Mitochondrial dysfunction and glaucoma', *J Glaucoma*, 18: 93-100.
24. Kosior-Jarecka, E., D. Wrobel-Dudzinska, U. Lukasik, T. Aung, C. C. Khor, J. Kocki, and T. Zarnowski. 2016. 'Plasma endothelin-1 and single nucleotide polymorphisms of endothelin-1 and endothelin type A receptor genes as risk factors for normal tension glaucoma', *Mol Vis*, 22: 1256-66.
25. Krishnamoorthy, Raghu R., Vidhya R. Rao, Rachel Dauphin, Ganesh Prasanna, Christina Johnson, and Thomas Yorio. 2008. 'Role of the ETB receptor in retinal ganglion cell death in glaucomaThis article is one of a selection of papers published in the special issue (part 1 of 2) on Forefronts in Endothelin', *Canadian Journal of Physiology and Pharmacology*, 86: 380-93.
26. Langmead, B., and S. L. Salzberg. 2012. 'Fast gapped-read alignment with Bowtie 2', *Nat Methods*, 9: 357-9.
27. Lau, J., M. Dang, K. Hockmann, and A. K. Ball. 2006. 'Effects of acute delivery of endothelin-1 on retinal ganglion cell loss in the rat', *Exp Eye Res*, 82: 132-45.
28. Lau, Y. E., J. J. Galligan, D. L. Kreulen, and G. D. Fink. 2006. 'Activation of ETB receptors increases superoxide levels in sympathetic ganglia in vivo', *Am J Physiol Regul Integr Comp Physiol*, 290: R90-5.
29. Lee, S., L. Sheck, J. G. Crowston, N. J. Van Bergen, E. C. O'Neill, F. O'Hare, Y. X. Kong, V. Chrysostomou, A. L. Vincent, and I. A. Trounce. 2012. 'Impaired complex-I-linked

respiration and ATP synthesis in primary open-angle glaucoma patient lymphoblasts', *Invest Ophthalmol Vis Sci*, 53: 2431-7.

30. Leske, M. C., A. Heijl, M. Hussein, B. Bengtsson, L. Hyman, and E. Komaroff. 2003. 'Factors for glaucoma progression and the effect of treatment: the early manifest glaucoma trial', *Arch Ophthalmol*, 121: 48-56.
31. Li, B., and C. N. Dewey. 2011. 'RSEM: accurate transcript quantification from RNA-Seq data with or without a reference genome', *BMC Bioinformatics*, 12: 323.
32. Li, S., A. Zhang, W. Cao, and X. Sun. 2016. 'Elevated Plasma Endothelin-1 Levels in Normal Tension Glaucoma and Primary Open-Angle Glaucoma: A Meta-Analysis', *J Ophthalmol*, 2016: 2678017.
33. Lopez-Riquelme, N., C. Villalba, C. Tormo, A. Belmonte, C. Fernandez, G. Torralba, and F. Hernandez. 2015. 'Endothelin-1 levels and biomarkers of oxidative stress in glaucoma patients', *Int Ophthalmol*, 35: 527-32.
34. McGrady, Nolan R., Alena Z. Minton, Dorota L. Stankowska, Shaoqing He, Hayden B. Jefferies, and Raghu R. Krishnamoorthy. 2017. 'Upregulation of the endothelin A (ETA) receptor and its association with neurodegeneration in a rodent model of glaucoma', *BMC Neuroscience*, 18: 27.
35. Minton, A. Z., N. R. Phatak, D. L. Stankowska, S. He, H. Y. Ma, B. H. Mueller, M. Jiang, R. Luedtke, S. Yang, C. Brownlee, and R. R. Krishnamoorthy. 2012. 'Endothelin B receptors contribute to retinal ganglion cell loss in a rat model of glaucoma', *PLoS One*, 7: e43199.
36. Morrison, J. C., C. G. Moore, L. M. Deppmeier, B. G. Gold, C. K. Meshul, and E. C. Johnson. 1997. 'A rat model of chronic pressure-induced optic nerve damage', *Exp Eye Res*, 64: 85-96.

37. Narayan, Santosh, Ganesh Prasanna, Raghu R. Krishnamoorthy, Xinyu Zhang, and Thomas Yorio. 2003. 'Endothelin-1 Synthesis and Secretion in Human Retinal Pigment Epithelial Cells (ARPE-19): Differential Regulation by Cholinergics and TNF-α', *Investigative Ophthalmology & Visual Science*, 44: 4885-94.
38. Nickells, R. W., G. R. Howell, I. Soto, and S. W. John. 2012. 'Under pressure: cellular and molecular responses during glaucoma, a common neurodegeneration with axonopathy', *Annu Rev Neurosci*, 35: 153-79.
39. Nickells, R. W., and H. R. Pelzel. 2015. 'Tools and resources for analyzing gene expression changes in glaucomatous neurodegeneration', *Exp Eye Res*, 141: 99-110.
40. Osborne, N. N. 2010. 'Mitochondria: Their role in ganglion cell death and survival in primary open angle glaucoma', *Exp Eye Res*, 90: 750-7.
41. Osborne, N. N., and S. del Olmo-Aguado. 2013. 'Maintenance of retinal ganglion cell mitochondrial functions as a neuroprotective strategy in glaucoma', *Curr Opin Pharmacol*, 13: 16-22.
42. Palmiter, R. D. 1974. 'Magnesium precipitation of ribonucleoprotein complexes. Expedient techniques for the isolation of undergraded polysomes and messenger ribonucleic acid', *Biochemistry*, 13: 3606-15.
43. Panda, A. C., J. L. Martindale, and M. Gorospe. 2017. 'Polysome Fractionation to Analyze mRNA Distribution Profiles', *Bio Protoc*, 7.
44. Pinazo-Duran, M. D., V. Zanon-Moreno, J. J. Garcia-Medina, and R. Gallego-Pinazo. 2013. 'Evaluation of presumptive biomarkers of oxidative stress, immune response and apoptosis in primary open-angle glaucoma', *Curr Opin Pharmacol*, 13: 98-107.

45. Prasanna, G., C. Hulet, D. Desai, R. R. Krishnamoorthy, S. Narayan, A. M. Brun, A. M. Suburo, and T. Yorio. 2005. 'Effect of elevated intraocular pressure on endothelin-1 in a rat model of glaucoma', *Pharmacol Res*, 51: 41-50.
46. Prasanna, Ganesh, Raghu Krishnamoorthy, Abbot F. Clark, Robert J. Wordinger, and Thomas Yorio. 2002. 'Human Optic Nerve Head Astrocytes as a Target for Endothelin-1', *Investigative Ophthalmology & Visual Science*, 43: 2704-13.
47. Quigley, H. A. 1999. 'Neuronal death in glaucoma', *Prog Retin Eye Res*, 18: 39-57.
48. ———. 2019. '21st century glaucoma care', *Eye (Lond)*, 33: 254-60.
49. Quigley, H. A., and A. T. Broman. 2006. 'The number of people with glaucoma worldwide in 2010 and 2020', *Br J Ophthalmol*, 90: 262-7.
50. Robinson, M. D., D. J. McCarthy, and G. K. Smyth. 2010. 'edgeR: a Bioconductor package for differential expression analysis of digital gene expression data', *Bioinformatics*, 26: 139-40.
51. Rosenthal, R., and M. Fromm. 2011. 'Endothelin antagonism as an active principle for glaucoma therapy', *Br J Pharmacol*, 162: 806-16.
52. Srinivasan, S., and N. G. Avadhani. 2012. 'Cytochrome c oxidase dysfunction in oxidative stress', *Free Radic Biol Med*, 53: 1252-63.
53. Stokely, M. E., S. T. Brady, and T. Yorio. 2002. 'Effects of endothelin-1 on components of anterograde axonal transport in optic nerve', *Invest Ophthalmol Vis Sci*, 43: 3223-30.
54. Tezel, G. 2008. 'TNF-alpha signaling in glaucomatous neurodegeneration', *Prog Brain Res*, 173: 409-21.

55. Tham, Y. C., X. Li, T. Y. Wong, H. A. Quigley, T. Aung, and C. Y. Cheng. 2014. 'Global prevalence of glaucoma and projections of glaucoma burden through 2040: a systematic review and meta-analysis', *Ophthalmology*, 121: 2081-90.
56. Thanos, S., and R. Naskar. 2004. 'Correlation between retinal ganglion cell death and chronically developing inherited glaucoma in a new rat mutant', *Exp Eye Res*, 79: 119-29.
57. Vass, C., C. Hirn, T. Sycha, O. Findl, P. Bauer, and L. Schmetterer. 2007. 'Medical interventions for primary open angle glaucoma and ocular hypertension', *Cochrane Database Syst Rev*: Cd003167.
58. White, Andrew JR, Janosch P Heller, Johahn Leung, Alessia Tassoni, and Keith R Martin. 2015. 'Retinal ganglion cell neuroprotection by an angiotensin II blocker in an ex vivo retinal explant model', *Journal of the Renin-Angiotensin-Aldosterone System*, 16: 1193-201.
59. Williams, P. A., J. M. Harder, and S. W. M. John. 2017. 'Glaucoma as a Metabolic Optic Neuropathy: Making the Case for Nicotinamide Treatment in Glaucoma', *J Glaucoma*, 26: 1161-68.
60. Yang, Z., H. A. Quigley, M. E. Pease, Y. Yang, J. Qian, D. Valenta, and D. J. Zack. 2007. 'Changes in gene expression in experimental glaucoma and optic nerve transection: the equilibrium between protective and detrimental mechanisms', *Invest Ophthalmol Vis Sci*, 48: 5539-48.
61. Yorio, T., R. Krishnamoorthy, and G. Prasanna. 2002. 'Endothelin: is it a contributor to glaucoma pathophysiology?', *J Glaucoma*, 11: 259-70.
62. Yu-Wai-Man, Patrick. 2012. 'Mitochondrial Dysfunction in Glaucoma—Closing the LoopMitochondrial Dysfunction in Glaucoma', *Investigative Ophthalmology & Visual Science*, 53: 2438-38.

63. Zanon-Moreno, V., J. J. Garcia-Medina, V. Zanon-Viguer, M. A. Moreno-Nadal, and M. D. Pinazo-Duran. 2009. 'Smoking, an additional risk factor in elder women with primary open-angle glaucoma', *Mol Vis*, 15: 2953-9.

Figure legends

Figure 1. a) Purity of primary RGC culture. Confocal representative images of pure RGC cultures immunolabeled with specific RGC markers, A) RBPMS (red), B) Brn3a (green) as well as with a specific marker for astrocytes/Muller cells, C) GFAP, while all isolated cells were stained with the D) nuclear dye DAPI (blue). A negative control immunostaining (Blank) in which the primary antibody was excluded showed no staining. Scale bar indicates 50 μm.

b) Quantitation of the RGC purity. Illustrated data are Mean±SEM from 3 independent experiments.

Figure 2. The DEGs in primary RGCs following ET-1 treatment for 24 hours were analyzed using the STRING database. The network nodes represent the proteins encoded by the DEGs. Seven different colored lines link a number of nodes and represent seven types of evidence used in predicting associations: green lines represent neighborhood evidence; red lines indicate the presence of fusion evidence; blue lines represent co-occurrence evidence; purple lines represent protein homology evidence; black lines represent co-expression evidence; pink lines represent experimental evidence; light blue lines represent database evidence; and yellow lines represent text-mining evidence.

Figure 3. Correlation heatmap, Principal Component Analysis and Ingenuity Pathway Canonical Network Analysis. (a) Heatmap analysis, clustering of samples based on Pearson's correlation showing hierarchical clustering of DEGs after ET-1 treatment. Rows representing genes are scaled, i.e., the value (z score) for a given gene in a given sample represents its deviation from the mean expression value of the gene across all samples in terms of its standard variation, with red denoting upregulation, and green downregulation. Each column represents a sample. Color key indicates relative levels of gene expression changes, with darker green indicating downregulation and darker red indicating upregulation. (b) PCA plot of samples shows the distribution of samples in the space of the first two components (PC1 and PC2). (c) Ingenuity Pathway Analysis of Canonical Pathway Enrichment. Z-score shows overall activation or suppression of the corresponding pathways.

Figure 4. qPCR validation of the expression of selected genes related to mitochondrial function, neurodegeneration or cell survival. Primary RGCs were either untreated (control) or treated with ET-1 for 24 hours following which total cellular RNA was isolated and subjected to qPCR analysis of gene expression. Relative mRNA expression values are plotted as a ratio to untreated control levels. Data are expressed as Mean±SEM (n=3-4 biological replicates). (*$p < 0.05$, **$p \leq 0.01$)

Figure 5. Immunofluorescence analysis of ATP5H and COX17 in control and ET-1 treated RGCs. Immunostaining for a) COX17 (red) and b) ATP5H (magenta) in primary RGCs. Scale bar, 50 μm and quantitation of COX17 and ATP5H (c, d) from five different images (n=5) following ET-1 treatment. Quantitation of fluorescence intensity of COX17 and ATP5H calculated

as integrated density/Brn3a positive 100 cells as determined from the five different images. Data are expressed as Mean±SEM (*P < 0.05).

Figure 6. Quantification of ATP production by Seahorse XF real-time ATP rate assay following ET-1 treatment at 4h and 24h in primary RGCs. (a) Kinetic profile of OCR measurements following ET-1 treatment at 4h and 24h. (b) ATP rate index indicating the changes in metabolic phenotype after ET-1 treatment at 4h and 24h. An increase in the XF ATP Rate Index represents a more oxidative / less glycolytic phenotype and vice-versa. (c) Metabolic flux analysis showing quantification of mitochondrial ATP production and glycolytic ATP production. Data shown are Mean±SEM (n=4 biological replicates and atleast 6 technical replicates), *p < 0.05, **p ≤ 0.01)

Figure 7. ATP5H and COX17 expression in retinas of adult Brown Norway rats following intravitreal administration of ET-1. a) Representative images. Immunostaining of retina sections probed for ATP5H (yellow) and COX17 (red) following ET-1, 50 (μM) intravitreal injection 24 hours. Scale bar, 50 μm. Relative fluorescent intensity for ATP5H (b) and COX17 (c) for the NFL; GC and IPL. Bars represent mean ± SEM (n = 6 animals/group). Asterisks indicate statistical significance *p < 0.05; **p < 0.01; by student's t-test. ONL outer nuclear layer, OPL outer plexiform layer, INL inner nuclear layer, IPL inner plexiform layer, GCL ganglion cell layer, NFL nerve fiber layer.

Figure 8. ATP5H and COX17 expression in Morrison's model of ocular hypertension following 2 week IOP elevation. a) Representative graph of IOP measurements for IOP elevated

(white circles) and contralateral control (black circles) eyes in adult male Brown Norway rats. b) Representative confocal microscopy images. Immunostaining of retina sections probed for ATP5H (green), COX17 (red), Brn3a (cyan) following 2 weeks of IOP elevation. C) Quantitation of the Relative fluorescent intensity for c) COX17 and D) ATP5H estimated by quantifying only Brn3a positive cells. Scale bar = 50 μm. Bars represent Mean ± SEM (n = 3 animals/group).

Figure 1

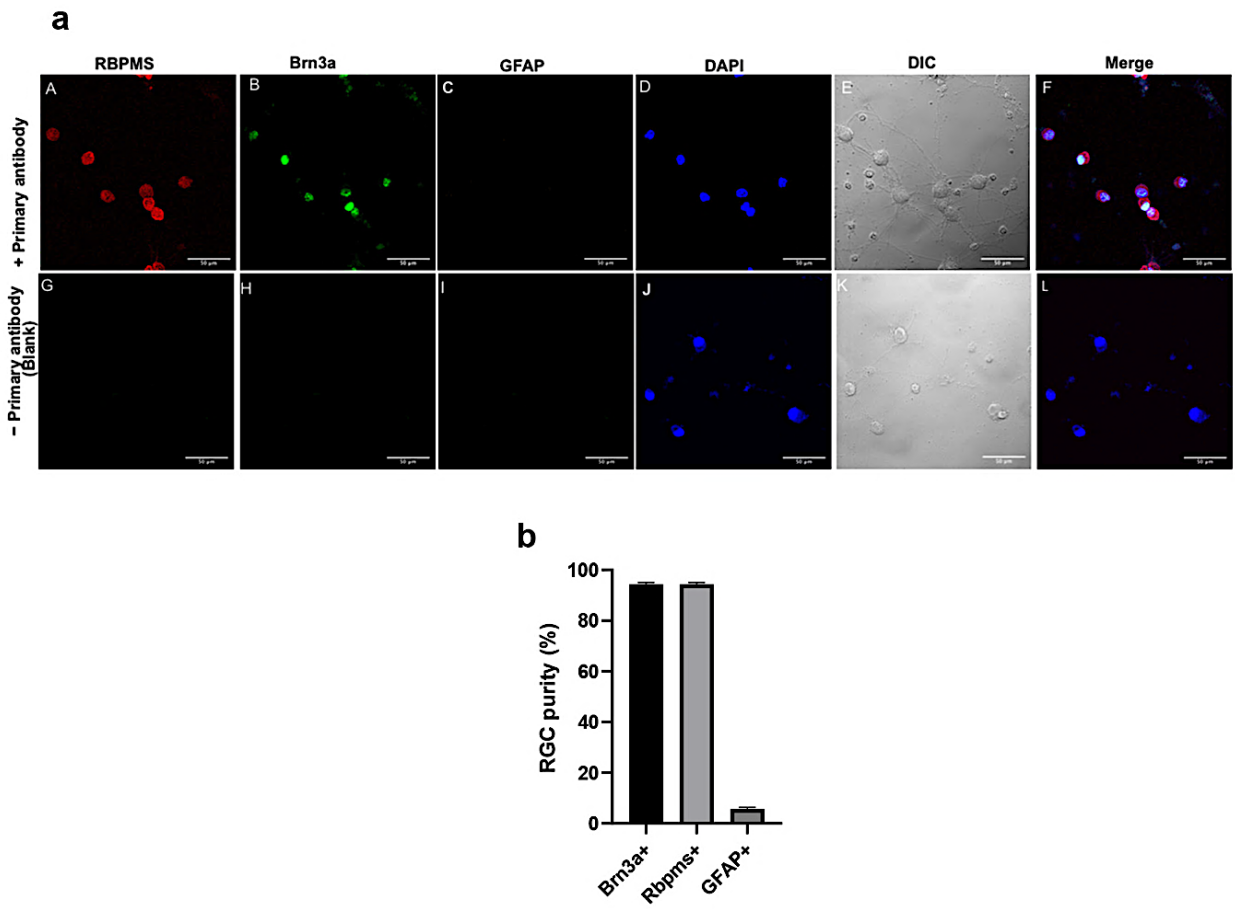
a
RBPMS
Brn3a
GFAP
DAPI
DIC
Merge
+ Primary antibody
– Primary antibody (Blank)
A
B
C
D
E
F
G
H
I
J
K
L
b
RGC purity (%)
100
80
60
40
20
0
Brn3a+
Rbpms+
GFAP+

Figure 2

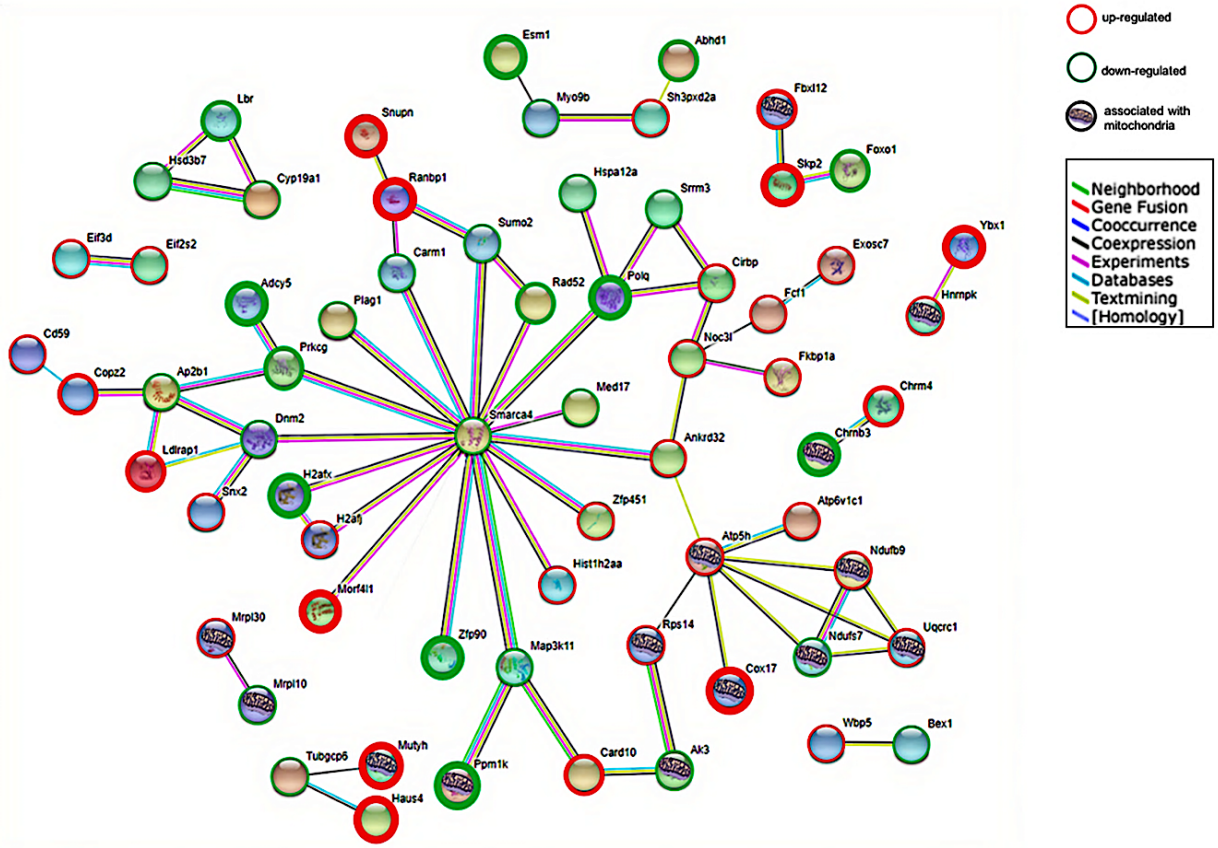
Esm1
Abhd1
Myo9b
Sh3pxd2a
Fbxl12
Lbr
Snupn
Skp2
Foxo1
Hsd3b7
Cyp19a1
Ranbp1
Hspa12a
Srrm3
Sumo2
Ybx1
Eif3d
Eif2s2
Carm1
Exosc7
Cirbp
Rad52
Polq
Fcf1
Hnrnpk
Adcy5
Plag1
Cd59
Noc3l
Fkbp1a
Prkcg
Copz2
Ap2b1
Med17
Chrm4
Dnm2
Smarca4
Ankrd32
Chrnb3
Ldlrap1
H2afx
Snx2
Zfp451
Atp6v1c1
H2afj
Atp5h
Ndufb9
Hist1h2aa
Morf4l1
Mrpl30
Rps14
Uqcrc1
Zfp90
Map3k11
Ndufs7
Mrpl10
Cox17
Wbp5
Bex1
Tubgcp6
Mutyh
Ppm1k
Card10
Ak3
Haus4
up-regulated
down-regulated
associated with mitochondria
Neighborhood
Gene Fusion
Cooccurrence
Coexpression
Experiments
Databases
Textmining
[Homology]

Figure 3

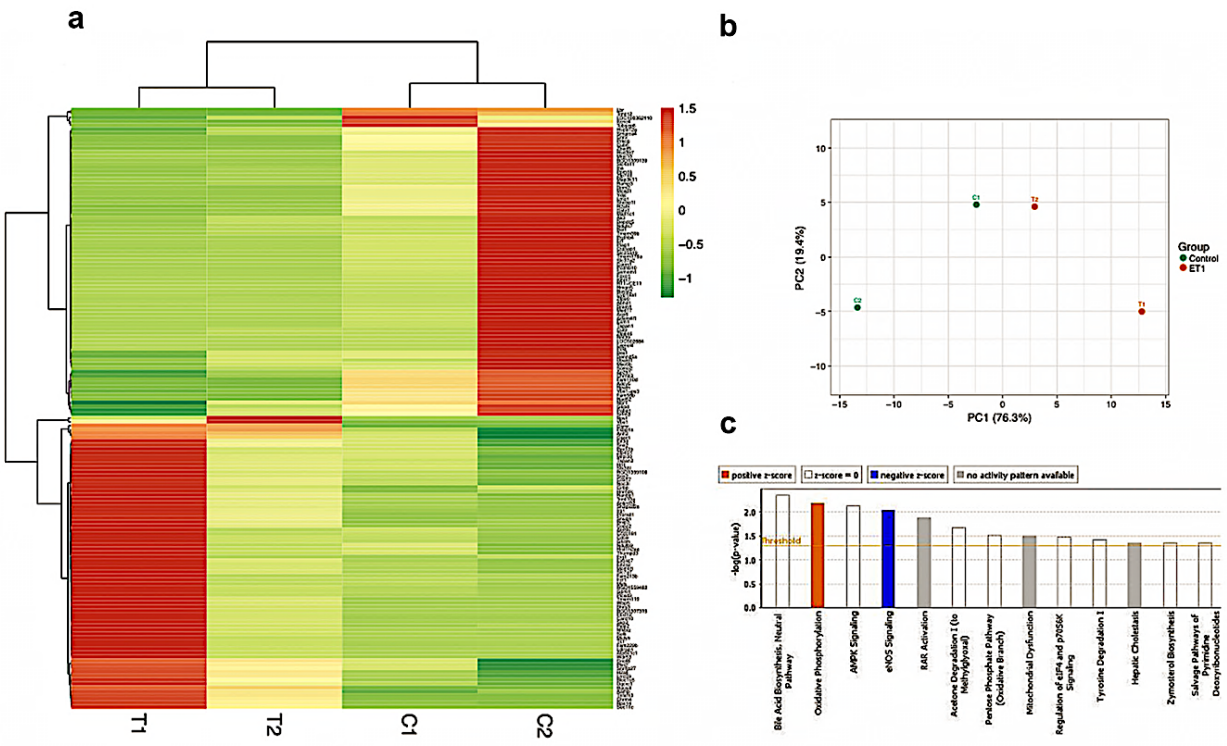
a
1.5
1
0.5
0
−0.5
−1
T1
T2
C1
C2
b
PC2 (19.4%)
PC1 (76.3%)
Group
Control
ET1
c
positive z-score
z-score = 0
negative z-score
no activity pattern available
-log(p-value)
Threshold
Bile Acid Biosynthesis, Neutral Pathway
Oxidative Phosphorylation
AMPK Signaling
eNOS Signaling
RAR Activation
Acetone Degradation I (to Methylglyoxal)
Pentose Phosphate Pathway (Oxidative Branch)
Mitochondrial Dysfunction
Regulation of eIF4 and p70S6K Signaling
Tyrosine Degradation I
Hepatic Cholestasis
Zymosterol Biosynthesis
Salvage Pathways of Pyrimidine Deoxyribonucleotides

Figure 4

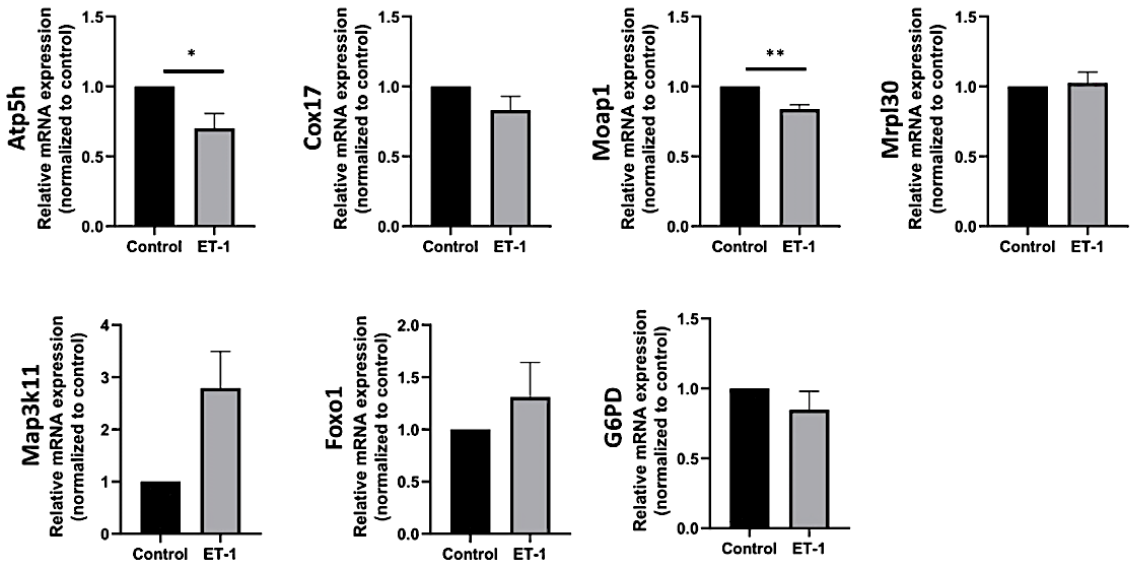
Atp5h
Relative mRNA expression (normalized to control)
1.5
1.0
0.5
0.0
*
Control
ET-1
Cox17
Relative mRNA expression (normalized to control)
1.5
1.0
0.5
0.0
Control
ET-1
Moap1
Relative mRNA expression (normalized to control)
1.5
1.0
0.5
0.0
**
Control
ET-1
Mrpl30
Relative mRNA expression (normalized to control)
1.5
1.0
0.5
0.0
Control
ET-1
Map3k11
Relative mRNA expression (normalized to control)
4
3
2
1
0
Control
ET-1
Foxo1
Relative mRNA expression (normalized to control)
2.0
1.5
1.0
0.5
0.0
Control
ET-1
G6PD
Relative mRNA expression (normalized to control)
1.5
1.0
0.5
0.0
Control
ET-1

Figure 5

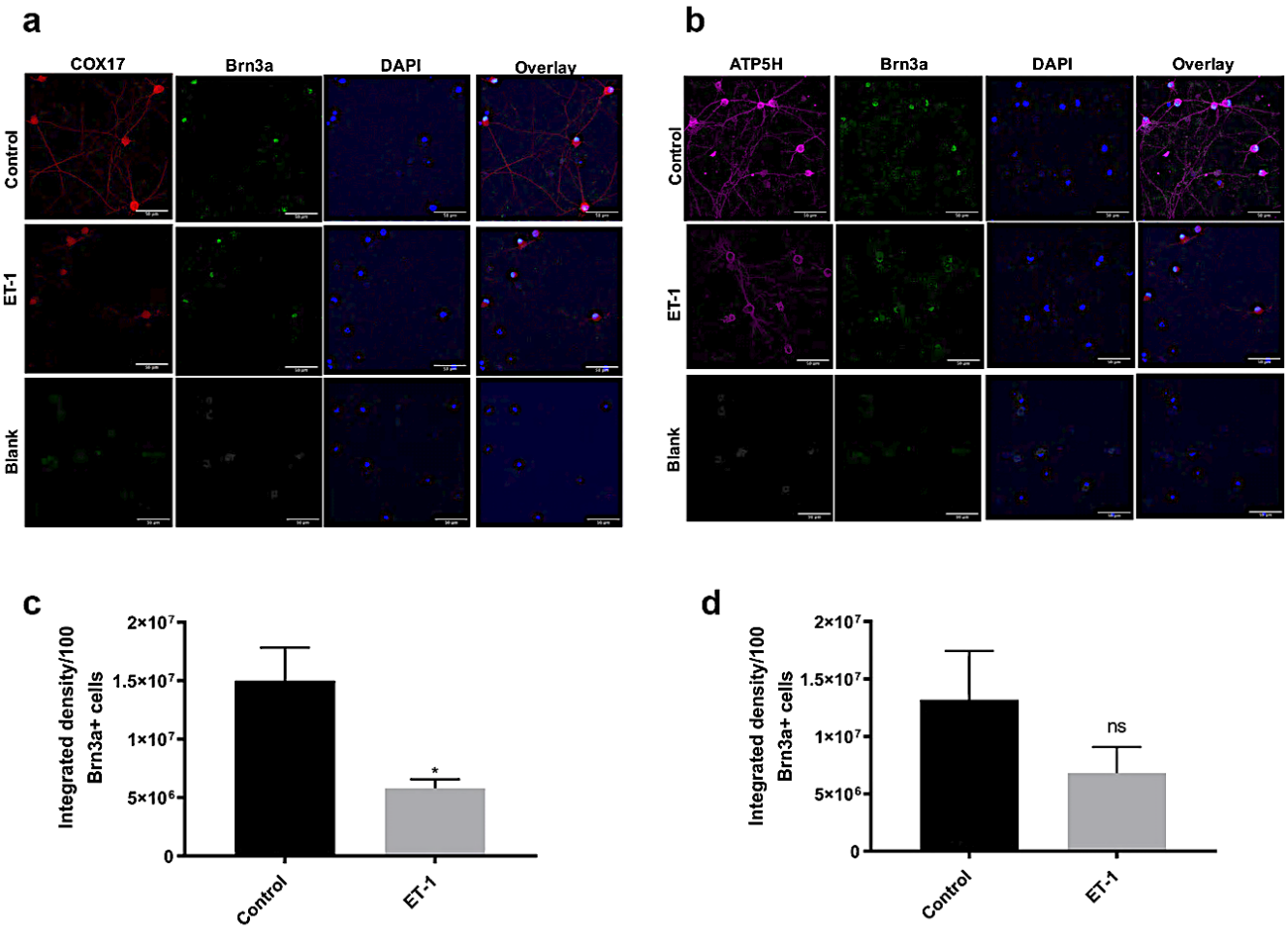
a
COX17
Brn3a
DAPI
Overlay
Control
ET-1
Blank
b
ATP5H
Brn3a
DAPI
Overlay
Control
ET-1
Blank
c
Integrated density/100 Brn3a+ cells
2×10^7
1.5×10^7
1×10^7
5×10^6
0
*
Control
ET-1
d
Integrated density/100 Brn3a+ cells
2×10^7
1.5×10^7
1×10^7
5×10^6
0
ns
Control
ET-1

Figure 6

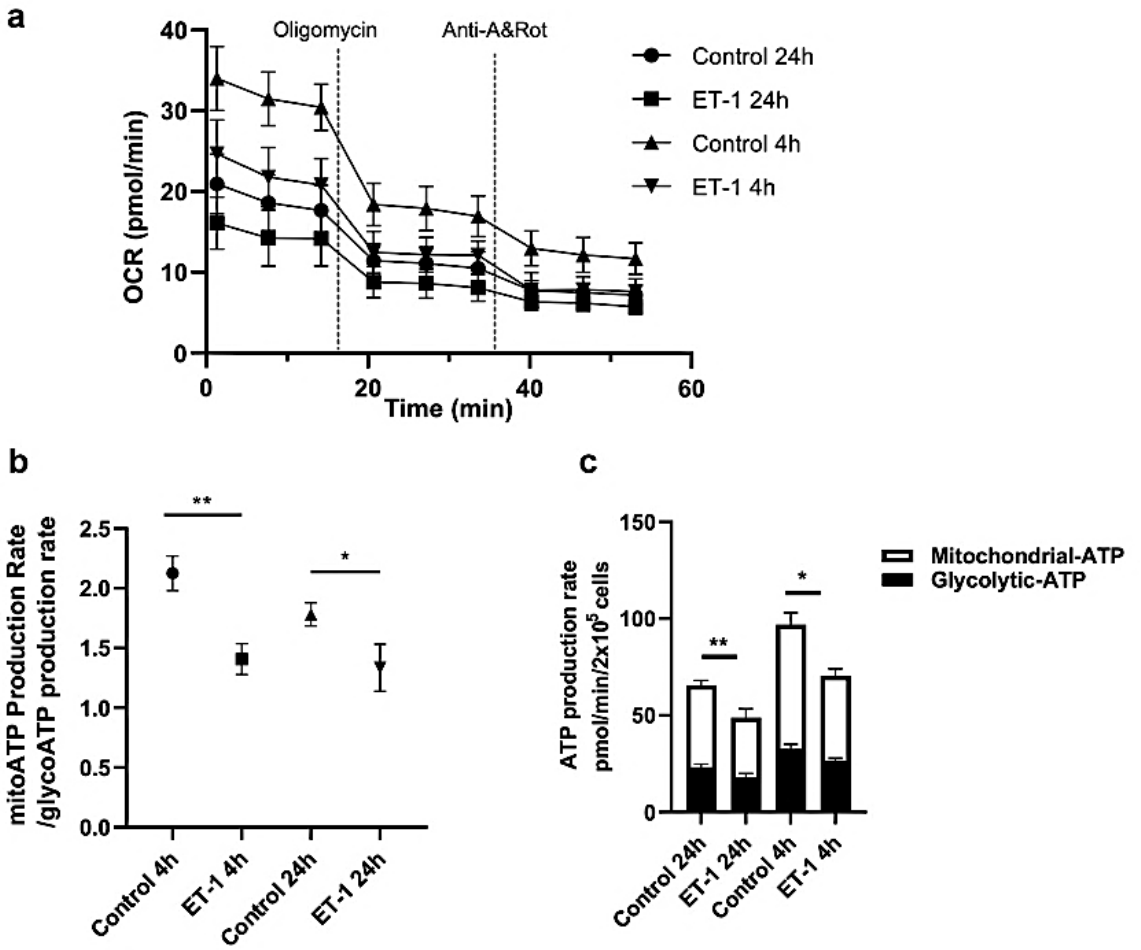
a
Oligomycin
Anti-A&Rot
Control 24h
ET-1 24h
Control 4h
ET-1 4h
OCR (pmol/min)
Time (min)
b
mitoATP Production Rate
/glycoATP production rate
**
*
Control 4h
ET-1 4h
Control 24h
ET-1 24h
c
ATP production rate
pmol/min/2x10^5 cells
Mitochondrial-ATP
Glycolytic-ATP
**
*
Control 24h
ET-1 24h
Control 4h
ET-1 4h

Figure 7

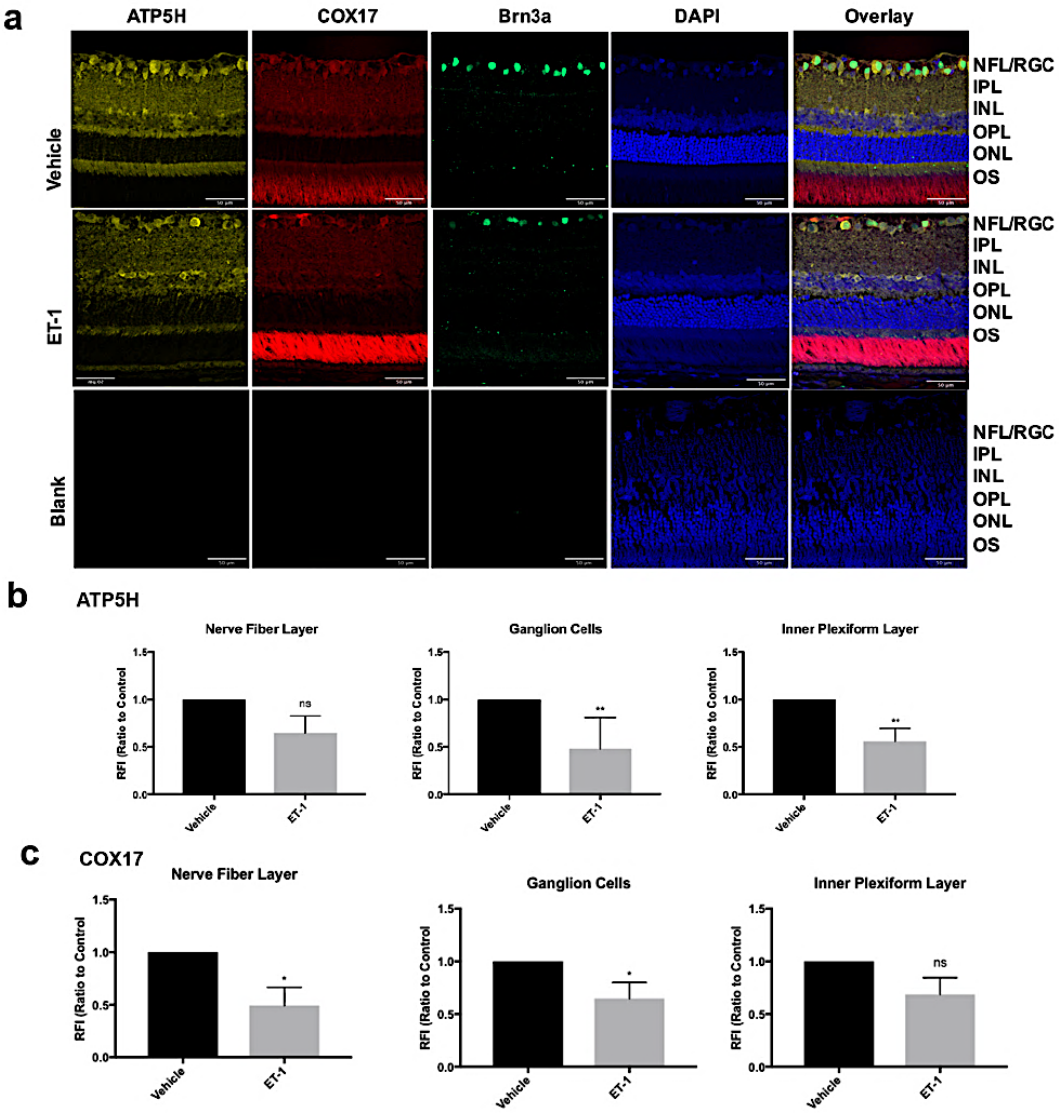
a
ATP5H
COX17
Brn3a
DAPI
Overlay
Vehicle
ET-1
Blank
NFL/RGC
IPL
INL
OPL
ONL
OS
b
ATP5H
Nerve Fiber Layer
Ganglion Cells
Inner Plexiform Layer
RFI (Ratio to Control
ns
**
Vehicle
ET-1
c
COX17
Nerve Fiber Layer
Ganglion Cells
Inner Plexiform Layer
*
ns

Figure 8

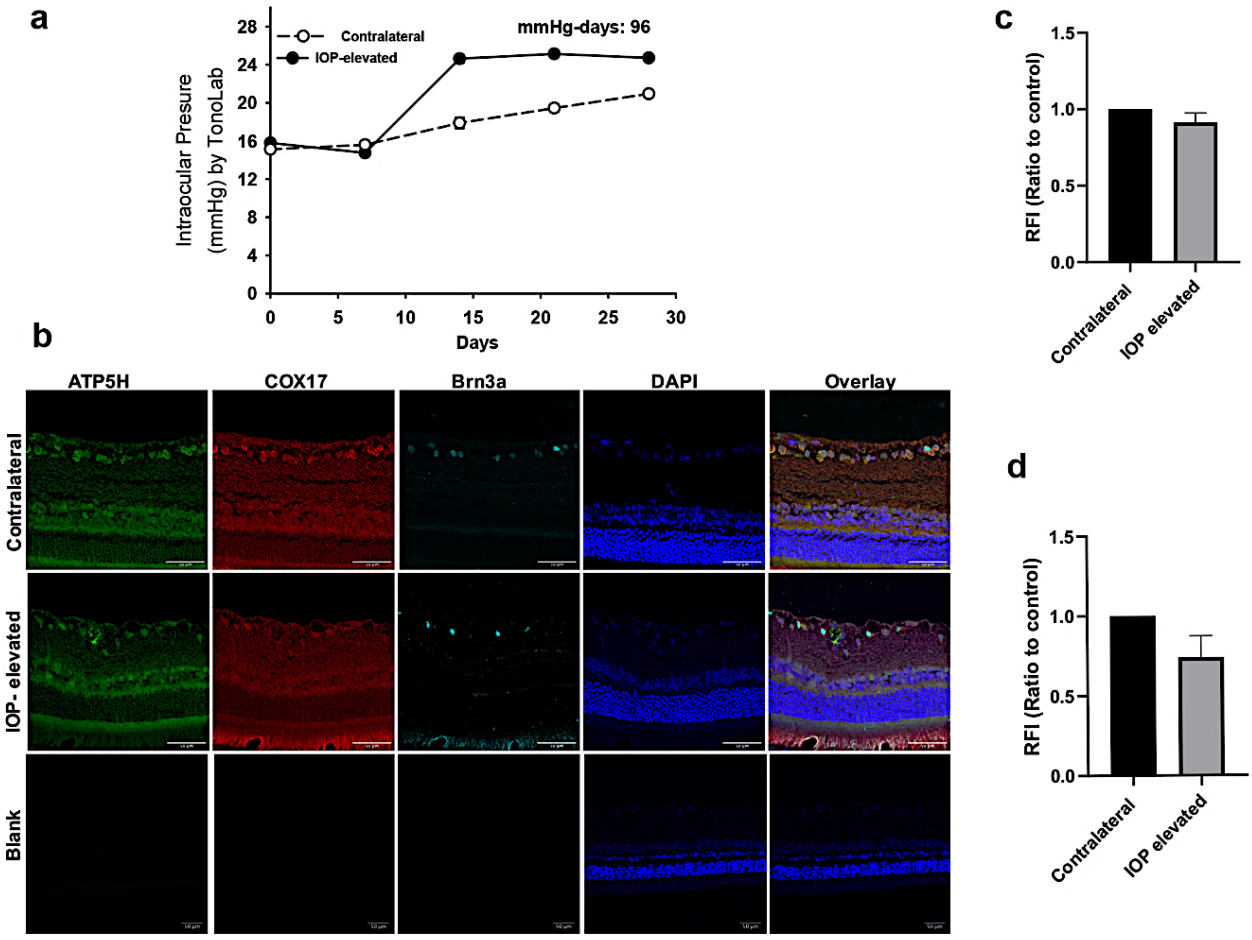
a
Contralateral
IOP-elevated
mmHg-days: 96
Intraocular Presure (mmHg) by TonoLab
Days
b
ATP5H
COX17
Brn3a
DAPI
Overlay
Contralateral
IOP- elevated
Blank
c
RFI (Ratio to control)
Contralateral
IOP elevated
d
RFI (Ratio to control)
Contralateral
IOP elevated

CHAPTER III

Decrease in mitophagosome formation is associated with glaucomatous neurodegeneration

Renuka M. Chaphalkar[1], Prabhavathi Maddineni[1], Bindu Kodati[1], Dorota L. Stankowska[1], Jude Prah[3], Shaohua Yang[1], Gulab Zode[1] and Raghu R. Krishnamoorthy[1*]

North Texas Eye Research Institute, [1]Department of Pharmacology and Neuroscience, UNT Health Science Center, Fort Worth, Texas 76107, United States. [2]Department of Microbiology, Immunology and Genetics, UNT Health Science Center, Fort Worth, Texas 76107, United States. [3] Department of Basic and Translational Sciences, School of Dental Medicine, University of Pennsylvania, Philadelphia, PA 19104, United States.

Abstract

Glaucoma is a heterogenous group of optic neuropathies characterized by degeneration of optic nerve axons and progressive loss of retinal ganglion cells (RGCs), ultimately leading to vision loss. Elevation of intraocular pressure (IOP) is a major risk factor in development of glaucoma. Endothelin-1 (ET-1), a potent vasoactive peptide has been shown to cause neurodegenerative effects in animal models of glaucoma. However, the exact mechanisms underlying ET-1 mediated neurodegeneration in glaucoma remains largely unknown. Using a Seahorse mitostress assay, we report that ET-1 treatment causes significant decline in various parameters of mitochondrial function, including, ATP production, maximal respiration and spare capacity in cultured RGCs at

4 and 24 hour time points. We hypothesized that this decline in mitochondrial function in RGCs may lead to an impairment in the mitochondrial quality control and disruption of the mitophagy pathway. In cultured RGCs we observed a decrease in mitophagy following ET-1 treatment for 24 h. Using the Morrison's model of ocular hypertension, we investigated here for the first time, changes in mitophagosome formation by analyzing the co-localization between LC-3B and TOM20 specifically in RGCs. We also injected ET-1 in the transgenic GFP-LC3 mice, to analyze the formation of mitophagosomes in vivo following 24 h. In Morrison's model of ocular hypertension, as well as in ET-1 injected GFP-LC3 mice, we found a decrease in co-localization of LC3-TOM20, indicating an impairment in mitophagosome formation. Taken together, these results demonstrate that both ocular hypertension and ET-1 administration in rats produce changes in mitophagosome formation, which may lead to a decline in mitophagy, thus predisposing RGCs to neurodegeneration.

1. Introduction

Glaucoma is an optic neuropathy characterized by progressive degeneration of the optic nerve and loss of RGCs leading to visual impairment. Primary open angle glaucoma (POAG) is the most common form of disease, typically associated with elevated intraocular pressure (IOP) (Boland and Quigley, 2007; Weinreb et al., 2016). IOP is the only treatable risk factor in glaucoma and all current therapies for glaucoma are aimed at lowering IOP. However, even though IOP lowering approaches remain a gold standard for glaucoma therapy, it does not completely prevent progression of RGC loss (Leske et al. 2003; Pascale, Drago, and Govoni 2012). Hence neuroprotective therapies are needed to delay axonal injury and enhance the survival of RGCs, which will be important as additional therapeutic interventions in glaucoma.

Multiple factors can contribute to glaucomatous neurodegeneration, including oxidative stress (Chidlow et al., 2017; Pinazo-Duran et al., 2018), glutamate neurotoxicity (Seki and Lipton 2008; Nguyen et al. 2011), release of tumor necrosis factor (TNF-α) (Agarwal and Agarwal 2012; Tezel et al. 2001) and mitochondrial dysfunction (Abu-Amero et al., 2006; Chaphalkar et al., 2020; Williams et al., 2017) . One of the key factors implicated in pathogenesis of glaucoma is endothelin -1 (ET-1). ET-1 is a 21 amino-acid vasoactive peptide belonging to the endothelin family which has been shown to produce several neurodegenerative effects in animal models of glaucoma (Chauhan 2008; Minton et al. 2012; Yorio, Krishnamoorthy, and Prasanna 2002). Previous studies reported that ET-1 levels are elevated in the aqueous humor and circulation in patients with POAG (Choritz, Machert, and Thieme 2012; Li et al. 2016; Tezel et al. 1997) and in animal models of glaucoma (Källberg et al. 2002; Prasanna et al. 2005). Administration of peribulbar and intravitreal ET-1 administration has been shown to produce degeneration of optic nerve axons and RGC loss (Chauhan et al., 2004; Cioffi and Sullivan, 1999; Krishnamoorthy et al., 2008; Lau et al., 2006). ET-1 acts through two G- protein coupled receptors: endothelin receptor A (ET_A) and endothelin receptor B (ET_B). Both ET_A and ET_B receptors are abundantly expressed in various ocular tissues (Chauhan, 2008; MacCumber and D'Anna, 1994). An increase in ET_B receptor expression was observed following IOP elevation in Brown Norway rats and neurodegenerative changes were significantly attenuated in ET_B receptor knockout rats, compared to wild type rats, suggestive of a causative role of the ET_B receptor in glaucomatous neurodegeneration (Minton et al., 2012). However, the detailed mechanisms underlying ET-1 mediated RGC loss in glaucoma are still not clearly understood.

We have recently shown that ET-1 treatment in cultured RGCs resulted in a significant decline in ATP synthase expression, indicative of an impairment in mitochondrial dynamics and bioenergetics, which could be one mechanism by which ET-1 promotes neurodegeneration of RGCs in glaucoma (Chaphalkar et al., 2020). Mitochondria are the major source of ATP synthesis and essential for the excitability and survival of neurons. Neurons are highly dependent on mitochondrial respiration to maintain the synaptic transmission and the dynamic mitochondrial trafficking between the soma and axons. Thus, mitochondrial dysfunction and defective clearance of impaired mitochondria (defective mitophagy) could be detrimental to neuronal health. Dysfunction in mitochondrial function disrupts mitochondrial quality control mechanisms that contributes to progression of several neurodegenerative disorders (Lin and Beal 2006). Mitophagy is one of the important quality control mechanism which is crucial for maintaining the mitochondrial quality control and cellular homeostasis (Wang et al., 2019). Mitophagy is a highly specialized form of autophagy and involves selective removal of damaged mitochondria in response to various stress conditions, including, increased production of reactive oxygen species (ROS) (Wang et al., 2012), hypoxia (Liu et al., 2012), mitochondrial depolarization (Matsuda et al., 2010) and protein misfolding. Hence mitophagy plays a pivotal role in preventing accumulation of dysfunctional mitochondria, possibly protecting from neuronal death.

Dysregulation of mitophagy (both an increase and decrease) contributes to the pathology of several neurodegenerative diseases including Parkinson's disease, Alzheimer's disease, Huntington's disease and Amyotrophic lateral sclerosis (Wang, Liu, and Lu 2019). The study of mechanisms of mitophagy in glaucoma is still limited and needs further exploration (Dai, Hu, and Sun 2018; Hirt et al. 2018; Hu et al. 2018). The goal of the present study was to investigate whether there is an

involvement of mitophagy pathway to target the damaged mitochondria for degradation following ET-1 treatment in RGCs. In this study, we observed a decrease in the mitophagosome density in cultured RGCs following ET-1 treatment for 24 h. We also found a significant decrease in the formation of mitophagosomes in RGCs (autophagosomes with engulfed mitochondria) in retinas with IOP-elevation for 2 weeks in adult Brown Norway rats. Our data suggests that ET-1 mediated impairment of mitochondrial bioenergetics can result in an accumulation of defective mitochondria, hence disrupting the regulation of mitophagy.

2. Materials and Methods

2.1 Primary RGC isolation

Female timed-pregnant Sprague-Dawley rats were obtained from Charles River Laboratories (Wilmington, MA, USA). Primary rat RGCs were isolated using a Thy-1.1 antibody-panning method (Barres et al., 1988). Briefly, post-natal day 4-6 rat pups were euthanized, and the isolated retinas were treated with 4.5 units/ml of papain solution to dissociate the retinal cells. The cell suspension was subsequently incubated for 10 minutes with a rabbit anti-macrophage antibody and transferred to a to a petri dish coated with a goat anti-rabbit IgG (H+L chain) antibody for 35 minutes. Cells that were not attached to the coated anti-rabbit IgG were transferred to a petri-dish coated with anti-Thy1.1 antibody for 60 minutes with intermittent shaking. After washing 3 to 5 times with DPBS, RGCs were then dissociated by trypsin treatment and then collected by centrifugation. Isolated RGCs were seeded either directly in a Seahorse XF96 Cell Culture Microplate or on 35mm Mattek glass bottom dishes, No 1.5 coverslip coated with poly-D lysine and mouse-laminin. Cells were cultured in serum-free Dulbecco's modified Eagle's medium containing brain-derived neurotrophic factor (BDNF) (50 ng/ml; Peprotech, Rocky Hill, NJ,

USA), ciliary neurotrophic factor (10 ng/ml; Peprotech), and forskolin (5 ng/ml; Sigma-Aldrich Corp.). Primary RGCs were maintained for a week at 37 °C in a humidified atmosphere of 10% CO_2 and 90% air to firmly attach and allow neurite outgrowth to occur. One-third volume of the culture medium was changed every two days. The purity of the culture obtained were routinely between 90%-95%.

2.2 ET-1 treatment

ET-1 peptide was purchased from Bachem (Torrance, CA) and dissolved to obtain the working stock concentration of 100 μM. The seeding density of the primary RGCs was approximately 25,000 cells/well for a Seahorse XF96 Cell Culture Microplate and 20,000 cells/ well for a 35mm Mattek glass bottom dish containing No 1.5 coverslip (0.16-0.19 mm thickness). Primary RGCs were allowed to grow in culture for one week to promote neurite outgrowth and then treated with 100 nM ET-1 (final concentration) for either 4h or 24h, while untreated RGCs served as controls.

2.3 Seahorse Extracellular flux analysis

Agilent Seahorse XFe96 analyzer was used to measure Oxygen consumption rate (OCR), basal respiration, extracellular acidification rate (ECAR), H^+ (Proton) leak, maximal respiration, spare respiratory capacity and ATP-linked respiration. Briefly, primary RGCs were isolated from post-natal day 4–6 rat pups. he RGCs were seeded RGC medium in a poly-D-lysine coated seahorse plate and maintained in culture for one week to allow neurite outgrowth. The RGCs were either untreated or treated with ET-1 for 4 h or 24 h in trophic factor-free medium. Seahorse Mito Stress kit was used to determine the effects on ET-1 on mitochondrial respiration in primary RGCs. A day prior to the experiment seahorse sensor cartridge was hydrated with water and incubated in a

non-CO_2 incubator at 37 °C. Two hours before the experiment, the water was replaced with a seahorse calibrant. One hour before the experiment, assay medium was prepared. Seahorse XF base medium was supplemented with 1 mM pyruvate, 2 mM glutamine and 10 mM glucose (Agilent, USA) and pH adjusted to 7.4. The RGC culture medium was then replaced with 180 μl of the supplemented Seahorse XF base medium and the cells incubated in a non-CO_2 incubator at 37 °C for 1 hour. While the cell culture microplates were incubating for an hour, solutions of oligomycin, FCCP, and Rotenone/Antimycin A (Agilent, USA) were prepared in the seahorse medium to achieve final concentrations of 1.5 μM, 2 μM, and 0.5 μM respectively when injected. The appropriate volumes: 20, 22 and 25 μl of Oligomycin, FCCP, and Rotenone/Antimycin A, respectively, were injected into the drug delivery ports A, B, C of the hydrated sensor cartridge and loaded into the seahorse XF analyzer to calibrate for 30 minutes. The calibration plate was replaced with the cell culture plate and oxygen consumption (OCR) and extracellular acidification rate (ECAR) was monitored following the sequential injection of Oligomycin, FCCP, and Rotenone/Antimycin A, with each cycle set as 3 min (mix), 2 min (delay) and measurements for 3 minutes. The Mito Stress test was carried out for two time points of ET-1 treatment (4 h and 24 h). Data was normalized to the cell number of each well by Calcein AM assay.

2.4 Immunofluoroscence

Primary RGCs were labelled with MitoTracker™ Deep Red FM (ThermoFisher Scientific) and LysoTracker™ Red DND-99 (ThermoFisher Scientific) to stain the mitochondria and lysosomes, respectively, according to manufacturer's instructions. In brief, the RGC medium was removed and cells were washed once with DMEM medium. Prewarmed (37°C) staining solution containing MitoTracker at the final concentration of 25nM and Lysotracker at the final concentration of 50nM

were added to the live cells and incubated for 30 min at 37°C. Cells were counterstained with Hoechst 33342 to label cell nuclei and Z-stack images were taken at 40x in a Zeiss LSM 510 laser scanning confocal microscope. Quantitation of co-localization puncta was analysed by measuring Manders' overlap coefficient using the method described in section 2.5.

2.5 Animals

All protocols and procedures were in accordance with the policies of the Association for Research in Vision and Ophthalmology (ARVO) for use of animals in research and approved by the Institutional Animal Care and Use Committee (IACUC) (animal protocol #IACUC-2017-0024) at the University of North Texas Health Science Center at Fort Worth, TX, USA. Retired breeder Brown Norway rats (Charles River Laboratories, Wilmington, MA) in the age group of 8 to 12 months were used to induce ocular hypertension by Morrison's glaucoma model. Male and female homozygous GFP-LC3 (Tg-GFP-LC3/6J) mice, 4 to 5 months old, on a C57BL6 background were a kind gift from Dr. Noboru Mizushima and used to monitor formation of autophagosomes in vivo (Mizushima et al., 2004). The GFP-LC3 mice were used to quantify the autophagosomes in retina sections obtained following intravitreal ET-1 injection in these mice as described below.

2.6 Immunohistochemistry

Rat eyes were enucleated and a small incision (approximately 4-5 mm) was made just posterior to the limbus and the eye was fixed in 4% paraformaldehyde (PFA) in phosphate buffered saline (PBS) for 30 min. After fixation, an incision was made along the entire circumference of the limbus to remove the entire anterior segment completely including the lens. The posterior segment was fixed in 4% PFA for an additional 3 hours. The tissue was rinsed with 70% ethanol and later embedded in paraffin. Sagittal retinal sections through the optic nerve head (7μm) were obtained,

de-paraffinized in xylene, and rehydrated with a graded series of ethanol. Following permeabilization, retinal sections were blocked for 1 hour with 5% normal donkey serum containing 5% BSA in PBS and incubated with the appropriate primary antibodies overnight.

Mice were euthanized by approved methods, 24h after intravitreal injection of ET-1 (2 µl of 500 µM), Death of the mice was confirmed by the absence of respiration and heartbeat, following which, a unilateral thoracotomy was performed. Mice eyes were enucleated carefully and fixed immediately in 4% PFA solution for 16 hours at 4 °C. The fixed eyes were washed briefly with PBS for 15 min and the tissue was submersed in sucrose gradient solutions of 10%, 20% and 30% sucrose for 16 hours at 4 °C. Eyes were embedded in OCT compound and cryopreserved in -80°C until further use. Using a cryostat, OCT embedded retinal sections of 10μm thickness were obtained. Blocking was carried out using 5% normal donkey serum containing 5% BSA in PBS for 1 hour. Primary antibodies used were mouse anti-TOM20 (1:100, #WH0009804M1ab69611, Millipore Sigma), rabbit anti-LC3B (1:100, #L7543, Millipore Sigma) and goat anti-Brn3a (1:200, #sc31984, Santa Cruz Biotechnology). Secondary antibody incubation for 1 hr was carried out at room temperature. Secondary antibodies used were either donkey anti-mouse Alexa 546 (1:1000, Invitrogen), donkey anti-rabbit Alexa 647 (1:1000, Invitrogen) or donkey anti-goat 488 (1:1000, Invitrogen). Retinal sections incubated with no primary antibody served as the blank to assess non-specific staining by the secondary antibodies. Sections were mounted using Prolong® Gold antifade reagent with DAPI (P36931, Invitrogen). Z-stack images (60X magnification) were taken using a Zeiss LSM 880 Airyscan Confocal Laser Scanning microscope.

2.7 Quantitation of co-localization of immunofluoroscent primary RGCs

Colocalization analysis of primary RGCs stained with either Mitotracker /Lysotracker and LC3/TOM20 were performed using Coloc2 (Fiji's plugin for co-localization analysis). Background subtraction was carried out by a Rolling-Ball Background Subtraction of 50 pixels. Primary RGCs were outlined using the freehand drawing tool. Similarly, for the retina sections, freehand region of interest (ROI) tool was used to outline the RGC layer. Point spread function (PSF) was calculated using the Colocalization Test to estimate PSF number. For this study, PSF was set to 10 and Costes randomizations were set to 100. Mander's overlap coefficient corresponding to the TOM20 image channel was used to quantify the number of mitochondria co-localizing with LC3 as described by (Dunn et al., 2011). For primary RGCs, at least 40-50 cells per group (control vs ET-1) were imaged to quantify the co-localization between Mitotracker and Lysotracker.

2.8 Induction of ocular hypertension using Morrison model in adult Brown Norway rats

IOP elevation was carried out in one eye of four retired breeder Brown Norway rats while the companion eye was used as the corresponding contralateral control eye by injection of hypertonic saline through episcleral veins. Briefly, rats were sedated by inhalation of isoflurane and anaesthesia was ensured by lack of a toe pinch reflex. Following a small conjunctival incision to expose the episcleral veins, hypertonic saline (1.8 M NaCl) was injected into an episcleral vein using a glass needle (TIP01TW1F, World Precision Instruments) at a rate of 309 μL/min for 10 to 20 seconds. Approximately, 50 to 100 µl of hypertonic saline was injected into the episcleral veins producing scarring of the trabecular meshwork. IOP was measured two times per week using a hand-held TonoLab tonometer (iCare, Finland). Six IOP measurements were averaged for each IOP measurement and ten IOP measurements were obtained for each eye. IOP plots were generated

from IOP values obtained from the surgically treated IOP elevated eye as well as the contralateral control eye. The IOP exposure in each rat was computed by the integral product of the extent of IOP elevation and the number of days of IOP elevation (expressed as mm Hg-days).

2.9 Intravitreal injection of ET-1

ET-1 peptide was purchased from Bachem (Torrance, CA) and dissolved to a stock concentration of 500 μM. 3 GFP/LC3 mice were intravitreally injected in one eye with 2 μl of 500 μM ET-1 in water while the contralateral eye was injected with water. Mice were euthanized 24 hours after injection using carbon dioxide (100%).

Statistical analysis

GraphPad Prism 8 (La Jolla, CA, USA) was used to perform statistical analysis. The two experimental groups (control vs treated) were compared by Student's t-test. Statistical significance of the experimental data was described as *$p < 0.05$; **$p < 0.01$, ***$p<0.001$, ****$p<0.0001$. Data are presented as mean ±SEM.

3. Results

3.1 ET-1 significantly decreases mitochondrial respiration following ET-1 treatment in primary RGCs

Our previous data (Chaphalkar et al., 2020) showed that ET-1 treatment for 4h and 24h significantly declined the rate of ATP production in cultured RGCs. This indicated a possibility

that ET-1 treatment generated constant metabolic stress in the primary RGCs, which prompted us to evaluate the effect of ET-1 on mitochondrial respiratory function. We determined the OCR following ET-1 treatment for 4h and 24hr using the Seahorse XF Cell Mito Stress Test kit, before and after injecting oligomycin, FCCP, and rotenone/antimycin A. OCR measurements were carried out following sequential injections of modulators of the electron transport chain, namely, oligomycin (1.5 μM), FCCP (2 μM), as well as rotenone & antimycin A (0.5 μM each). These OCR measurements enable us to measure the key parameters of mitochondrial function including basal respiration, maximal respiration, ATP-linked mitochondrial respiration, proton leak and spare respiratory capacity.

Representative OCR profiles in primary RGCs following ET-1 4h and 24h are depicted in Fig. 1A and 1B. After oligomycin injection, the OCR was decreased for both 4h and 24h time points of ET-1 (Fig. 1A and 1B). For the 4h time-point of ET-1 treatment, we observed a significant decrease of 29% in the basal rate of respiration from 28.8 ± 1.7 to 20.38 ± 1.9 ($p=0.006$). This decrease indicates a significant decline in endogenous ATP synthetic capacity of the cells with ET-1 treatment. The maximal respiration was significantly reduced by 34% with a decrease from 39.69 ± 3.2 to 26.2 ± 2.7 ($p=0.008$). A decrease in maximal respiratory capacity is revealed by a reduction in FCCP-stimulated respiration of the cells, since FCCP causes the mitochondria to function at maximal activity resulting in rapid oxidation of mitochondrial substrates to meet this metabolic challenge. This significant decrease in the maximal respiratory OCR of the ET-1 treated RGCs compared to the control indicates the effect of ET-1 to cause mitochondrial dysfunction (a decreased capacity to respond to an increased energy demand). There was also a significant decrease of 31% observed in ATP-linked OCR with ET-1 compared to control from 19.65 ± 1.47

to 13.50 ± 1.22 (p=0.007). The spare respiratory capacity which is a measurement of the difference between the basal respiration and protonophore-stimulated respiration was significantly reduced at ET-1 4h by 53% compared to the control. The spare respiratory capacity was decreased from 10.85±1.7 to 5.82±1.0 (p=0.036) with ET-1 treatment for 4h (Fig. 1C). This signifies a decreased capability of the RGCs to respond to an increased demand of ATP and withstand metabolic stress within the cells.

For the 24h time-point of ET-1 treatment, there was a decrease in basal respiration with ET-1 by 30% from 31.99 ± 2.38 to 22.29 ±3.5 (p=0.03) compared to the control RGCs. There was a significant decrease in maximal respiration by 28% from 48.65±3.23 to 34.79 ± 3.5 (p=0.01). ATP-linked respiration reduced by 45% from 23.25 ± 1.6 to 12.84 ± 0.72 (p<0.0001) (Fig 1D). There was an appreciable decrease of 25% in the spare respiratory capacity from 16.66 ± 3.8 to 12.51 ± 2.3, although it was not statistically significant.

In addition, the decline in ATP-linked OCR observed at ET-1 24h was more drastic than the ET-1 4h time point. There was no significant difference observed in proton leak at both time-points compared to the control. The above results were representative of three independent biological replicates (n=3).

3.2 ET-1 decreases co-localization of mitotracker and lysotracker in primary RGCs

Impairment of mitochondrial bioenergetics in primary RGCs following ET-1 implied a possibility of a compromise in the mitochondrial quality control system. Maintaining a healthy mitochondrial network requires a clearance of accumulated defective mitochondria and one of the mechanism of mitochondrial clearance occurs via a process called mitophagy (Ashrafi and Schwarz, 2013). The

initial step in mitophagy pathway process is the recruitment of damaged mitochondria to the autophagosomes, a double-membraned structure that incorporates the Atg family protein, LC3, which is used as a selective marker of autophagosomes. We investigated whether there is a change in the mitophagy with ET-1 compared to the basal levels (control) in primary RGCs.

Primary rat RGCs were treated with ET-1 for 24h, following which the co-localization of MitoTracker Deep Red and Lysotracker was analyzed. MitoTracker red allows the visualization of active mitochondria, while Lysotracker was used to label the lysosomes. In cell culture studies, co-localization between MitoTracker and LysoTracker or mitochondrial and lysosomal proteins provides a measurement of mitophagy. The co-localization of MitoTracker and LysoTracker is indicative of mitophagy (Redmann et al., 2018). Quantification of co-localization puncta further acts as a reliable indicator of occurrence of mitophagy in the cell.

Immunocytochemistry revealed that there was a robust staining for MitoTracker red and Lysotracker in control RGCs, suggestive of robust mitophagy occurring under basal conditions (Fig. 2A). However, following a 24h of ET-1 treatment, there was a decrease in the co-localization intensity of MitoTracker and LysoTracker, suggesting a reduction in mitophagy compared to the untreated control cells. The merge panel showed that, with ET-1 treatment, there was a decrease in co-localization puncta of MitoTracker and LysoTracker. Quantitation of the co-localization pixels between MitoTracker and LysoTracker was measured by Mander's overlap co-efficient (MOC) using a Coloc2 plugin on ImageJ. There was a significant decrease in MOC from 0.43 ± 0.04 to 0.22 ± 0.04 ($p<0.01$, $n=3$ per group, Student's t-test). These results indicate a decrease in mitophagy in primary RGCs with ET-1 treatment (24h) compared to control.

3.3 Elevated IOP decreases formation of mitophagosomes in adult Brown Norway rats in retinal ganglion cells

Injection of hypertonic saline into episcleral veins was used to elevate IOP in one eye (Morrison et al., 1997). Four retired breeder Brown Norway rats were IOP elevated in one eye using the other eye as the contralateral control. As seen in Fig. 3A, IOP elevation was detected 10 days after surgery and remained elevated for 2 weeks following which the rats were euthanized. Representative mean values of IOP exposure during for the study were 96 mmHg-days.

Retina sections were obtained from rats and immunostaining was carried out using the antibodies to LC3B and TOM20. We measured the cellular distribution of the autophagosome adapter protein LC3B and the mitochondrial outer membrane marker Tom20, specifically in the RGC layer of these retina sections. The LC3B antibody used for the study recognizes the cytosolic LC3 form, LC3B-I as well as autophagosome membrane bound form, LC3B-II. The number of mitochondrial autophagosomes in retinas of IOP-elevated eye compared to the contralateral eyes was measured by quantifying the co-localization puncta between LC3B and TOM20. Images obtained from the Airyscan confocal image Z-stacks, were analyzed for estimating the Mander's overlap co-efficient in the ganglion cell layer. The co-localization puncta were significantly decreased in IOP-elevated eyes compared to the contralateral eye (Fig. 3B). The Coloc2 plugin on ImageJ, was used to determine the Mander's overlap coefficient and Pearson's correlation co-efficient, corresponding to the proportion of colocalized pixels (LC3B and TOM20 positive) over TOM20 positive pixels. tM1 or tM2 (thresholded Mander's coefficient) value corresponding to TOM20 channel was used for quantitation. IOP elevation significantly decreased tM value 0.69 ± 0.02 to 0.44 ± 0.04 ($p<0.0001$, n=4 retinas, Student's t-test) (Fig. 3C).

Taken together, the data indicated that there was a significant decrease, (approximately 2-fold) in the number of mitophagosome formation in IOP-elevated rat eyes compared to the contralateral eyes.

3.4 ET-1 treatment for 24h decreases autophagosome formation in GFP-LC3 transgenic mice in retinal ganglion cells

To determine if there is an ET-1-mediated change in number of mitophagosome formation, we carried out the *in vivo* studies using GFP-LC3 transgenic mice. The GFP-LC3 mice ubiquitously expresses green fluorescent protein (GFP)-fused LC3 (GFP-LC3) under the constitutive CAG promoter (cytomegalovirus immediate-early (CMVie) enhancer and chicken β-actin promoter). LC3, the mammalian homologue of yeast Atg8, is present on the phagophore as well as on autophagosomal membrane, hence when GFP-LC3 is expressed, punctate structures are observed by fluorescence microscopy. This transgenic model allows us to monitor occurrence of autophagy by performing immunohistochemistry of frozen sections and analyzing the stained sections using a fluorescent microscope (Wang, Liu, and Lu 2019). The mice were intravitreally injected with ET-1 (1 nmole in 1 μl) (24 h) in one eye while the contralateral eye was injected with vehicle (water). Analysis of the co-localization of the puncta corresponding to LC3B positive and TOM20 positive overlapping pixels was performed using the Coloc2 plugin in ImageJ. We assessed the immunoreactivity for LC3B and TOM20 co-localization in ganglion cells. In the vehicle treated eyes, co-localization of the immunoreactivity for LC3B and TOM20 was higher, compared to the ET-1 injected retina (Fig. 4A).

Quantitation analysis was carried out by estimating the Mander's overlap co-efficient. There was a significant decrease in the tM1 or tM2 values corresponding to the TOM20 channel from 0.52 ± 0.02 to 0.45±0.01 ($p=0.01$, $n=3$, Student's t-test) (Fig. 4B). These results implied that there was a significant decline in the number of mitophagosomes with ET-1 treatment for 24h in the ganglion cell layer.

4. Discussion

Previous studies have reported that there is an increased mitochondrial dysfunction in aging population (Cui et al., 2012; Jang et al., 2018; Trifunovic and Larsson, 2008) and importantly, age is an established risk factor in development of glaucoma (Leske et al., 1994; Mitchell et al., 1996; Rochtchina et al., 2002). With age, increased oxidative stress and ROS production can trigger mitochondrial dysfunction which could further exacerbate the accumulation of ROS to form a vicious cycle accelerating the cellular damage. Hence, oxidative stress and mitochondrial dysfunction are key contributors to several neurodegenerative diseases (Muddapu et al. 2020). There have been several review articles illustrating the involvement of chronic oxidative stress and ROS leading to RGC loss in glaucoma (Chrysostomou et al. 2013; Izzotti, Bagnis, and Sacca 2006; Osborne and del Olmo-Aguado 2013). However, there is a lack of explanation of the cause of vulnerability of RGCs to mitochondrial damage. One of the important possible explanation underlying the susceptibility of the RGCs to mitochondrial dysfunction is their unique metabolic requirements and complex architecture. Mitochondrial biosynthesis occurs in the RGC soma, located in the ganglion cell layer, but the energy requirements extend to axonal as well as dendritic arbors projecting into the inner plexiform layer to establish synaptic connections with other retinal neurons. Hence, the synapses in dendritic arbors are densely packed with mitochondria because an

extraordinarily high amount of energy is required to synthesize and release neurotransmitters, organize the synaptic vesicle pool, regulate calcium homoeostasis and restore the ion gradients at the active sites (Vos, Lauwers, and Verstreken 2010).

In this study, we have investigated the effects of ET-1 treatment on mitochondrial function at two time points (4 h and 24 h) in cultured RGCs and *in vivo* using GFP-LC3 transgenic mice (at 24 h). We found that in primary RGCs at both time points of ET-1 treatment, there was a significant decline in the key mitochondrial bioenergetic parameters, including, ATP-linked respiration, basal respiratory capacity, maximum respiratory capacity and spare respiratory capacity (Fig. 1). These findings suggest that one of the mechanisms underlying ET-1 mediated neurodegeneration in RGCs involves mitochondrial dysfunction and alterations in oxidative phosphorylation pathway. In our previous study, we observed a decrease in expression of key mitochondrial proteins, cytochrome c oxidase copper chaperone (COX17) (3- fold), and ATP synthase, H^+ transporting mitochondrial F0 complex (ATP5H), following 2 weeks of IOP elevation in Morrison's model of glaucoma (Chaphalkar et al., 2020). A decrease in the critical components of the electron transport chain and oxidative phosphorylation machinery could create conditions favorable for generation of reactive oxygen species. Increased oxidative stress by ET_B receptor activation could possibly be a strong contributor leading to impairment of mitochondrial bioenergetics in RGCs. For instance, (Lau et al. 2006) have demonstrated an appreciable increase in superoxides in inferior mesenteric ganglion in rats infused intravenously with sarafotoxin (an ET_B receptor agonist). One possible mechanism by which ET_B receptor activation elevates oxidative stress is through activation of NADPH oxidase (Dammanahalli and Sun 2008; Tam et al. 2019). Reactive oxygen species including superoxides are known to produced opening of the permeability transition pore, dissipating the mitochondrial membrane potential, thereby producing mitochondrial damage and

compromising the ability to synthesize ATP. Preserving basal mitochondrial homeostasis is therefore critically important to respond to this mitochondrial damage and maintain the quality control of mitochondria.

As briefly mentioned in the introduction, mitophagy is the only way a cell can eliminate the damaged mitochondria which makes it a crucial component of mitochondrial quality control. We observed that there is a decrease in mitophagy in cultured RGCs with 24h of ET-1 treatment (Fig.2). Usually during mitophagy, when mitochondria are depolarized, a E3 ubiquitin ligase (Parkin) is recruited to the outer mitochondrial membrane due to accumulation of PTEN-induced kinase1 (PINK1), facilitating ubiquitination of outer mitochondrial membrane proteins leading to PINK1/Parkin mediated mitophagy (Jin and Youle 2012). Parkin ubiquitinates several outer mitochondrial membrane proteins. Optineurin and NDP52 are two autophagy receptors with LC-3 interacting region (LIR) domains that bind to ubiquitinated outer mitochondrial proteins, bringing the mitochondria closer to the phagophore and induce autophagy (Villa, Marchetti, and Ricci 2018). This process is initiated by sequestering the individual damaged mitochondria by recruiting the phagophore protein LC3, leading to the formation of mitophagosomes and their subsequent fusion with lysosomes (Wong and Holzbaur 2015). In the present study, we assessed the changes in mitophagosome formation following IOP elevation of 2 weeks in adult Brown Norway rats. This *in vivo* study showed a significant decrease in co-localization of LC3B-TOM20 indicating a decrease in mitophagosome formation in the RGC layer (Fig. 3). Previous studies have demonstrated that there is an increase in the number of mitophagosomes and mitophagy was observed in the glaucomatous D2 mice (Kim et al., 2015). Similarly, overexpression of parkin exerted a significant protective effect on RGCs and partially restored dysfunction of mitophagy in

response to cumulative IOP elevation (Dai et al., 2018). However, a significant increase in number of autophagosomes was observed in the optic nerve of aging DBA/2J mice at all ages compared to the age-matched controls, but surprisingly these defective mitochondria were not targeted towards autophagosomes indicating lack of mitophagy initiation (Coughlin et al., 2015). Contrary to our findings, Hirt et al., (2018) reported an overactivation of autophagy as a potential cellular mechanism leading to ON degeneration in the chronic hypertensive DBA/2J mice. Some these discrepancies in the findings could be due to the glaucoma model and the duration of IOP elevation at which autophagy is being assessed.

It is evident from all the previous studies in literature that different experimental models, timing of analysis following onset of IOP elevation as well as age of the animals are critical in evaluation of activation of autophagy and measurement of autophagic flux. In 12 month old DBA/2J mice, there was a decrease in protein levels of LC3, p62 and LAMP1 in RGCs suggesting a decreased autophagy which is contradictory to several other studies. However, in RGCs of DBA/2J::GFP-LC3 mice, an increased amounts of autophagosome-associated LC3 (LC3-II, LC3 puncta) was found, however the autophagic flux was diminished in the outflow pathway region of DBA/2J hypertensive mice compared to age-matched C57BL/6J (Hirt et al., 2018). Meanwhile, our LC3-TOM20 co-localization data in GFP-LC3 mice intravitreally injected with ET-1 showed a decrease in the co-localization puncta indicating a decrease in mitophagosome formation (Fig. 4). It can be inferred from all these studies that an increase in autophagic vacuoles or mitophagosomes is not necessarily indicative of progression towards an increase in mitophagy or autophagy. Failure of mitophagosomes to fuse with lysosomes or impairment in lysosomal degradative capacity or lysosomal destabilization can lead to an impairment in the mitophagic flux.

In summary, we have described here for the first time, an impairment in formation of mitophagosomes in RGCs following Morrison's model of IOP elevation as well as in ET-1 injected GFP-LC3 mice and in primary RGCs *in vitro*. Mitophagy in RGCs has not been studied extensively and it would be interesting to further investigate the pathway following formation of mitophagosomes. Whether the mitophagosomes are transported to the lysosomes for degradation triggering induction of mitophagy or if there is an accumulation and inefficient recycling of mitophagosomes resulting in a potential defect in mitophagy pathway remains to be seen. Interplay of different events including mitochondrial fusion/fission dynamics, mitochondrial biogenesis and degradation play a key role in formation of mitophagosomes and ultimately regulation of the process of mitophagy. Regardless, our findings suggest an impairment in formation of mitophagosomes and mitochondrial dysregulation specifically in RGCs, which may help to understand the mechanism of mitochondrial dysfunction in neurodegeneration of glaucoma.

References

1. Abu-Amero, K.K., Morales, J., Bosley, T.M., 2006. Mitochondrial abnormalities in patients with primary open-angle glaucoma. Invest Ophthalmol Vis Sci 47, 2533-2541.
2. Ashrafi, G., Schwarz, T.L., 2013. The pathways of mitophagy for quality control and clearance of mitochondria. Cell Death & Differentiation 20, 31-42.
3. Barres, B.A., Silverstein, B.E., Corey, D.P., Chun, L.L., 1988. Immunological, morphological, and electrophysiological variation among retinal ganglion cells purified by panning. Neuron 1, 791-803.

4. Boland, M.V., Quigley, H.A., 2007. Risk factors and open-angle glaucoma: classification and application. J Glaucoma 16, 406-418.
5. Chaphalkar, R.M., Stankowska, D.L., He, S., Kodati, B., Phillips, N., Prah, J., Yang, S., Krishnamoorthy, R.R., 2020. Endothelin-1 Mediated Decrease in Mitochondrial Gene Expression and Bioenergetics Contribute to Neurodegeneration of Retinal Ganglion Cells. Sci Rep 10, 3571.
6. Chauhan, B.C., 2008. Endothelin and its potential role in glaucoma. Canadian Journal of Ophthalmology 43, 356-360.
7. Chauhan, B.C., LeVatte, T.L., Jollimore, C.A., Yu, P.K., Reitsamer, H.A., Kelly, M.E.M., Yu, D.-Y., Tremblay, F.o., Archibald, M.L., 2004. Model of Endothelin-1–Induced Chronic Optic Neuropathy in Rat. Investigative Ophthalmology & Visual Science 45, 144-152.
8. Chidlow, G., Wood, J.P.M., Casson, R.J., 2017. Investigations into Hypoxia and Oxidative Stress at the Optic Nerve Head in a Rat Model of Glaucoma. Front Neurosci 11, 478.
9. Choritz, L., Machert, M., Thieme, H., 2012. Correlation of endothelin-1 concentration in aqueous humor with intraocular pressure in primary open angle and pseudoexfoliation glaucoma. Invest Ophthalmol Vis Sci 53, 7336-7342.
10. Cioffi, G.A., Sullivan, P., 1999. The Effect of Chronic Ischemia on the Primate Optic Nerve. European Journal of Ophthalmology 9, S34-S36.
11. Dunn, K.W., Kamocka, M.M., McDonald, J.H., 2011. A practical guide to evaluating colocalization in biological microscopy. American Journal of Physiology-Cell Physiology 300, C723-C742.

12. Källberg, M.E., Brooks, D.E., Garcia-Sanchez, G.A., Komàromy, A.M., Szabo, N.J., PhD, L.T., 2002. Endothelin 1 Levels in the Aqueous Humor of Dogs With Glaucoma. Journal of Glaucoma 11, 105-109.
13. Krishnamoorthy, R.R., Rao, V.R., Dauphin, R., Prasanna, G., Johnson, C., Yorio, T., 2008. Role of the ETB receptor in retinal ganglion cell death in glaucomaThis article is one of a selection of papers published in the special issue (part 1 of 2) on Forefronts in Endothelin. Canadian Journal of Physiology and Pharmacology 86, 380-393.
14. Lau, J., Dang, M., Hockmann, K., Ball, A.K., 2006. Effects of acute delivery of endothelin-1 on retinal ganglion cell loss in the rat. Experimental Eye Research 82, 132-145.
15. Liu, L., Feng, D., Chen, G., Chen, M., Zheng, Q., Song, P., Ma, Q., Zhu, C., Wang, R., Qi, W., Huang, L., Xue, P., Li, B., Wang, X., Jin, H., Wang, J., Yang, F., Liu, P., Zhu, Y., Sui, S., Chen, Q., 2012. Mitochondrial outer-membrane protein FUNDC1 mediates hypoxia-induced mitophagy in mammalian cells. Nature Cell Biology 14, 177-185.
16. MacCumber, M.W., D'Anna, S.A., 1994. Endothelin Receptor-Binding Subtypes in the Human Retina and Choroid. Archives of Ophthalmology 112, 1231-1235.
17. Matsuda, N., Sato, S., Shiba, K., Okatsu, K., Saisho, K., Gautier, C.A., Sou, Y.-s., Saiki, S., Kawajiri, S., Sato, F., Kimura, M., Komatsu, M., Hattori, N., Tanaka, K., 2010. PINK1 stabilized by mitochondrial depolarization recruits Parkin to damaged mitochondria and activates latent Parkin for mitophagy. Journal of Cell Biology 189, 211-221.
18. Minton, A.Z., Phatak, N.R., Stankowska, D.L., He, S., Ma, H.-Y., Mueller, B.H., Jiang, M., Luedtke, R., Yang, S., Brownlee, C., Krishnamoorthy, R.R., 2012. Endothelin B Receptors Contribute to Retinal Ganglion Cell Loss in a Rat Model of Glaucoma. PLOS ONE 7, e43199.

19. Mizushima, N., Yamamoto, A., Matsui, M., Yoshimori, T., Ohsumi, Y., 2004. In vivo analysis of autophagy in response to nutrient starvation using transgenic mice expressing a fluorescent autophagosome marker. Mol Biol Cell 15, 1101-1111.
20. Morrison, J.C., Moore, C.G., Deppmeier, L.M., Gold, B.G., Meshul, C.K., Johnson, E.C., 1997. A rat model of chronic pressure-induced optic nerve damage. Exp Eye Res 64, 85-96.
21. Nguyen, D., Alavi, M.V., Kim, K.Y., Kang, T., Scott, R.T., Noh, Y.H., Lindsey, J.D., Wissinger, B., Ellisman, M.H., Weinreb, R.N., Perkins, G.A., Ju, W.K., 2011. A new vicious cycle involving glutamate excitotoxicity, oxidative stress and mitochondrial dynamics. Cell Death Dis 2, e240.
22. Pinazo-Duran, M.D., Shoaie-Nia, K., Zanon-Moreno, V., Sanz-Gonzalez, S.M., Del Castillo, J.B., Garcia-Medina, J.J., 2018. Strategies to Reduce Oxidative Stress in Glaucoma Patients. Curr Neuropharmacol 16, 903-918.
23. Redmann, M., Benavides, G.A., Wani, W.Y., Berryhill, T.F., Ouyang, X., Johnson, M.S., Ravi, S., Mitra, K., Barnes, S., Darley-Usmar, V.M., Zhang, J., 2018. Methods for assessing mitochondrial quality control mechanisms and cellular consequences in cell culture. Redox Biology 17, 59-69.
24. Tezel, G., Kass, M.A., Kolker, A.E., Becker, B., Wax, M.B., 1997. Plasma and aqueous humor endothelin levels in primary open-angle glaucoma. Journal of glaucoma 6, 83-89.

Tezel, G.l.n., Li, L.Y., Patil, R.V., Wax, M.B., 2001. TNF-α and TNF-α Receptor-1 in the Retina of Normal and Glaucomatous Eyes. Investigative Ophthalmology & Visual Science 42, 1787-1794.

25. Wang, Y., Liu, N., Lu, B., 2019. Mechanisms and roles of mitophagy in neurodegenerative diseases. CNS Neurosci Ther 25, 859-875.

26. Wang, Y., Nartiss, Y., Steipe, B., McQuibban, G.A., Kim, P.K., 2012. ROS-induced mitochondrial depolarization initiates PARK2/PARKIN-dependent mitochondrial degradation by autophagy. Autophagy 8, 1462-1476.
27. Weinreb, R.N., Leung, C.K., Crowston, J.G., Medeiros, F.A., Friedman, D.S., Wiggs, J.L., Martin, K.R., 2016. Primary open-angle glaucoma. Nat Rev Dis Primers 2, 16067.
28. Williams, P.A., Harder, J.M., Foxworth, N.E., Cochran, K.E., Philip, V.M., Porciatti, V., Smithies, O., John, S.W.M., 2017. Vitamin B₃ modulates mitochondrial vulnerability and prevents glaucoma in aged mice. Science 355, 756-760.
29. Yorio, T., Krishnamoorthy, R., Prasanna, G., 2002. Endothelin: Is It a Contributor to Glaucoma Pathophysiology? Journal of Glaucoma 11, 259-270.
30. Agarwal, R., Agarwal, P., 2012. Glaucomatous neurodegeneration: an eye on tumor necrosis factor-alpha. Indian J Ophthalmol 60, 255-261.
31. Chauhan, B.C., 2008. Endothelin and its potential role in glaucoma. Canadian Journal of Ophthalmology 43, 356-360.
32. Choritz, L., Machert, M., Thieme, H., 2012. Correlation of endothelin-1 concentration in aqueous humor with intraocular pressure in primary open angle and pseudoexfoliation glaucoma. Invest Ophthalmol Vis Sci 53, 7336-7342.
33. Chrysostomou, V., Rezania, F., Trounce, I.A., Crowston, J.G., 2013. Oxidative stress and mitochondrial dysfunction in glaucoma. Curr Opin Pharmacol 13, 12-15.
34. Dai, Y., Hu, X., Sun, X., 2018. Overexpression of parkin protects retinal ganglion cells in experimental glaucoma. Cell Death & Disease 9, 88.
35. Dammanahalli, K.J., Sun, Z., 2008. Endothelins and NADPH oxidases in the cardiovascular system. Clin Exp Pharmacol Physiol 35, 2-6.

36. Hirt, J., Porter, K., Dixon, A., McKinnon, S., Liton, P.B., 2018. Contribution of autophagy to ocular hypertension and neurodegeneration in the DBA/2J spontaneous glaucoma mouse model. Cell Death Discovery 4, 75.
37. Hu, X., Dai, Y., Zhang, R., Shang, K., Sun, X., 2018. Overexpression of Optic Atrophy Type 1 Protects Retinal Ganglion Cells and Upregulates Parkin Expression in Experimental Glaucoma. Front Mol Neurosci 11, 350.
38. Izzotti, A., Bagnis, A., Sacca, S.C., 2006. The role of oxidative stress in glaucoma. Mutat Res 612, 105-114.
39. Jin, S.M., Youle, R.J., 2012. PINK1- and Parkin-mediated mitophagy at a glance. Journal of Cell Science 125, 795-799.
40. Källberg, M.E., Brooks, D.E., Garcia-Sanchez, G.A., Komàromy, A.M., Szabo, N.J., PhD, L.T., 2002. Endothelin 1 Levels in the Aqueous Humor of Dogs With Glaucoma. Journal of Glaucoma 11, 105-109.
41. Lau, J., Dang, M., Hockmann, K., Ball, A.K., 2006. Effects of acute delivery of endothelin-1 on retinal ganglion cell loss in the rat. Experimental Eye Research 82, 132-145.
42. Leske, M.C., Heijl, A., Hussein, M., Bengtsson, B., Hyman, L., Komaroff, E., Group, f.t.E.M.G.T., 2003. Factors for Glaucoma Progression and the Effect of Treatment: The Early Manifest Glaucoma Trial. Archives of Ophthalmology 121, 48-56.
43. Li, S., Zhang, A., Cao, W., Sun, X., 2016. Elevated Plasma Endothelin-1 Levels in Normal Tension Glaucoma and Primary Open-Angle Glaucoma: A Meta-Analysis. J Ophthalmol 2016, 2678017.
44. Lin, M.T., Beal, M.F., 2006. Mitochondrial dysfunction and oxidative stress in neurodegenerative diseases. Nature 443, 787-795.

45. Minton, A.Z., Phatak, N.R., Stankowska, D.L., He, S., Ma, H.-Y., Mueller, B.H., Jiang, M., Luedtke, R., Yang, S., Brownlee, C., Krishnamoorthy, R.R., 2012. Endothelin B Receptors Contribute to Retinal Ganglion Cell Loss in a Rat Model of Glaucoma. PLOS ONE 7, e43199.
46. Muddapu, V.R., Dharshini, S.A.P., Chakravarthy, V.S., Gromiha, M.M., 2020. Neurodegenerative Diseases – Is Metabolic Deficiency the Root Cause? Frontiers in Neuroscience 14.
47. Nguyen, D., Alavi, M.V., Kim, K.Y., Kang, T., Scott, R.T., Noh, Y.H., Lindsey, J.D., Wissinger, B., Ellisman, M.H., Weinreb, R.N., Perkins, G.A., Ju, W.K., 2011. A new vicious cycle involving glutamate excitotoxicity, oxidative stress and mitochondrial dynamics. Cell Death Dis 2, e240.
48. Osborne, N.N., del Olmo-Aguado, S., 2013. Maintenance of retinal ganglion cell mitochondrial functions as a neuroprotective strategy in glaucoma. Curr Opin Pharmacol 13, 16-22.
49. Pascale, A., Drago, F., Govoni, S., 2012. Protecting the retinal neurons from glaucoma: lowering ocular pressure is not enough. Pharmacol Res 66, 19-32.
50. Prasanna, G., Hulet, C., Desai, D., Krishnamoorthy, R.R., Narayan, S., Brun, A.-M., Suburo, A.M., Yorio, T., 2005. Effect of elevated intraocular pressure on endothelin-1 in a rat model of glaucoma. Pharmacological Research 51, 41-50.
51. Seki, M., Lipton, S.A., 2008. Targeting excitotoxic/free radical signaling pathways for therapeutic intervention in glaucoma. Prog Brain Res 173, 495-510.
52. Tam, S.W., Feng, R., Lau, W.K., Law, A.C., Yeung, P.K., Chung, S.K., 2019. Endothelin type B receptor promotes cofilin rod formation and dendritic loss in neurons by inducing oxidative stress and cofilin activation. J Biol Chem 294, 12495-12506.

53. Tezel, G., Kass, M.A., Kolker, A.E., Becker, B., Wax, M.B., 1997. Plasma and aqueous humor endothelin levels in primary open-angle glaucoma. Journal of glaucoma 6, 83-89.

54. Tezel, G.l.n., Li, L.Y., Patil, R.V., Wax, M.B., 2001. TNF-α and TNF-α Receptor-1 in the Retina of Normal and Glaucomatous Eyes. Investigative Ophthalmology & Visual Science 42, 1787-1794.

55. Villa, E., Marchetti, S., Ricci, J.E., 2018. No Parkin Zone: Mitophagy without Parkin. Trends Cell Biol 28, 882-895.

56. Vos, M., Lauwers, E., Verstreken, P., 2010. Synaptic Mitochondria in Synaptic Transmission and Organization of Vesicle Pools in Health and Disease. Frontiers in Synaptic Neuroscience 2.

57. Wong, Y.C., Holzbaur, E.L., 2015. Temporal dynamics of PARK2/parkin and OPTN/optineurin recruitment during the mitophagy of damaged mitochondria. Autophagy 11, 422-424.

58. Yorio, T., Krishnamoorthy, R., Prasanna, G., 2002. Endothelin: Is It a Contributor to Glaucoma Pathophysiology? Journal of Glaucoma 11, 259-270.

Figure legends

Figure 1. ET-1 decreases oxygen consumption rate (OCR) at 4h and 24h in primary RGCs.

A. Representative OCR profiles showing OCR recordings at baseline and after treatment with oligomycin, FCCP and rotenone/Antimycin A at ET-1 4h. **B.** Representative OCR profiles showing OCR recordings at baseline and after treatment with oligomycin, FCCP and rotenone/Antimycin A at ET-1 24h. **C.** Bar graphs showing quantitation of mitochondrial parameters including basal respiration, maximal respiration, ATP-linked respiration, spare respiratory capacity and proton leak at ET-1 4h. **D.** Bar graphs showing quantitation of mitochondrial parameters including basal respiration, maximal respiration, ATP-linked respiration, spare respiratory capacity and proton leak at ET-1 24h. Data represented as the mean ± SEM, (Student's t-test, n=3 biological replicates per group), significance at * $p < 0.05$, ** $p < 0.01$, *** $p < 0.001$, **** $p < 0.0001$.

Figure 2. ET-1 (24h) mediated decrease in co-localization of lysotracker and mitotracker in cultured primary RGCs

A. Primary RGCs were stained with Mitotracker Deep Red and Lysotracker Red (25nM) following ET-1 treatment for 24h. A decrease in co-staining (yellow) of mitotracker and lysotracker was found following ET-1 treatment indicative of decreased mitophagy. **B.** Quantitation of co-localization puncta was determined by Mander's overlap co-efficient. Data represented as the mean ± SEM, (Student's t-test, n=3 biological replicates per group), significance at ** $p < 0.01$. Data represented as mean ±SEM

Figure 3. Elevated IOP in Brown Norway rats decreases formation of mitophagosomes in retinal ganglion cells.

A. IOP was elevated by the Morrison's model of glaucoma in rats for 2 weeks – Representative graph of IOP measurements for IOP elevated (black circles) and contralateral control (white circle) eyes in adult Brown Norway rats. **B.** Retina sections obtained were stained using anti-LC3B (component of autophagosome) and anti- TOM20 (outer mitochondrial membrane protein). IOP elevated rats showing a significant decrease in co-localization puncta (as shown in white arrows) in RGCs. **C.** Quantitation of co-localization between LC3B(red) and TOM20 (green) was determined by Mander's overlap co-efficient (n=4, ***p<0.001). Scale bar =10μm. Data represented as mean ±SEM

Figure 4. ET-1 treatment for 24h decreases mitophagosome formation in GFP-LC3 transgenic mice in retinal ganglion cells.

A. OCT sections showing a significant decrease in co-localization puncta (as shown in white arrows) between GFP-LC3 (green) and anti-TOM20 (yellow) following intravitreal ET-1 injection (24h). **B.** Quantitation of co-localization between GFP-LC3 and TOM20 was determined by Mander's overlap co-efficient (n=3, *p<0.05). Scale bar =10μm. Data represented as mean ±SEM.

Figure 1

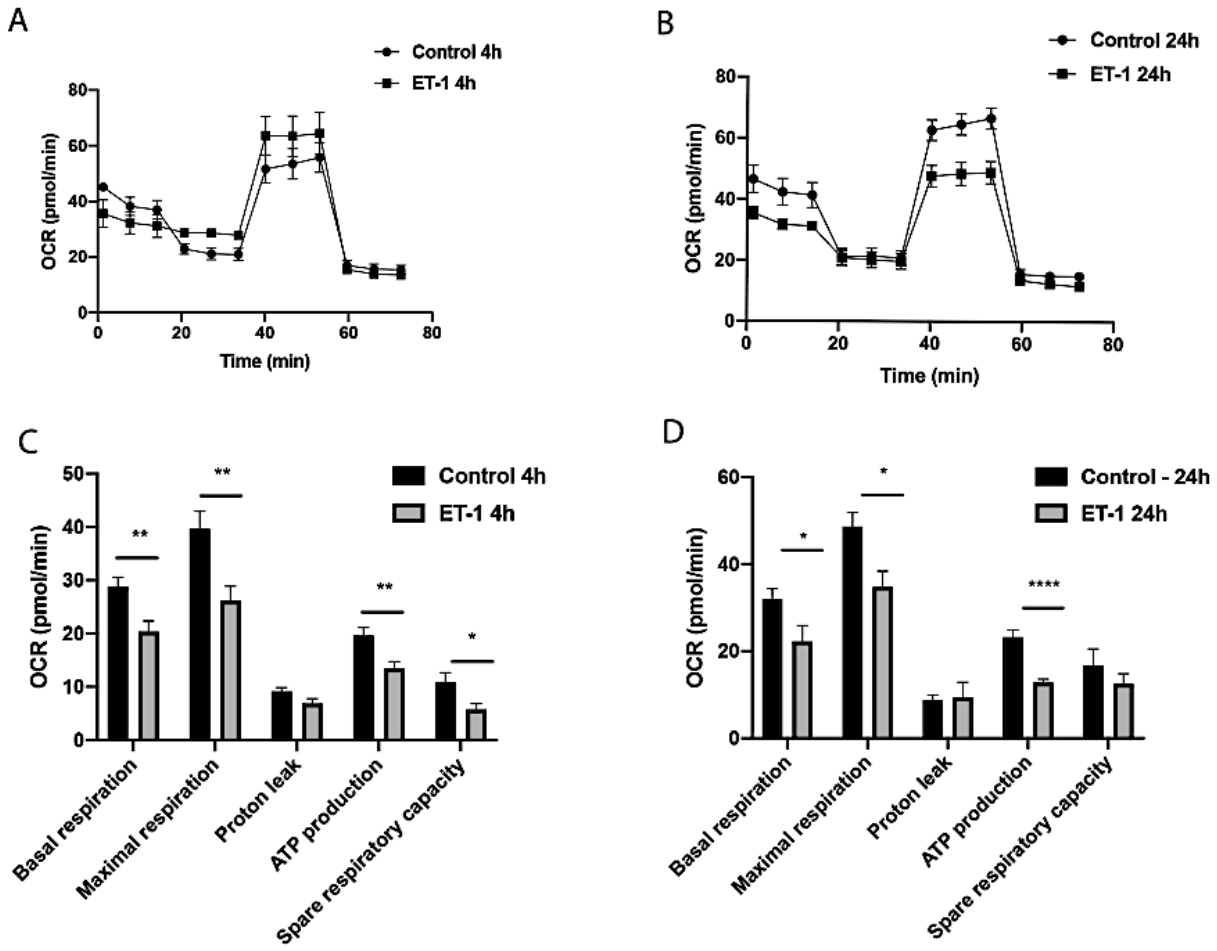
A
Control 4h
ET-1 4h
OCR (pmol/min)
Time (min)
B
Control 24h
ET-1 24h
OCR (pmol/min)
Time (min)
C
Control 4h
ET-1 4h
OCR (pmol/min)
Basal respiration
Maximal respiration
Proton leak
ATP production
Spare respiratory capacity
D
Control - 24h
ET-1 24h
OCR (pmol/min)
Basal respiration
Maximal respiration
Proton leak
ATP production
Spare respiratory capacity

Figure 2

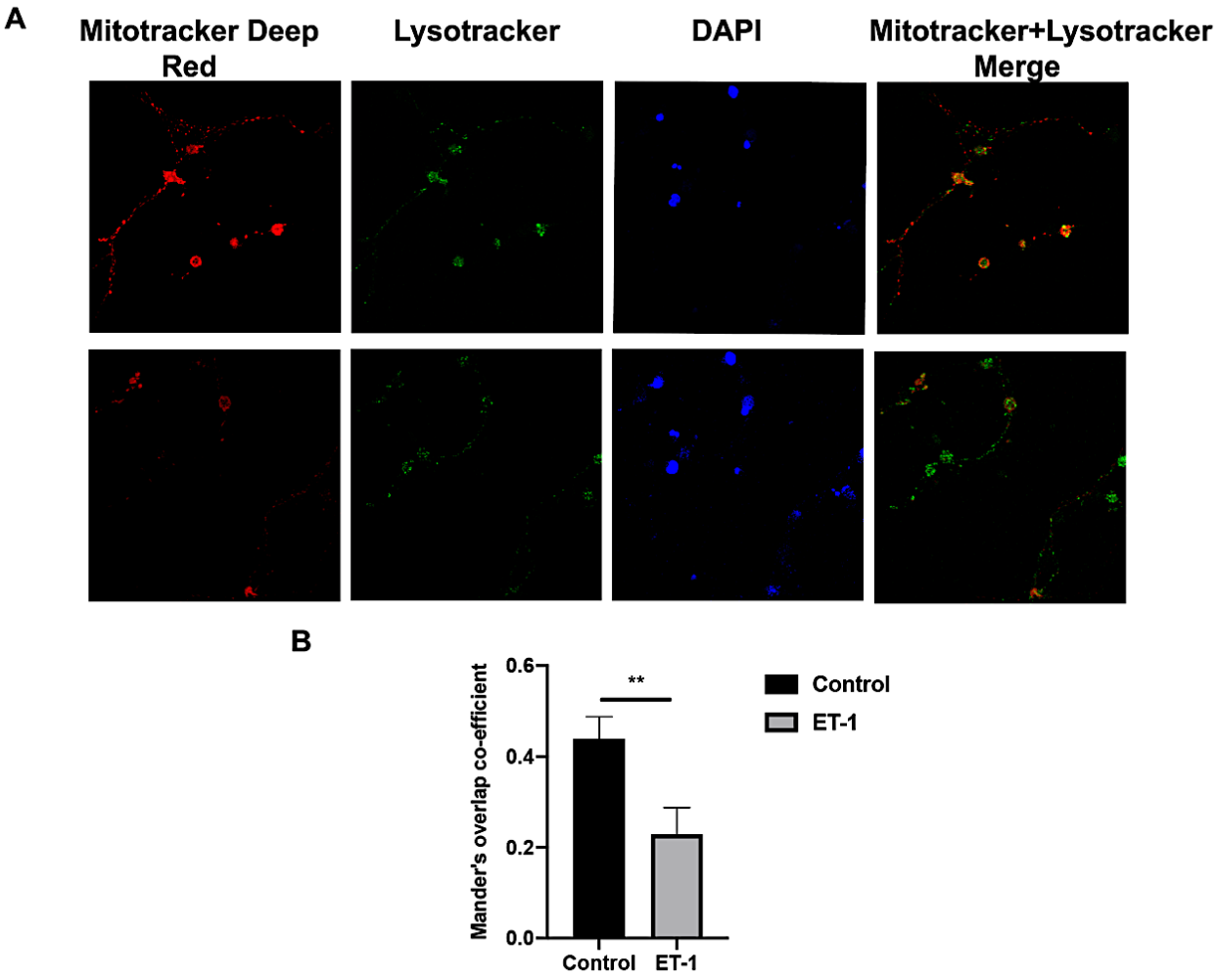
A
Mitotracker Deep Red
Lysotracker
DAPI
Mitotracker+Lysotracker Merge
B
Mander's overlap co-efficient
0.6
0.4
0.2
0.0
**
Control
ET-1
Control
ET-1

Figure 3

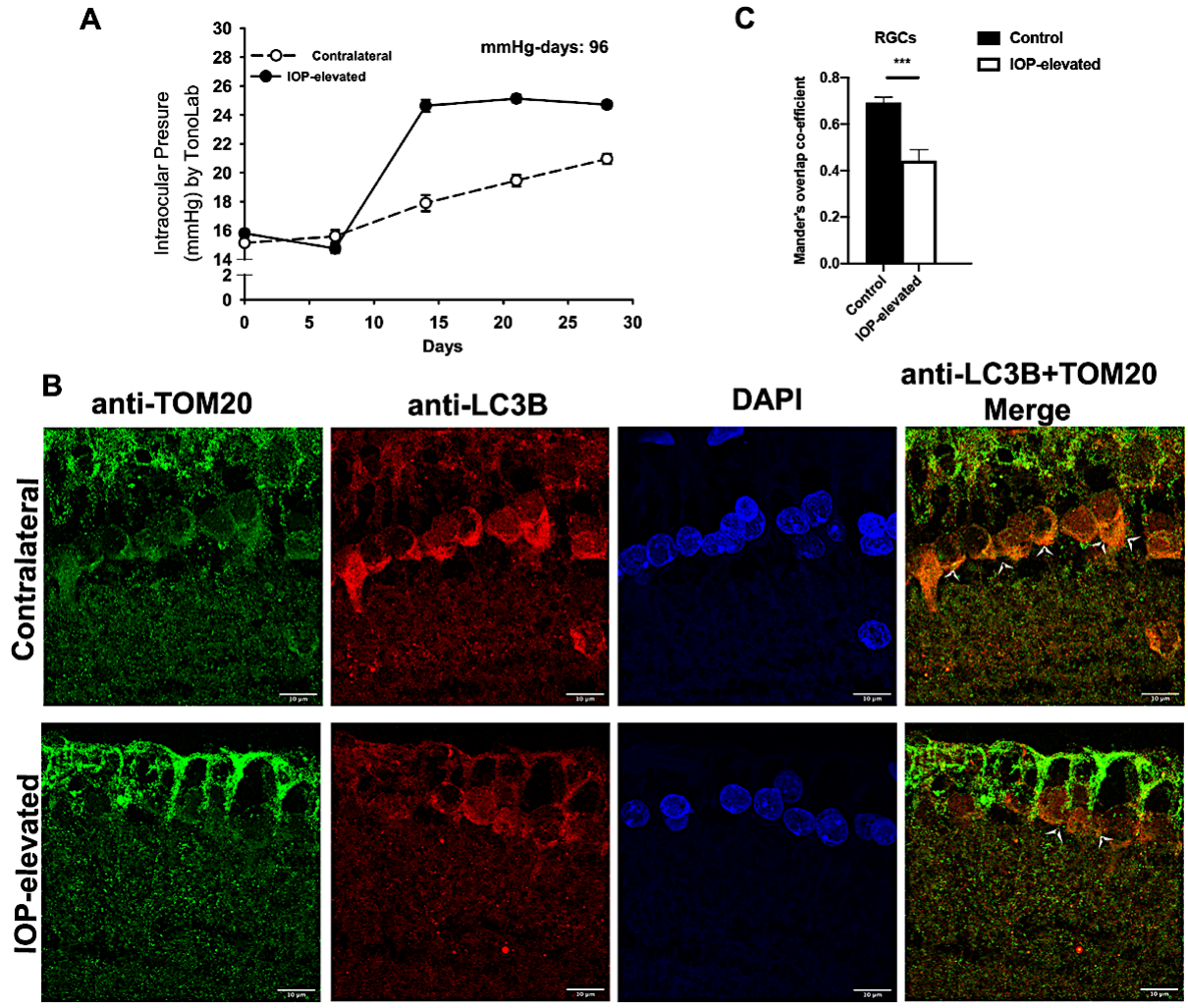
A
Contralateral
IOP-elevated
mmHg-days: 96
Intraocular Presure (mmHg) by TonoLab
Days
C
RGCs
***
Control
IOP-elevated
Mander's overlap co-efficient
Control
IOP-elevated
B
anti-TOM20
anti-LC3B
DAPI
anti-LC3B+TOM20 Merge
Contralateral
IOP-elevated

Figure 4

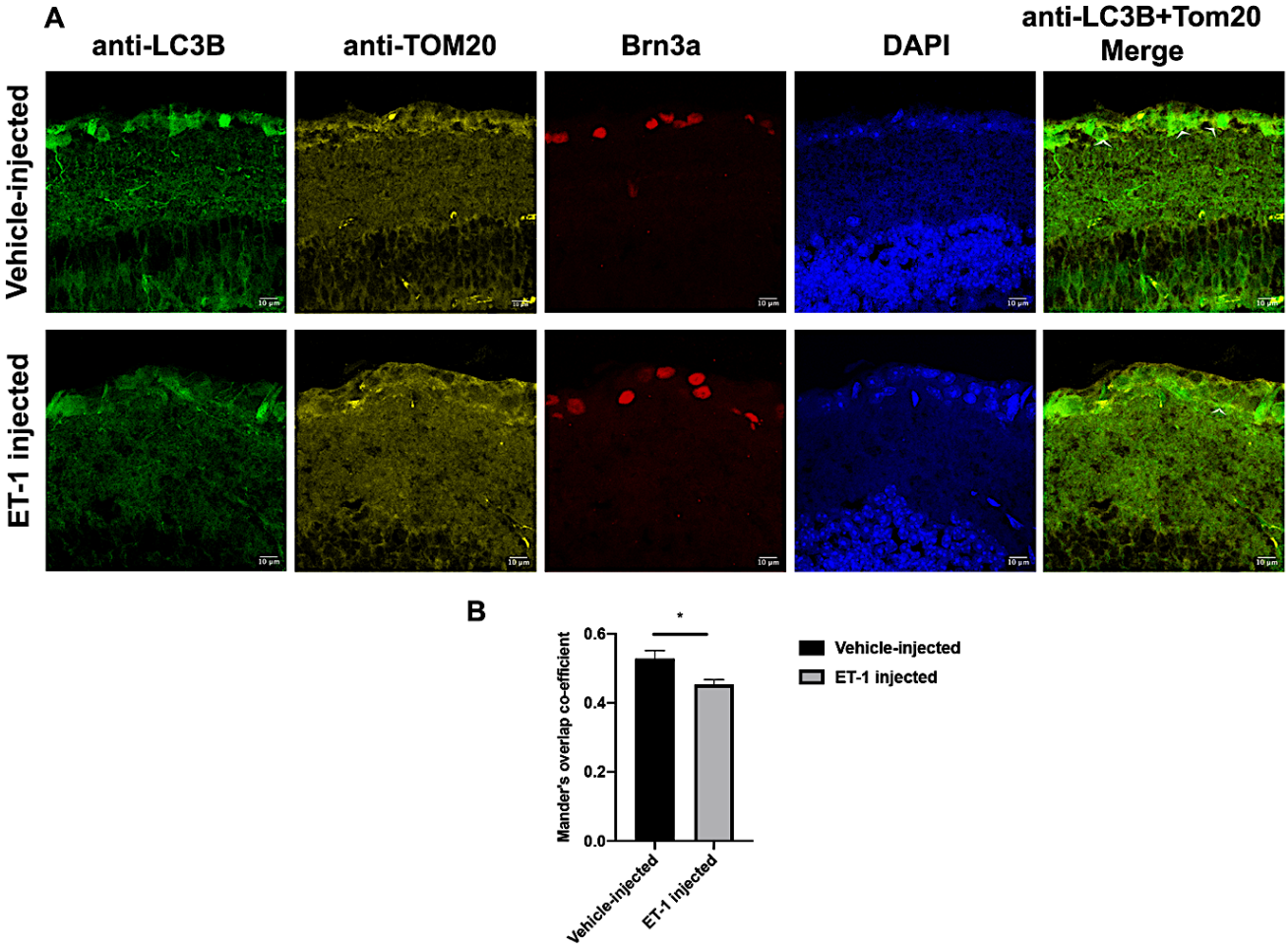
A
anti-LC3B
anti-TOM20
Brn3a
DAPI
anti-LC3B+Tom20
Merge
Vehicle-injected
ET-1 injected
B
Mander's overlap co-efficient
0.6
0.4
0.2
0.0
*
Vehicle-injected
ET-1 injected
Vehicle-injected
ET-1 injected

CHAPTER IV

DISCUSSION

Glaucoma is an optic neuropathy, commonly associated with elevated IOP that afflicts nearly 1% of world population (approximately 80 million patients world-wide) and 3 million patients in the United States (Quigley and Broman, 2006; Tham et al., 2014). Age is a prominent risk factor for glaucoma and people over the age of forty have increased incidence of glaucoma (Guedes et al., 2011). With improvements in health care and rapid developments in medical diagnoses and surgical treatments, longevity has increased all over the world, which is reflected in increased prevalence of glaucoma. Other risk factors include, race (African-American or Hispanic are the most affected), family history of glaucoma, and use of steroid medications (Tielsch et al., 1991; Quigley et al., 2001; Varma et al., 2004; Clark and Wordinger, 2008). Primary open angle glaucoma (POAG) accounts for the majority of glaucoma patients, where the obstruction to outflow of aqueous humor from the trabecular meshwork is a major contributor to IOP elevation. If IOP elevation is either undetected or untreated, it could produce damage to the optic nerve, leading to apoptotic cell death of RGCs, producing visual field defects, ultimately leading to a loss of vision.

There are two major hypotheses to explain the etiology of glaucoma: The “mechanical” hypothesis contends that increased IOP mechanically damages the axons of the RGCs, leading to subsequent degenerative effects. The “vascular” hypothesis posits that abnormal blood flow or vasospasm at the optic nerve head produces ischemic injury to the axons leading to neurodegeneration. The detailed mechanisms contributing to pathological changes in the trabecular meshwork as well as neurodegenerative effects in the RGCs and their axons are still

being elucidated. Clearly, glaucoma is a heterogenous group of multi-factorial neurodegenerative diseases, which needs to be understood in more detail at the genetic, cellular, and molecular level.

The mainstay of glaucoma treatment is lowering IOP by either reducing aqueous humor formation or increased outflow (mainly through the uveoscleral pathway) using a number of pharmacological agents, including, β-adrenergic antagonists, carbonic anhydrase inhibitors and prostaglandin analogs. A recent major development in the field was the development of Rhopressa, which directly targets the trabecular meshwork leading to increased outflow through the conventional outflow pathway. Use of these medications has been very effective in slowing down the progression of the disease. Most of these require self-administration of the medications (mainly eye drops) and life-long treatments. However, prolonged use of most of these IOP lowering treatments produces a number of undesirable side-effects, leading to poor patient compliance (Newman-Casey et al., 2020). Moreover, neurodegenerative effects persist in some patients despite lowering IOP, which is reflected in unilateral (38%) or bilateral blindness (14%) after 20 years of treatment (Peters et al., 2013). There is a pressing need for neuroprotection in glaucoma as a complement to existing therapies.

Several approaches for neuroprotection are being tested in animal models of glaucoma, however, few have managed to reach clinical trials. In two large-scale multi-center, randomized double-masked placebo-controlled Phase III clinical trials, the NMDA antagonist, memantine, failed to meet the primary endpoint of improvement in the visual field in patients with glaucoma. This was an unexpected setback in the field of neuroprotection in glaucoma. **Hence, there is an unmet need to develop neuroprotective treatments as additional therapeutic modalities, which are being sought in several ongoing studies** (Levin et al., 2017; Quigley, 2019). Several

targets for neuroprotection have emerged from pre-clinical studies using animal models of glaucoma, including, neurotrophins, TNF-α, and Complement C1q (Mueller et al., 2011). The endothelin family of vasoactive peptides and their ET_A and ET_B receptors have emerged as strong candidates to target for neuroprotection in glaucoma. Endothelins act through both vascular and cellular mechanisms to promote neurodegeneration of RGCs and their axons.

ET-1 was discovered in the cardiovascular system from the pioneering work of Yanagisawa et al., (1988) who identified, isolated and cloned this 21 amino acid peptide from the supernates of cultured porcine aortic endothelial cells and provided evidence for its potent vasoconstrictor activity (Yanagisawa et al., 1988). The endothelin family comprises of three members of 21 amino acid peptides (ET-1, ET-2 and ET-3) which are encoded by separate genes in the human genome. There is considerable sequence homology between the endothelin peptides: ET-1 and ET-2 differ by only two amino acids, while ET-1 and ET3 differ by 6 amino acids. The two major classes of G protein coupled receptors of endothelins (ET_A and ET_B receptors) are responsible for the biphasic hemodynamic response to intravenous administration of ET-1 in animals: a transient hypotension and a sustained hypertension. Over the past two decades, endothelins have gained prominence in glaucoma research for their neurodegenerative effects in animal models of glaucoma (Yorio et al., 2002; Rosenthal and Fromm, 2011; Shoshani et al., 2012). ET-1 has been shown to be elevated both in the aqueous humor and circulation of primary open angle glaucoma patients (Choritz et al., 2012; Li et al., 2016). Some of the earlier studies in rabbits reported a prolonged decrease in IOP, which could possibly occur by the ability of ET-1 to inhibit Na/K-ATPase (Prasanna et al., 2001). Studies from Dr. Stamer's lab using a gel contraction assay, have shown the ability of ET-1 to produce a contraction of the TM, which was reversed by a NO donor (Dismuke et al., 2014), which could have implications for the

ability of ET-1 to elevate IOP. ET-1 has the ability to either contract or relax the ciliary muscle in different species (Kamikawatoko et al., 1995; Millar et al., 1995). The differential effects of ET-1 on the ciliary muscle versus the trabecular meshwork, could account for the discrepancies in the findings about effect of ET-1 on IOP regulation. However, in the posterior segment of the eye, ET-1 produces a number of neurodegenerative effects. These occur through both vascular and cellular effects that could be targeted for neuroprotection in glaucoma.

Exogenous ET-1 administration has been shown to decrease optic nerve head and choroidal blood flow in rabbits, monkeys and humans (Orgul et al., 1996; Cioffi and Sullivan 1999; Kiel, 2000; Polak et al., 2001and Sugiyama et al., 2011). Emre et al., (2005) found that POAG patients with worsening of the visual field despite lowering IOP had higher circulating levels of ET-1. This could be indicative of the role of ET-1 in long-term neurodegenerative effects. Chauhan et al., (2004) showed that administration of low doses of ET-1 not affecting hemodynamics of the optic nerve head vasculature produced significant RGC loss and damage to optic nerve axons in rats, indicative of vasculature-independent neurodegenerative effects of ET-1.

Much of the earlier work on ocular endothelins was aimed at understanding the source of ocular endothelins and stimuli involved in promoting ET-1 release (Tao et al., 1998, Prasanna et al., 1998; Zhang et al, 2003). The optic nerve head astrocytes and retinal pigment epithelium are good sources of ET-1 in the posterior segment of the eye (Prasanna et al., 2005 and Narayan et al. 2003). Hypoxia, a prominent risk factor contributing to the etiology of glaucoma (Tezel et al., 2004; Chidlow et al., 2017; Jassim and Inman, 2019) stimulates ET-1 release possibly through the HIF-1 since there is a HIF-1 element in the promoter region of the ET-1 gene. Hypoxia could promote ET-1 release from vascular endothelial cells, and optic nerve head astrocytes

(Kourembanas et al, 1991; Desai et al., 2005) which in turn could produce vasoconstriction leading to a vicious cycle of hypoxia and ET-1 release. Apart from the vasculature, cellular factors known to be elevated in glaucoma, including TNF-α and TGF-β have been shown to induce the expression of ET-1. TNF-α treatment has been shown to promote ET-1 release from cultured transformed human ciliary non-pigmented epithelial cells (Prasanna et al., 1998). TGF-β was found to result in a 7-fold increase in prepro ET-1 mRNA expression and also stimulate ET-1 peptide release from cultured primary as well as transformed human trabecular meshwork cells (Von Zee et al., 2012).

Even though ET-1 has been shown in multiple studies to produce axonal degeneration and apoptotic cell death of RGCs, the detailed mechanisms are not completely understood. In this dissertation, several mitochondrial mechanisms contributing to RGC loss were addressed. The impetus for assessing mitochondrial mechanisms came from the RNA-seq analyses of the translatome in primary RGCs treated with ET-1. Gene Ontology (GO) classification carried out using statistical overrepresentation tests revealed a significant enrichment in the differentially expressed genes (DEG) set encoding various cellular components that are characteristic of mitochondrion, endocytic vesicle membrane and cytoplasmic stress granules. Genes identified in these sets can be interrogated and pursued further for assessment of their role in neurodegeneration. Following ET-1 treatment, twenty-three (15%) of the 156 differentially expressed genes had known or predicted mitochondrial function, of which oxidative phosphorylation emerged as the top-most enriched pathway.

Another notable change in gene expression was the decrease in FOXO-1 expression following ET-1 treatment in RGCs. FOXOs are thought to play an important role in regulating genes governing the formation of autophagosomes and their fusion with lysosomes (Cheng,

2019). In response to oxidative stress, FOXOs along with PINK1 promote apoptosis (Sengupta et al, 2009). This prompted us assess ET-1 mediated changes in autophagy in RGCs. Analysis of ET-1 mediated changes in gene expression in primary cultures of RGCs is a good starting point, to get an insight into gene expression changes happening *in vivo* in the RGCs following intravitreal ET-1 administration and during ocular hypertension. In our study, we found strikingly similar changes in key components of the mitochondrial proteins in RGCs, both in culture and in vivo. We also wanted to address the mechanisms by which ET-1 treatment produced these changes in mitochondrial bioenergetics.

The ET_B receptor appears to have a causative role in promoting glaucomatous neurodegeneration, which was evidenced by significant neuroprotection of RGCs and their axons in ET_B receptor-deficient rats, compared to wild type rats during ocular hypertension (Minton et al., 2012). IOP elevation also produced an increase in ET_B receptor levels in the RGC layer, suggesting the possibility that enhanced stimulation and signaling via ET_B receptors are contributors to RGC loss. Interestingly, the ET_B receptor levels are also elevated by cyclical stretch (up to 20% elongation, 0.5 Hz, 6 h) using a Flexcell in cultured rat aortic smooth muscle cells. Exogenous addition of ET-1 to the cells subjected to cyclical stretch produced increased apoptotic cell death (Cattaruzza et al., 2000). It could be speculated that similar mechanotransduction effects that occur during IOP spikes and fluctuations might generate increased expression of the ET_B receptor in RGCs. Activation of the ET_B receptor *in vivo*, by infusion of the ET_B receptor agonist, sarafotoxin 6c, was found to increase superoxide levels in sympathetic ganglia in male Sprague-Dawley rats (Li et al., 2008). One possible mechanism by which ET_B receptor activation elevates oxidative stress is through activation of NADPH oxidase (Tam et al., 2019, Dammanahalli and Sun, 2008;). In addition, we have shown that IOP elevation

produces an upregulation of the ET_A receptor in the RGC layer in rats (McGrady et al., 2017). ET-1 acting through the ET_A receptor elevates intracellular Ca^{2+} through G_q protein coupled activation of phospholipase Cβ and subsequent IP_3 mediated release of Ca^{2+} from intracellular stores (Tao et al., 1998; Prasanna et al., 2002). ROS and elevated intracellular calcium have been shown to promote opening of the permeability transition pore in the mitochondria, leading to a decline in the mitochondrial membrane potential. Depolarization of the mitochondrial membrane potential causes PINK1 to be stabilized in the outer mitochondrial membrane, which recruits the ubiquitin ligase, Parkin to the damaged mitochondria. Parkin ubiquitinates several substrates which recruit the autophagy receptors, optineurin and calcium binding coiled-coiled domain 2 (NDP52) proteins which have a LC3-interacting regions that interact with LC-3 protein (characteristic of autophagosomes) and bring the autophagy machinery for engulfment of the mitochondria (Villa et al., 2018).

The second part of the dissertation was focused on ET-1 mediated decrease in mitophagy in primary RGCs. Mitophagy is a bulk degradation process by which long-lived and damaged mitochondria are enclosed by a double membraned cupped structure called phagophore, which form autophagosomes that ultimately fuse with lysosomes resulting in degradation of faulty/damaged mitochondria. This is an essential function to maintain quality control of mitochondria, especially in very metabolically active cell types such as photoreceptors and RGCs. The autophagosome-lysosome pathway is disrupted in numerous neurodegenerative diseases (Chen et al., 2020). The most commonly assessed autophagy marker is the Atg8 protein, LC-3, which upon lipidation forms LC3-I, a selective marker of autophagosome. An increase in LC-3-postive puncta is often used as a surrogate marker of autophagy activation and increased autophagosome formation. Mitochondria play a pivotal role in sustenance of neurons and are

critical for axonal transport from the soma to the synaptic junctions. RGCs are very metabolically active with high oxygen consumption, hence mitochondria play a vital role in the RGCs to power crucial cell activities, including, anterograde and retrograde axonal transport and saltatory conduction through the axons of the optic nerve (Calkins, 2012; Inman and Harun-Or-Rashid, 2017). Unmyelinated axons at the optic nerve head require more energy (compared to myelinated axons) to propagate axon potentials since they lack saltatory conduction. Glaucomatous insults are thought to inhibit axonal transport leading to accumulation of mitochondria in the prelaminar region of the optic nerve head, leading to the generation of reactive oxygen species (Lin and Kuang, 2014, Eells et al., 2019).

Age is a risk factor in glaucoma which is reflected in a 50% decrease in the extent of mitochondrial transport in older mice after a glaucomatous insult, compared to that observed in in younger mice (Kimball et al., 2018). There are conflicting reports of either increase or decrease in mitophagy in animal models of glaucoma. Haas and Barnstable (2019a) showed that increasing expression of the mitochondrial uncoupler protein 2 (Ucp2) improved RGC survival, while deletion of Ucp2 paradoxically improved RGC survival by enhancing mitophagy following IOP elevation in mice (Haas and Barnstable, 2019b). OPA1 overexpression was found to protect RGCs by increasing mitochondria fusion and facilitating parkin mediated mitophagy in IOP elevated rats (Hu et al., 2018). In parkin-overexpressed glaucomatous rats, the ratio of LC3-II to LC3-I, LAMP1 level, and the number of mitophagosomes were increased at 2 weeks following intraocular pressure (IOP) elevation suggesting that increased mitophagy is a protective quality control mechanisms in RGCs (Dai et al., 2018). On the other hand, Hirt et al., (2018) demonstrated an increase in mitophagy in the RGCs in DBA/2J mice, based upon increased immunostaining for LC-3, compared to C57BL/6 mice. A recent study using MitoQC

mice demonstrated increased mitophagy in mice following optic nerve crush (Rosignol et al., 2020). Being a quality control process, it is possible that mitophagy is highly elevated following the traumatic injury to the optic nerve axons and remains elevated which could be detrimental and contributes to the rapid and drastic cell death in this model. Studies to demonstrate mitophagy were carried out by either immunoblot analyses or immunohistochemical co-localization of a mitochondrial marker with a lysosomal marker protein to draw conclusions about occurrence of mitophagy. Our study is the first to report preliminary findings of a decrease in mitophagy following IOP elevation as well as ET-1 treatment in RGCs.

In conclusion, this study addresses novel mitochondrial mechanisms contributing to ET-1 mediated decline in mitochondrial bioenergetics as well as mitophagy. The accumulation of faculty mitochondria that lack the capacity for ATP production could be a key mechanism predisposing RGCs to neurodegeneration. These findings have significant implications both for understanding the contribution of endothelin receptors to mitophagy as well as develop novel endothelin antagonists as neuroprotective agents for treatment of glaucoma.

References

1. Calkins DJ. (2012) Critical pathogenic events underlying progression of neurodegeneration in glaucoma. Prog Retin Eye Res. 2012 Nov;31(6):702-19. doi: 10.1016/j.preteyeres.2012.07.001. Epub 2012 Aug 1. Review.

2. Cattaruzza M, Dimigen C, Ehrenreich H, Hecker M. (2000) Stretch-induced endothelin B receptor-mediated apoptosis in vascular smooth muscle cells. FASEB J. 14(7):991-8.

3. Chauhan BC, LeVatte TL, Jollimore CA, Yu PK, Reitsamer HA, Kelly ME, Yu DY,Tremblay F, Archibald ML. (2004) Model of endothelin-1-induced chronic optic neuropathy n rat. Invest Ophthalmol Vis Sci. 45(1):144-52.

4. Chen G, Kroemer G, Kepp O. Mitophagy: An Emerging Role in Aging and Age-Associated Diseases. Front Cell Dev Biol. 2020 Mar 26;8:200. doi: 10.3389/fcell.2020.00200. eCollection 2020. Review.

5. Cheng Z. The FoxO-Autophagy Axis in Health and Disease. Trends Endocrinol Metab. 2019 Sep;30(9):658-671. doi: 10.1016/j.tem.2019.07.009. Review.

6. Chidlow G, Wood JPM, Casson RJ. (2017) Investigations into Hypoxia and Oxidative Stress at the Optic Nerve Head in a Rat Model of Glaucoma. Front Neurosci. 11:478. doi: 10.3389/fnins.2017.00478. eCollection 2017.

7. Choritz L, Machert M, Thieme H. Correlation of endothelin-1 concentration in aqueous humor with intraocular pressure in primary open angle and pseudoexfoliation glaucoma. Invest Ophthalmol Vis Sci. 2012 Oct 23;53(11):7336-42. doi: 10.1167/iovs.12-10216.

8. Cioffi GA, Sullivan P. (1999) The effect of chronic ischemia on the primate optic nerve. Eur J Ophthalmol. 9 Suppl 1:S34-6.

9. Clark AF, and Wordinger RJ. (2008) The role of steroids in outflow resistance. Exp Eye Res. 2009 Apr;88(4):752-9. doi: 10.1016/j.exer.2008.10.004. Epub 2008 Nov 1.Review.

10. Guedes G, Tsai JC, Loewen NA. Glaucoma and aging. Curr Aging Sci. 2011 Jul;4(2):110-7. Review.

11. Dai Y, Hu X, Sun X. (2018) Overexpression of parkin protects retinal ganglion cells in experimental glaucoma. *Cell Death Dis*. 9(2):88. Published 2018 Jan 24.

12. Dammanahalli KJ, and Sun Z. (2008) Endothelins and NADPH oxidases in the cardiovascular system. *Clin Exp Pharmacol Physiol.* 35(1):2-6. Review.

13. Desai D, He S, Yorio T, Krishnamoorthy RR, Prasanna G. (2004) Hypoxia augments TNF-alpha-mediated endothelin-1 release and cell proliferation in human optic nerve head astrocytes. Biochem Biophys Res Commun. 318(3):642–648.

14. Dismuke WM, Liang J, Overby DR, Stamer WD. (2014) Concentration-related effects of nitric oxide and endothelin-1 on human trabecular meshwork cell contractility. Exp Eye Res. 2014 Mar;120:28-35. doi:10.1016/j.exer.2013.12.012. Epub 2013 Dec27.

15. Eells JT. (2019) Mitochondrial Dysfunction in the Aging Retina. (2019) Biology (Basel). 8(2). pii: E31. doi: 10.3390/biology8020031. Review.

16. Emre M, Orgül S, Haufschild T, Shaw SG, Flammer J. (2005) Increased plasma endothelin-1 levels in patients with progressive open angle glaucoma. Br JOphthalmol. 89(1):60-3.

17. Hass DT, Barnstable CJ. (2019a) Cell Autonomous Neuroprotection by the Mitochondrial Uncoupling Protein 2 in a Mouse Model of Glaucoma. *Front Neurosci*. 2019;13:201.

18. Hass DT, Barnstable CJ. (2019b) Mitochondrial Uncoupling Protein 2 Knock-out Promotes Mitophagy to Decrease Retinal Ganglion Cell Death in a Mouse Model of Glaucoma. *J Neurosci*. 2019;39(18):3582–3596.

19. Hirt J, Porter K, Dixon A, McKinnon S, Liton PB. (2018) Contribution of autophagy to ocular hypertension and neurodegeneration in the DBA/2J spontaneous glaucoma mouse model. *Cell Death Discov.* 4:14. doi: 10.1038/s41420-018-0077-y. eCollection 2018. Erratum in: *Cell Death Discov.* 2019 Jul 10;5:116.

20. Inman DM, Harun-Or-Rashid M. (2017) Metabolic Vulnerability in the Neurodegenerative Disease Glaucoma. Front Neurosci. 11:146. doi:10.3389/fnins.2017.00146. eCollection 2017. Review.

21. Jassim AH, Inman DM. (2019) Evidence of Hypoxic Glial Cells in a Model of Ocular Hypertension. Invest Ophthalmol Vis Sci. 60(1):1-15. doi: 10.1167/iovs.18-24977.

22. Kamikawatoko S, Tokoro T, Azuma H, Hamasaki H, Ishida A. (1995) The effects of endothelin-1 on isolated bovine ciliary muscles. Exp Eye Res. 1995 Nov;61(5):559-64.

23. Kiel JW. (2000) Endothelin modulation of choroidal blood flow in the rabbit. Exp Eye Res. 71(6):543-50.

24. Kimball EC, Jefferys JL, Pease ME, Oglesby EN, Nguyen C, Schaub J, Pitha I, Quigley HA. (2018) The effects of age on mitochondria, axonal transport, and axonal degeneration after chronic IOP elevation using a murine ocular explant model. *Exp Eye Res*. 172:78–85.

25. Kourembanas S, Marsden PA, McQuillan LP, Faller DV. (1991) Hypoxia induces endothelin gene expression and secretion in cultured human endothelium. J Clin Invest. 88(3):1054-7.

26. Li M, Dai X, Watts S, Kreulen D, Fink G. (2008) Increased superoxide levels in ganglia and sympathoexcitation are involved in sarafotoxin 6c-induced hypertension. Am J Physiol Regul Integr Comp Physiol. 295(5):R1546-54. doi: 10.1152/ajpregu.00783.2007. Epub 2008 Sep 3.

27. Li S, Zhang A, Cao W, Sun X. (2016) Elevated Plasma Endothelin-1 Levels in Normal Tension Glaucoma and Primary Open-Angle Glaucoma: A Meta-Analysis. J Ophthalmol. 2016;2016:2678017. Epub 2016 Nov 14. Review.

28. Lin WJ, Kuang HY. (2014) Oxidative stress induces autophagy in response to multiple noxious stimuli in retinal ganglion cells. Autophagy. 10(10):1692-701. Review.

29. Levin LA, Crowe ME, Quigley HA; Lasker/IRRF Initiative on Astrocytes and Glaucomatous Neurodegeneration Participants. Neuroprotection for glaucoma: Requirements for clinical translation. Exp Eye Res. 2017 Apr;157:34-37.

30. McGrady NR, Minton AZ, Stankowska DL, He S, Jefferies HB, Krishnamoorthy RR. (2017) Upregulation of the endothelin A (ET(A)) receptor and its association with neurodegeneration in a rodent model of glaucoma. BMC Neurosci. 18(1):27.

31. Millar C, Poyer JF, Gabelt BT, Kaufman PL. (1995) Endothelin subtypes: effect on isolated rhesus monkey ciliary muscle. J Pharmacol Exp Ther. 275(3):1143-7.

32. Minton AZ, Phatak NR, Stankowska DL, He S, Ma HY, Mueller BH, Jiang M, Luedtke R, Yang S, Brownlee C, Krishnamoorthy RR. (2012) Endothelin B receptors contribute to retinal ganglion cell loss in a rat model of glaucoma. PLoS One.7(8):e43199. doi: 10.1371/journal.pone.0043199. Epub 2012 Aug 20.

33. Mueller, BM, Stankowska DL and Krishnamoorthy RR (2011) Neuroprotection in glaucoma. In *Glaucoma: Basic and Clinical Concepts*, InTech Publishers.

34. Narayan S, Prasanna G, Krishnamoorthy RR, Zhang X, Yorio T. (2003) Endothelin-1 synthesis and secretion in human retinal pigment epithelial cells (ARPE-19): differential regulation by cholinergics and TNF-alpha. *Invest Ophthalmol Vis Sci*. 2003;44(11):4885–4894. doi:10.1167/iovs.03-0387

35. Newman-Casey PA, Niziol LM, Gillespie BW, Janz NK, Lichter PR, Musch DC. (2020)The Association between Medication Adherence and Visual Field Progression in the Collaborative Initial Glaucoma Treatment Study. Ophthalmology. 127(4):477-483. doi: 10.1016/j.ophtha.2019.10.022. Epub 2020 Jan 10.

36. Orgül S, Cioffi GA, Bacon DR, Van Buskirk EM. (1996) An endothelin-1-induced model of

chronic optic nerve ischemia in rhesus monkeys. *J Glaucoma.* 5(2):135-8.

37. Peters D, Bengtsson B, Heijl A. (2013) Lifetime risk of blindness in open-angle glaucoma. Am J Ophthalmol. 156(4):724-30. doi:10.1016/j.ajo.2013.05.027. Epub 2013 Aug 7.

38. Polak K, Petternel V, Luksch A, Krohn J, Findl O, Polska E, Schmetterer L. (2001) Effect of endothelin and BQ123 on ocular blood flow parameters in healthy subjects. Invest Ophthalmol Vis Sci.;42(12):2949-56.

39. Prasanna G, Dibas A, Tao W, White K, Yorio T. (1998) Regulation of endothelin-1 in human non-pigmented ciliary epithelial cells by tumor necrosis factor-alpha. *Exp Eye Res.* 66(1):9-18.

40. Prasanna G, Dibas A, Hulet C, Yorio T. (2001) Inhibition of Na(+)/K(+)-atpase by endothelin-1 in human nonpigmented ciliary epithelial cells. J Pharmacol Exp Ther. 296(3):966-71.

41. Prasanna G, Hulet C, Desai D, Krishnamoorthy RR, Narayan S, Brun AM, Suburo AM, Yorio T. Effect of elevated intraocular pressure on endothelin-1 in a rat model of glaucoma. Pharmacol Res. 2005;51(1):41–50. doi:10.1016/j.phrs.2004.04.006

42. Quigley, HA (2019) Glaucoma neuroprotection trials are practical using visual field outcomes. American Academy of Ophthalmology (Editorial:pp 69-71) Elsevier Inc. (ISBN 2589-4196/19)

43. Quigley HA, West SK, Rodriguez J, Munoz B, Klein R, Snyder R. (2001) The prevalence of glaucoma in a population-based study of Hispanic subjects: Proyecto VER. Arch Ophthalmol. 119(12):1819-26.

44. Quigley HA, Broman AT. (2006) The number of people with glaucoma worldwide in 2010 and 2020. Br J Ophthalmol. 2006;90:262–267

45. Rosenthal R, Fromm M. (2011) Endothelin antagonism as an active principle for glaucoma therapy. Br J Pharmacol. 162(4):806-16. doi: 10.1111/j.1476-5381.2010.01103.x. Review.

46. Rosignol I, Villarejo-Zori B, Teresak P, Sierra-Filardi E, Pereiro X, Rodríguez-Muela N, Vecino E, Vieira HLA, Bell K, Boya P. (2020) The mito-QC Reporter for Quantitative Mitophagy Assessment in Primary Retinal Ganglion Cells and Experimental Glaucoma Models. Int J Mol Sci. 21(5). pii: E1882. doi: 10.3390/ijms21051882.

47. Sengupta, A., Molkentin, JD., Yutzey, KE. (2009). FOXO transcription factors promote autophagy in cardiomyocytes. J Biol Chem, 284(41), 28319- 28331.

48. Shoshani YZ, Harris A, Shoja MM, Rusia D, Siesky B, Arieli Y, Wirostko B. (2012) Endothelin and its suspected role in the pathogenesis and possible treatment of glaucoma. Curr Eye Res. 37(1):1-11. doi: 10.3109/02713683.2011.622849. Epub 2011 Oct 26. Review.

49. Sugiyama T, Shibata M, Kajiura S, Okuno T, Tonari M, Oku H, Ikeda T. (2011) Effects of fasudil, a Rho-associated protein kinase inhibitor, on optic nerve head blood flow in rabbits. Invest Ophthalmol Vis Sci. 52(1):64-9. doi: 10.1167/iovs.10-5265.

50. Tao W, Prasanna G, Dimitrijevich S, Yorio T. (1998) Endothelin receptor A is expressed and mediates the [Ca2+]i mobilization of cells in human ciliary smooth muscle, ciliary nonpigmented epithelium, and trabecular meshwork. Curr Eye Res. 17(1):31-8.

51. Tezel G, Wax MB. (2004) Hypoxia-inducible factor 1alpha in the glaucomatous retina and optic nerve head. Arch Ophthalmol. 122(9):1348-56.

52. Tham YC, Li X, Wong TY, Quigley HA, Aung T, Cheng CY. (2014) Global prevalence of glaucoma and projections of glaucoma burden through 2040: a systematic review and meta-analysis. Ophthalmology. 121(11):2081-90. doi: 10.1016/j.ophtha.2014.05.013. Epub 2014 Jun 26. Review.

53. Tielsch JM, Sommer A, Katz J, Royall RM, Quigley HA, Javitt J. (1991) Racial variations in the prevalence of primary open-angle glaucoma. The Baltimore Eye Survey. JAMA. 266(3):369-74.

54. Varma R, Ying-lai M, Francis BA, et al. "Prevalence of open-angle glaucoma and ocular hypertension in Latinos: The Los Angeles Latino Eye Study." Ophthalmology. 2004; 111:1439-1448.

55. Villa E, Marchetti S, Ricci JE. (2018) No Parkin Zone: Mitophagy without Parkin. Trends Cell Biol. 28(11):882-895. doi: 10.1016/j.tcb.2018.07.004. Epub 2018 Aug 13. Review.

56. Von Zee CL, Langert KA, Stubbs EB Jr. (2012) Transforming growth factor-β2 induces synthesis and secretion of endothelin-1 in human trabecular meshwork cells.Invest Ophthalmol Vis Sci. 53(9):5279-86. doi: 10.1167/iovs.11-9289.

57. Yanagisawa M, Kurihara H, Kimura S, Tomobe Y, Kobayashi M, Mitsui Y, Yazaki Y, Goto K, Masaki T. (1988) A novel potent vasoconstrictor peptide produced by vascularendothelial cells. Nature. 1988 Mar 31;332(6163):411-5.

58. Yorio T, Krishnamoorthy R, Prasanna G. (2002) Endothelin: is it a contributor to glaucoma pathophysiology? J Glaucoma. 2002 Jun;11(3):259-70. Review.

59. Zhang X, Krishnamoorthy RR, Prasanna G, Narayan S, Clark A, Yorio T. (2003) Dexamethasone regulates endothelin-1 and endothelin receptors in human non-pigmented ciliary epithelial (HNPE) cells. Exp Eye Res. 76(3):261-72.

CHAPTER V

FUTURE DIRECTIONS

1. Sustaining mitochondrial function and bioenergetics using endothelin-receptor antagonists.

The Seahorse XF ATP rate assay and Mitostress assay will be carried in primary RGCs at two time points of ET-1 treatment (4 h and 24 h) following pretreatment with endothelin-receptor antagonists. This will help to determine if mitochondrial bioenergetics and function could be sustained by blockage of endothelin receptors. The assay will provide a measurement of cellular respiration by recording and quantifying multiple parameters including oxygen consumption rate (OCR), ATP production rate from both glycolytic and mitochondrial pathways and ATP rate index. These assays will provide a comprehensive analysis of mitochondrial function and indicate if endothelin receptor antagonists exert neuroprotective function through their ability to sustain mitochondrial function.

2. Measuring mitophagic flux in primary RGCs treated with ET-1 (4 h and 24 h)

Mitophagy is a two-step process in which damaged mitochondria are first targeted by Pink1/Parkin proteins and then eliminated by autophagic machinery. To determine the relative degree of mitochondrial-targeted turnover and if ET-1 induced/decreased mitophagy in primary RGCs, primary RGCs will be treated with ET-1 for 4 h and 24 h, after which the expression levels of mitophagy markers PINK1, Parkin, and Drp1 will be determined by Western blotting. Protein levels of macroautophagy machinery: **a)** autophagosome initiation marker (Beclin 1), **b)** autophagosome formation marker (LC3B-II) and

c) autophagy degradation marker (SQSTM1 or p62) will also be measured. A mitophagy inducer carbonyl cyanide 3-chlorophenylhydrazone (CCCP) will be used as a positive control.

3. To study whether there is an initiation of mitophagy in RGCs

In this study, we showed an impairment of mitophagosome formation in RGCs of GFP-LC3 mice injected with ET-1 (24 h) and in ocular hypertensive rats. Understanding whether these mitophagosomes will further be degraded by the lysosomes or their transport to the lysosomes would be disrupted, it would be necessary to probe for antibodies specific to LC3B, Lamp1 (lysosomal marker), Tom 20, Pink1 and Parkin. The co-localization analysis will be carried in retina sections of ocular hypertensive rats (2 weeks IOP elevation) as well as in GFP-LC3 mice injected with ET-1 (24h). Z-stack images will be obtained using a confocal microscope with an Airyscan detector to allow clear visualization of co-localization puncta.

4. Immunohistochemical analyses to determine if LC-3B, TOM20 and LAMP-1 expression is decreased in wild type rats, and enhanced in ET_A receptor- and ET_B receptor knockout rats at 1, 3, 7 and 14 days of IOP elevation

IOP elevation will be carried out in wild type and RGC-specific ET_A- and ET_B-knockout rats (in the Brown Norway background) using the Morrison model. Previous data revealed decreased co-staining of LC-3B and TOM20 following two weeks of IOP elevation in retired Breeder Brown Norway rats. A time course IOP elevation including 1, 3, 7 and 14 days will be done to determine the effect of endothelin receptor deletion on mitophagy. After sacrificing the rats, sagittal frozen sections will be obtained and mitophagy will be assessed by immunostaining for TOM-20, LC-3B and LAMP 1. Co-localization analysis of staining between TOM-20 LC-3B and LAMP-1 will be an indication of engulfment of mitochondria in the autophagosome and its transit to the lysosomes. It will be determined if there is a decline in mitophagy in the RGCs in

wild type rats and an enhancement in mitophagy in either the RGC-specific ET_A/ET_B-receptor knockout rats, compared to the wild type rats following IOP elevation.

CHAPTER VI

SUPPLEMENTAL CHAPTER

Publications

1. **Chaphalkar, R. M**., Stankowska, D. L., He, S., Kodati, B., Phillips, N., Prah, J., Yang, S., & Krishnamoorthy, R. R., Endothelin-1 Mediated Decrease in Mitochondrial Gene Expression and Bioenergetics Contribute to Neurodegeneration of Retinal Ganglion Cells: *Scientific Reports*. 10(1), 3571, (2020).

2. **Chaphalkar, R. M.,** Maddineni P., Kodati, B., Stankowska D.L., Prah, J., Yang, S., Zode G and Krishnamoorthy, R. R. Impairment of mitophagosome formation in glaucomatous neurodegeneration. Submitted to *Experimental Eye Research.*

3. Stankowska, D.L., Nam, M. H., Nahomi, R. B., **Chaphalkar, R. M.,** Nandi, S. K., Fudala, R., Krishnamoorthy, R. & Nagaraj, R. H., Correction: Systemically administered peptain-1 inhibits retinal ganglion cell death in animal models: implications for neuroprotection in glaucoma In : *Cell Death Discovery*. 5, 1, 122, (2019).

4. Stankowska D.L., Millar C., Kodati B., Behera S., **Chaphalkar, R.M.,** Nguyen T., Nguyen K., Krishamoorthy R.R., Ellis D and Acharya S., Nanoencapsulated Hybrid Compound SA-2 with Long Lasting Intraocular Pressure Lowering Activity in Rodent Eyes. Submitted to *Molecular Vision.*

5. Stankowska D.L., Zhang W., Krishnamoorthy V., Harris P., Hall T., **Chaphalkar R.,** Kodati B., Chavala S and Krishnamoorthy R.R., The Endothelin Receptor Antagonist Macitentan Ameliorates Endothelin-Mediated Vasoconstriction and Promotes Neuroprotection of Retinal Ganglion Cells in Rats. Submitted to *Molecular Vision.*